An Ac Polarographic Study Of Some Electrochemical Reaction Mechanisms.

Citation

EVILIA, RONALD FRANK. *An Ac Polarographic Study Of Some Electrochemical Reaction Mechanisms*. 1969, https://preserve.lehigh.edu/lehigh-scholarship/graduate-publications-theses-dissertations/theses-dissertations/ac-polarographic.

70-1720

EVILIA, Ronald Frank, 1943-
AN AC POLAROGRAPHIC STUDY OF
SOME ELECTROCHEMICAL REACTION
MECHANISMS.

Lehigh University, Ph.D., 1969
Chemistry, analytical

University Microfilms, Inc., Ann Arbor, Michigan

AN AC POLAROGRAPHIC STUDY OF SOME ELECTROCHEMICAL REACTION MECHANISMS

by

Ronald Frank Evilia

A Dissertation
Presented to the Graduate Committee
of Lehigh University
in Candidacy for the Degree of
Doctor of Philosophy
in
Chemistry

Lehigh University
1969

CERTIFICATE OF APPROVAL

Approved and recommended for acceptance as a dissertation in partial fulfillment of the requirements for the degree of Doctor of Philosophy.

May 22, 1969
(date)

James Diefenderfer
Professor in Charge

Accepted April 7, 1969
(date)

Special committee directing
the doctoral work of Mr.
Ronald Frank Evilia

James Diefenderfer
Dr. A. James Diefenderfer,
Chairman

William E. Ohnesorge
Dr. William E. Ohnesorge

Ned D. Heindel
Dr. Ned D. Heindel

Thomas R. Ortolano
Dr. Thomas R. Ortolano

ACKNOWLEDGEMENTS

The author thanks Professor A. James Diefenderfer for his encouragement and guidance. He also thanks Professor W. E. Ohnesorge for many helpful discussions.

Thanks are also given to the department of Saline Water for a research assistantship and to Lehigh University for the student chemical society fellowship.

DEDICATION

To Debbie

TABLE OF CONTENTS

LIST OF FIGURES

LIST OF TABLES

ABSTRACT

The construction of an ac-dc polarograph is described. The dc section of the polarograph is of standard design. The ac section makes use of a commercially available lockin amplifier. The instrument is tested with the model system $Cd^{2+} + 2e \rightleftharpoons Cd(Hg)$ and is found to be equal to or better than previously described ac polarographs. This design is considered superior to the previous ones because it is easier to construct and to operate than the other available designs.

The mechanism of the electrochemical reduction of the monohalopyridines is studied with the instrument. The dc polarographic half-wave potential is found to vary with pH (over a range of pH's determined by the isomer being reduced). The half-wave potential is determined by the isomer being reduced and the pH of the solution. At high pH it is observed that all isomeric iodopyridines reduce with the same reduction half-wave potential. The polarographically measured pKa's values of the various pyridinium species are in poor agreement with the literature values.

Two mechanisms for the halopyridine reductions are proposed: an acidic mechanism and an alkaline mechanism. The acidic mechanism is a two step process which explains the pKa values on the basis of the stability of the intermediate. The alkaline mechanism is an EC mechanism in which the carbon-halogen bond is polarized prior to electron transfer.

The catalytic oxidation of uranium (III) by nitrate ion was studied by ac polarography. The reaction mechanism was not a simple collisional process. The observed rate law is:

$$\text{Rate} = k_1(NO_3^-)^x - k_2(UO_2^{2+})^y$$

A mechanism involving an "electron bridge" between the electrode and nitrate ions is proposed from the rate law.

The mechanism of reduction of UO_2^+ to U^{3+} is found to be:

$$\begin{aligned} UO_2^+ &+ e^- \longrightarrow UO_2 \\ UO_2 &+ 4H^+ \longrightarrow U^{4+} + H_2O \\ U^{4+} &+ e^- \rightleftharpoons U^{3+} \end{aligned}$$

The reduction of uranium (V) to uranium (III) in the presence of nitrate ion is found to give ac polarographic data inconsistent with any mechanism studied theoretically.

INTRODUCTION

This dissertation discusses three topics which are not closely related to each other. The techniques used are the same, but the emphasis and interpretation are different.

The first section discusses the construction of the ac - dc polarograph used for the two subsequent chemical investigations. The main emphasis in the construction of the instrument section is the design and evaluation of the ac polarographic operation of the instrument. Familiarity with dc polarography and instrumentation is assumed.

Much of the interpretation of the subsequent sections is based upon ac polarographic data; the mechanistic interpretation of these data has only recently become available (1). A brief discussion of ac polarographic theory follows.

Ac polarography has been known for many years but, lacking adequate theoretical studies, it has not been used extensively except for quantitative analysis. Due to the rather unsophisticated approach to ac polarography taken in the past, there have been many misconceptions as to what an ac polarographic wave means. For example, for many years it was thought that an irreversible electron transfer reaction would not give a wave, but several recent treatments have shown that irreversible processes do give rise to ac polarographic waves, although of decreased current magnitude (2,3,4). Much of the reason for the inadequate theory is the great mathematical complexity which can only be solved now by means of digital computer approximation techniques.

The first step toward rectifying the theoretical inadequacies was taken by Matsuda who developed a method of dealing with systems more complicated than the simple Nernstian charge transfer mechanism (5). Recently Smith has devoted himself to the problem using the original work of Matsuda as a starting point. He has considered many general reaction mechanisms. A complete discussion of Smith's work is beyond the interest and need of this dissertation, however, the general approach will be discussed briefly. The original works should be consulted for a more complete description of the theoretical solutions.

The first system to be investigated theoretically was, of course, the reversible (Nerstian) charge transfer system represented by

$$\mathrm{Ox} + \mathrm{ne} = \mathrm{Red}$$

where the partial differential equations and boundary values for a stationary planar electrode are (1,6):

$$\frac{\partial\, \mathrm{Cox}}{\partial\, t} = \mathrm{Dox}\frac{\partial^2 \mathrm{Cox}}{\partial\, X^2} \quad (1) \qquad t=0,\ \text{any } X \quad \begin{array}{l} \mathrm{Cox} = \mathrm{Cox}^{*} \\ \mathrm{Cred} = \mathrm{Cred}^{*} \end{array} \quad (3)$$

$$\frac{\partial\, \mathrm{Cred}}{\partial\, t} = \mathrm{Dred}\frac{\partial^2 \mathrm{Cred}}{\partial\, X^2} \quad (2) \qquad \begin{array}{l} t > 0 \\ X \rightarrow \infty \end{array} \quad \begin{array}{l} \mathrm{Cox} \rightarrow \mathrm{Cox}^{*} \\ \mathrm{Cred} \rightarrow \mathrm{Cred}^{*} \end{array} \quad (4)$$

$$t > 0,\ X=0 \quad \mathrm{Dox}\frac{\partial\, \mathrm{Cox}}{\partial\, X} = -\mathrm{Dred}\frac{\partial\, \mathrm{Cred}}{\partial\, X} = \frac{i(t)}{\mathrm{nFA}} \quad (5)$$

$$\mathrm{Cox} = \mathrm{Cred}(\mathrm{Dred}/\mathrm{Dox})^{\frac{1}{2}}\exp(\mathrm{nF}/\mathrm{Rt}(E(t) - E^{r}_{\frac{1}{2}})) \quad (6)$$

Equation (6) is simply the Nernst equation written in terms of the dc reversible half-wave potential and rearranged to solve for C_{ox}. Using the method of Laplace transforms to solve the above boundary value problem yields (1):

$$\underset{x=0}{Cox} = \overset{*}{C}ox - \int_0^t \frac{i(t-u)du}{nFA(D_o \pi u)^{\frac{1}{2}}} \quad (7) \qquad Cred = \overset{*}{C}red + \int_0^t \frac{i(t-u)du}{nFA(D_r \pi u)^{\frac{1}{2}}} \quad (8)$$

Assuming that $C^*_{red}=0$ and substituting equations (7) and (8) into equation (6) and rearranging yields:

$$e^{-j(t)} - e^{-j(t)} \int_0^t \frac{\psi(t-u)du}{(\pi u)^{\frac{1}{2}}} = \int_0^t \frac{\psi(t-u)du}{(\pi u)^{\frac{1}{2}}} \qquad (9)$$

where $\psi(t) = \dfrac{i(t)}{nFA\overset{*}{C}oxD^{\frac{1}{2}}ox}$ $\quad j(t)=nF/RT(E(t)-E^r_{\frac{1}{2}})$

The potential of the electrode in an ac polarographic experiment is:

$$E(t) = E_{dc} - \Delta E \sin \omega t$$

Assuming that the E_{dc} term is constant and substituting the potential term into the above yields (1):

$$e^{-j(t)} = e^{-j} \exp(nF \Delta E/RT)(\sin \omega t) \quad (10) \qquad j=\frac{nF}{RT}(Edc-E^r_{\frac{1}{2}})$$

Smith then developed a power series expansion for the exponential terms as shown below:

$$\exp(nF\Delta E/RT)(\sin \omega t) = \sum_{p=0}^{\infty} (nF \Delta E/RT)^p \frac{(\sin \omega t)^p}{p!} \qquad (11)$$

$$\psi(t) = \sum_{p=0}^{\infty} \psi_p(t)(t)(nF \Delta E/RT)^p \qquad p= 0,1,2,\ldots\ldots$$

Then substituting back into equation (9) and equating equal powers of $\left(\frac{nF\Delta E}{RT}\right)^p$, a system of integral equations is obtained as below:

$$\frac{e^{-j}(\sin \omega t)^p}{p!} - \sum_{r=0}^{p} \frac{e^{-j}(\sin \omega t)^r}{r!} \int_0^t \frac{\psi_{p-r}(t-u)du}{(\pi u)^{\frac{1}{2}}} = \int_0^t \frac{\psi_p(t-u)du}{(\pi u)^{\frac{1}{2}}} \qquad (13)$$

This then is the general equation which must be solved for different faradaic components (values of p). The fundamental harmonic component is p=1, the second harmonic component is p=2, etc. The results of the solution of equation (13) as given by Smith are shown below for the fundamental and second harmonic components (1):

$$I(\omega t) = \frac{K\delta\omega^{\frac{1}{2}}}{4\cosh^2(j/2)} \qquad I(2\omega t) = \frac{2^{\frac{1}{2}}K\delta^2\omega^{\frac{1}{2}}\sinh(j/2)}{16\cosh^3(j/2)}$$

$$\delta = nF\Delta E/RT \qquad K = nFAC_o^{*}D_o^{\frac{1}{2}}$$

Thus the solution of even the Nernstian charge transfer problem is very complicated. If one considers non-Nernstian charge transfer problems, the Nernst equation must be replaced by the absolute rate expression (1,7):

$$\frac{i(t)}{nFAk_s} = \underset{x=0}{\mathrm{Cox}} \exp\left(\frac{\alpha nF}{RT}(E(t)-E^o)\right) - \underset{x=0}{\mathrm{Cred}} \exp\left(\frac{(1-\alpha)nF}{RT}(E(t)-E^o)\right)$$

If one also considers coupled chemical reactions, the boundary conditions must then be changed to fit the chosen reaction scheme. Consideration of non-linear diffusion and expanding electrode geometry adds further complications. The solution of the problem becomes too involved to be obtained by any exact techniques. Smith has, however, used digital computer approximation techniques to obtain solutions to many different boundary value problems. These solutions are available in the literature and will not be reproduced here (1,8,9,10,11,12,13). The solutions given in the literature present graphically the theoretical values of phase angle and current magnitude as functions of the critical parameters (electron transfer rate constants, chemical reaction rate constants, chemical equilibrium constants, transfer coefficients and half-wave potentials) for the various mechanisms.

Despite the now present wealth of theoretical ac polarographic data, the interpretation of experimental results is difficult. The reason for the interpretation difficulty is twofold. If one considers the "simple" phase angle data, all of the following variables affect the measured value: electron transfer rate constant, chemical reaction rate constant, transfer coefficient, chemical equilibrium constants, half-wave potential differences (two step mechanism). The current magnitude is affected by all of the above as well as by the mass transfer variables and electrode geometry (drop growth and fall) variables. The second interpretation difficulty is the great number of data treatments possible. An ac polarographic experiment generates a great deal of data which may be analyzed in several ways; this means that to analyze all the data in all the possible manners will require a great deal of time. While this is not a theoretical problem, it must be considered from an operational standpoint. These considerations limit the usefulness of ac polargraphic data.

Other techniques used in this work are well-known standard techniques: dc polarography, controlled potential electrolysis, potentiometry and shall not be discussed here. Ample descriptions of these techniques are available in standard texts (14,15).

The second section of this dissertation is concerned with the mechanism of the electrochemical reduction of the monohalopyridines. The dc polarographic data is stressed and ac polarography is used to add some details which could not be determined by other means. The halopyridine work illustrates the use of ac polarography for qualitative information. No attempt was made to determine rate constants for the proposed mechanism due to the unavailability of some necessary data (individual transfer coefficients, electron transfer rate constants, and individual half-wave potentials).

The third section is an ac polarographic study of the reaction of uranium (III) with nitrate ion. Uranium (III) is electrochemically generated from uranium (VI) (or U(IV)) and is then oxidized to uranium (IV) by nitrate ion. Ac polarographic data are used as the major argument in elucidation of the proposed mechanism.

CONSTRUCTION OF AN AC - DC POLAROGRAPH

Introduction

With the recent renewed interest in ac polarographic theory the need for adequate ac polarographic instrumentation has become obvious (1,2,3,4,5,8,9,10,11,12,13). A research quality ac polarograph must do several things. First it must control the dc potential of the working electrode as accurately as a dc polarograph. Second it must be able to superimpose upon the dc potential an alternating potential (usually sinusoidal) of known and variable magnitude and frequency. Third it must be able to measure the ac component of the total current which flows through the cell. In addition to the above "classic" requirements of an ac polarograph, the modern ac polarograph must also provide a means whereby the phase angle of the ac current, relative to the applied potential, can be measured. The reason for this last requirement is that modern theoretical studies have shown that the phase angle of the current is a useful method of determining kinetic parameters (1,8,9,10,11,12,13). The first three of the above requirements are rather easy to obtain. The last requirement, phase detection, however, presents a much more difficult problem.

Recently several workers have developed research quality operational amplifier based ac polarographs which meet all of the above requirements (14,15,16,17). A design using highly tuned twin T filters has been presented (14). This approach has the serious shortcoming that operation at several different frequencies is difficult because the tuned amplifiers must be retuned for each new frequency of operation. Because ac polarographic measurements are low level measurements (100 v) it is important that the noise level be as small as possible. Hence the very sharply tuned amplifiers are necessary. The highly tuned amplifiers lower the noise level by having very low gain at all but the desired frequency. This means that if one of the amplifiers (there are several tuned amplifiers in the instrument) is not tuned properly, the gain at the desired frequency will be very low also and no signal will be seen.

Another approach to accomplish the above aims has been the use of an analog computation technique (17). In this method, standard operational amplifier circuitry is used to control the working electrode potential and perform preliminary amplification of the ac signals. An oscillator is used to supply the sinusoidal signal. The phase and frequency detection are accomplished by means of an analog multiplication making use of the following trigonometric identities:

$$(a)\sin \omega t(b)\cos \omega t = \frac{ab}{2}(\sin 2\omega t)$$

$$(a)\sin \omega t(b)\sin \omega t = \frac{ab}{2}(1-\cos 2\omega t)$$

If the signals are of different frequency or phase, no constant (dc) component is obtained. The dc component is measured and is proportional to the magnitude of the signal in phase with the reference signal. One signal (sine term) is simply the appropriately amplified oscillator signal while the other signal is the properly amplified current signal (after being changed to a voltage signal). By phase shifting the oscillator signal by 90° the dc output becomes proportional to the 90° out of phase (quadrature) current signal. Hence, phase angles can be measured by taking first the in-phase and then the quadrature polarogram. This design has the advantage over the tuned amplifier technique in that the frequency and phase sensitivity is characteristic of the multiplication technique and, hence, highly tuned operational amplifiers are not needed and thus the tuning problems inherent with highly tuned amplifiers do not appear. It is also relatively easy to compensate for iR losses by this method. The major disadvantage with this method is the large amount of circuit wiring which must be done by the constructor (eleven operational amplifiers in addition to the analog multiplier-divider are needed) and the corresponding calibration problems.

The method of phase and frequency detection used in this laboratory and to be further described below eliminates the problems inherent with the tuned amplifier method without getting involved in the problems mentioned for the analog computation method. The polarograph uses a commercially available lock-in amplifier (Princeton Applied

Research, model HR-8) and standard operational amplifier potentiostat design to accomplish the result.

Theory of Operation

The potentiostat, ramp generator and dc current amplifier are constructed of Philbrick SP 656 solid state operational amplifiers in a configuration of standard design (16,20,21). A positive feedback loop was included in the instrument to compensate for iR losses by the method of Brown et. al. (which is only useful for stationary electrodes)(16). The follower amplifiers were SP 656's in the grounded output configuration (22) the instrument being of the voltage follower design since this design has been found to be more stable when positive feedback is employed than the current follower design (16).

The operation of the potentiostat section of the instrument can be understood by considering some basic characteristics of operational amplifiers. An inverting amplifier is essentially a high gain amplifier the output of which is reversed in sign from the input. A portion of the output signal is fed back to the input through an appropriate impedance. This tends to hold the input at (virtual) ground potential. If a feedback loop is not included, the amplifier will saturate (because it will try to bring the input to ground potential through an infinite impedance) and the amplifier cannot be used. The current drawn by the input of an operational amplifier (inverting amplifier) is very small and can be considered to be zero for out purposes. Consider the circuit shown below;

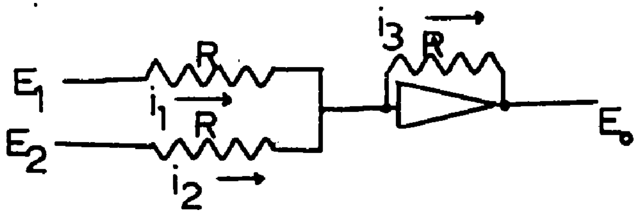

Assume all the resistors are equal, Eo is the output potential, E_1 and E_2 are the input potentials (relative to ground). Because the input current drawn by the amplifier (the triangle the base is the input, the apex is the output), $i_1+i_2= -i_3$ (Kirchhoff's law) and from Ohm's law: $i_1=E_1/R$, $i_2=E_2/R$, $i_3=E_o/R$. Hence, $-E_o=E_1+E_2$. This configuration can be generalized for any number of inputs. The resistors can be different values to get nonunity gains. For our purposes the output of this configuration is $E_o= -\sum E_i$. A similar analysis of different feedback and input impedances yields configurations which will perform many useful tasks (integration, differentiation, logarithm, etc.) and is the basis for analog computer solutions of many problems.

A follower amplifier has the following properties: input current extremely small (very high input impedance), unity gain, non-inverting. This means that the output potential is exactly the same as the input potential in both magnitude and sign. The advantage of the follower is that it will not load the source and hence can be used with high impedance sources (although it is not as good as an electrometer).

If we now consider the circuit shown below the basic reason why a three electrode potentiostat works is obvious:

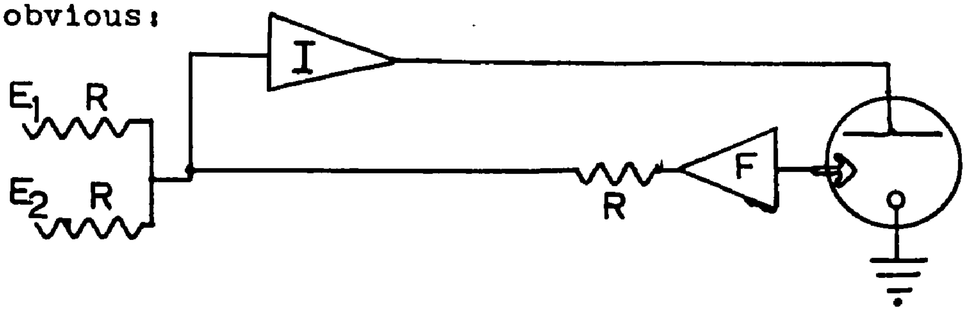

Because the output of the inverting amplifier is such that it will bring the input to ground potential, the output will increase until the output of the follower (which is the feedback loop) is $-\sum E_i$. This means that the input of the follower must be at $-\sum E_i$ relative to ground. Hence the reference electrode must be at $-\sum E_i$ relative to ground. Thus the working electrode, which is at ground potential, must be at $\sum E_i$ relative to the reference electrode. If one of the inputs is a linear ramp and the other a sine wave, we have the basic circuit of an ac polarograph less the current measuring device. Because the follower allows so little current to flow into its input, the reference electrode does not pull any appreciable current and all current flow occurs between the auxiliary electrode and the working electrode. The fact that so little current flows through the reference electrode has two advantages: the reference potential does not change significantly from experiment and high resistance salt bridges may be used because the iR drop is very small.

The alternating current functions of the polarograph are performed by the lock-in amplifier (LIA) mentioned in the previous section. The detailed operation of lock-in amplifiers can be found in several places (23,24). Basically the LIA is an ac voltmeter which responds only to signals of a specific frequency (the reference frequency) and in phase with the reference frequency. The LIA used in this work has a built-in reference oscillator (although operation with an external reference oscillator can easily be accomplished) the output of which after proper attenuation is used as the source of sinusoidal signal for the polarograph. The input signal to the LIA is "mixed" heterodyned with the reference signal producing sum and difference signals. The difference signal between the reference and the desired frequency is zero (dc) and this is the signal which is further amplified and filtered to remove components of noise frequencies close to the reference frequency. A block diagram of the lock-in amplifier is shown in Figure 1. A phase shifter is included in the circuit between the mixer and the reference oscillator so that the output can be made proportional to the component at any phase relative to the output of the reference oscillator. For ac polarography, the components of interest are the 0° (in phase) and 90° out of phase (quadrature) components of the current.

The ac current is measured by applying the voltage drop across a 500 ohm load resistor to the input of the LIA.

FIGURE 1

Block Diagram of the Lock-in-Amplifier

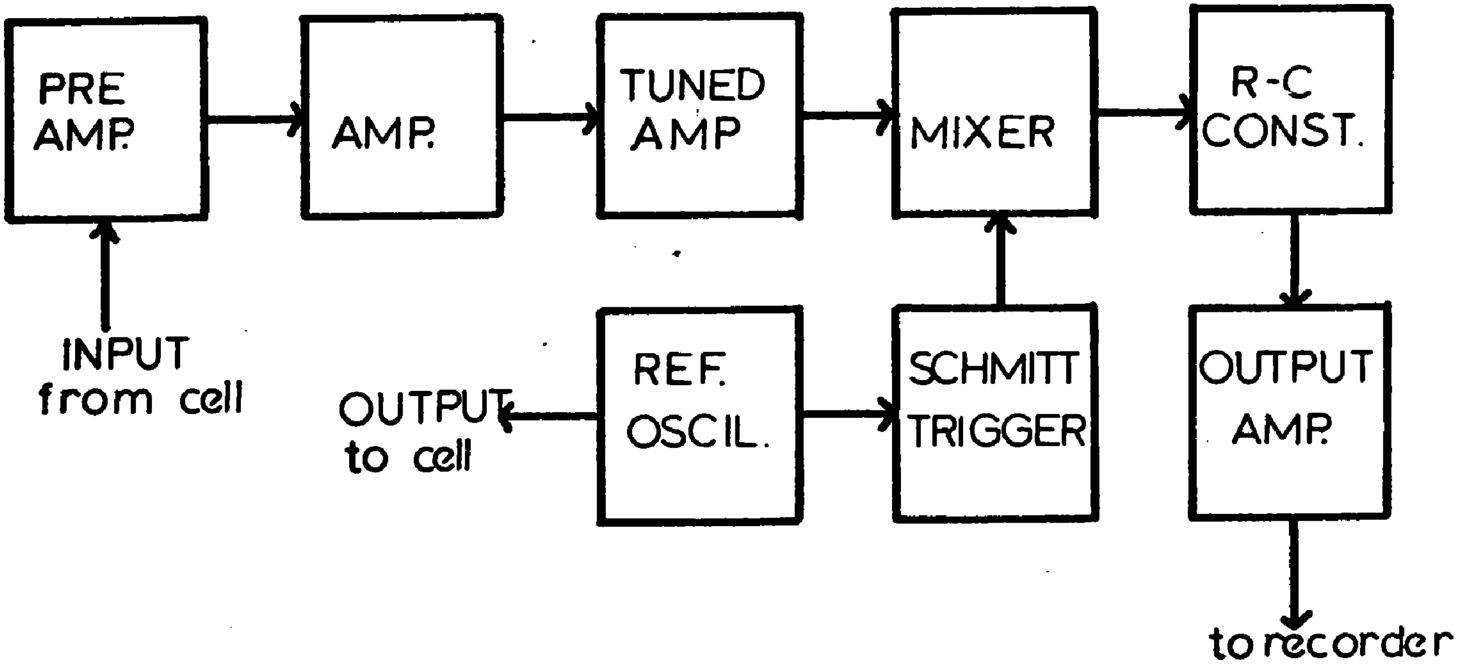
PRE AMP.
AMP.
TUNED AMP
MIXER
R-C CONST.
INPUT from cell
OUTPUT to cell
REF. OSCIL.
SCHMITT TRIGGER
OUTPUT AMP.
to recorder

The output of the LIA is then proportional to the current flowing through the cell at whatever phase the LIA is tuned. The output of the LIA can be changed from relative current to absolute current by means of the sensitivity setting of the LIA and Ohm's law.

Using the LIA eliminates the tuning problems associated with the highly tuned amplifier technique and the wiring and calibration problems of the analog computation technique.

Second harmonic ac polarography can be performed with relative ease using the LIA approach but is very difficult with the analog multiplication method because of the need for two synchronized oscillators. Second harmonic operation is also difficult with the tuned amplifier approach, because of tuning problems.

To do second harmonic ac polarography with the LIA polarograph and external oscillator is needed. The oscillator signal is applied to the cell through the summing amplifier in the same manner that the reference oscillator signal is applied for fundamental harmonic polarograms. The LIA is placed in the external reference mode and tuned to twice the oscillator frequency by applying the oscillator signal to the reference input terminal of the LIA through a rectifier. The rectification procedure changes the signal to one which is a summation of the fundamental and higher harmonics of the applied sine wave. This circuit is shown below:

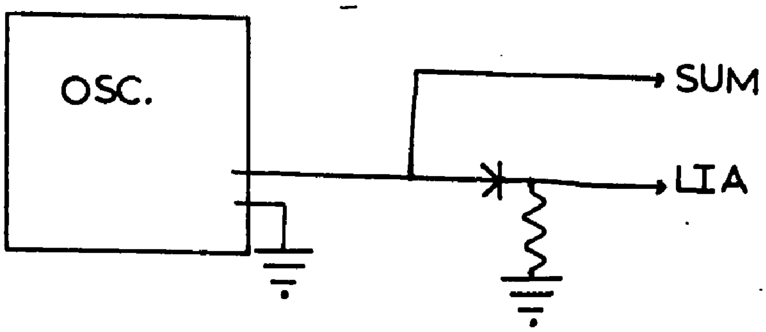

The LIA now responds to signals at twice the applied frequency. Hence, it is operating as a second harmonic ac polarograph. Third harmonic ac polarography can be performed in a similar manner by tuning to three times the applied frequency. Fourth and higher harmonics cannot be handled in this manner because of a lack of adequate signal strength to operate the reference channel of the LIA.

A complete schematic diagram of the instrument is shown in Figure 2.

FIGURE 2

Schematic Diagram of the ac-dc Polarograph

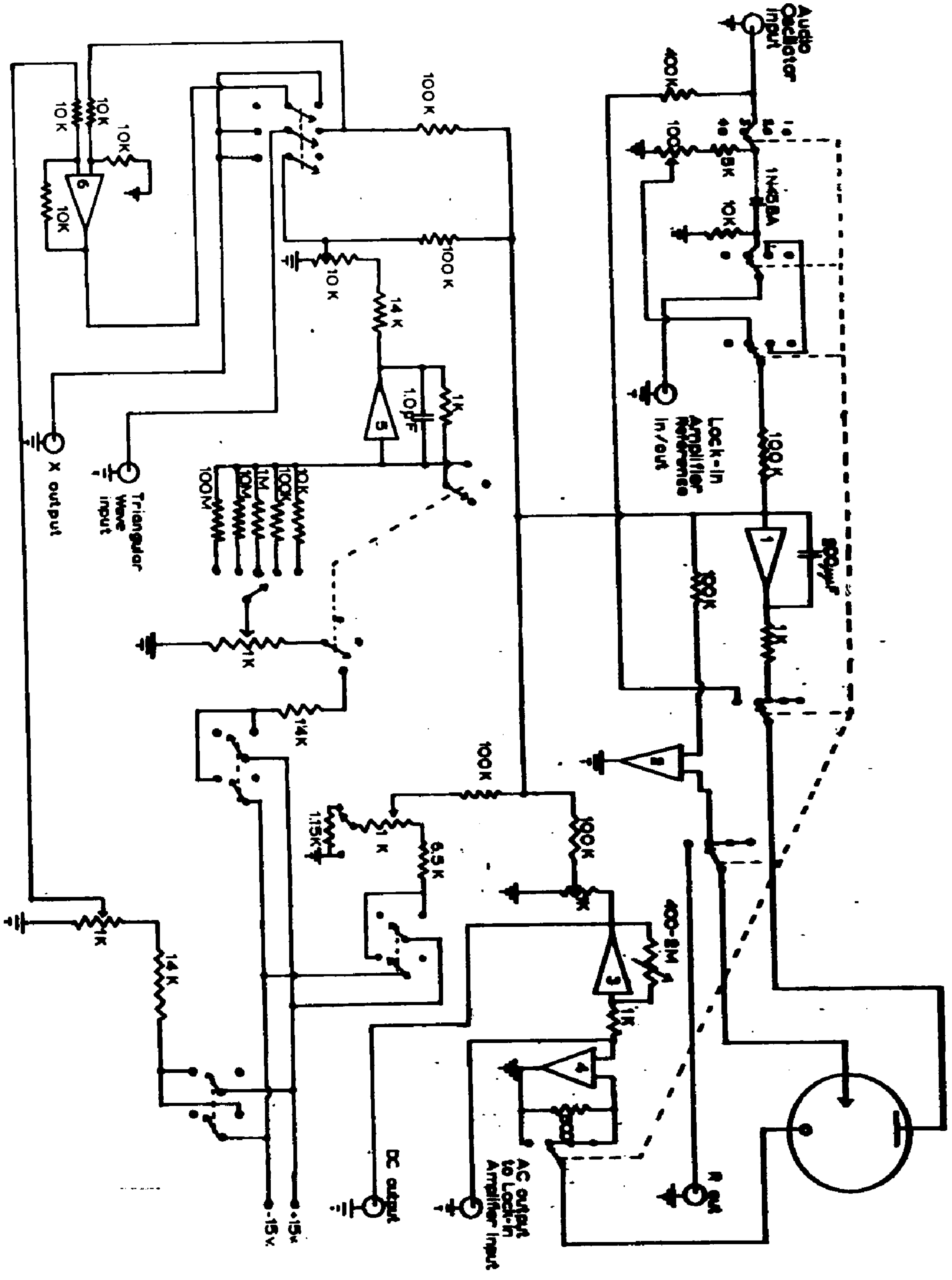
Audio Oscillator Input
400K
100K
8K
1N458A
10K
Lock-in Amplifier Reference in/out
100K
1
800pF
100K
1K
2
100K
100K
1K
400-8M
3
1K
4
AC output to Lock-in Amplifier input
R out
DC output
1.15K
1K
6.5K
14K
1K
10K
100K
1M
10M
100M
5
1.0pF
1K
14K
10K
100K
100K
6
10K
10K
10K
10K
Triangular Wave input
X output
1K
14K
+15v
-15v

INSTRUMENT EVALUATION

In order to evaluate the performance of the polarograph, the reversible reduction of cadmium ion to the amalgam was used as a model system,

$$Cd^{2+} + 2e^- \rightleftharpoons Cd(Hg)$$

The cadmium reduction has been extensively studied; the charge transfer reaction has been shown to be reversible (Nernstian) at the frequencies used in this work (25,26).

Ac polarography, by virtue of the derivitive (peak) output, has inherently better resolution capabilities than dc polarography. A difference in half-wave potentials of at least 100 mv is necessary to resolve two dc polarographic waves, while a difference in peak potentials of only 40 mv is necessary to resolve two ac polarographic peaks. Figure 3 shows an in-phase ac polarogram of a mixture of Cu^{2+}, Pb^{2+}, In^{3+}, Cd^{2+} and Zn^{2+}. As can be seen from the enlargement the In^{3+} and Cd^{2+} waves, which differ in dc polarographic half-wave potential by only 40 mv, can be resolved. Note also, the flat base line which indicates that the capacitive (quadrature) current has been effectively rejected by the LIA.

The reproducibility of the instrument was tested by running three consecutive polarograms over each other. A high time constant was used to damp out the dropping mercury electrode noise. The results of the reproducibility

FIGURE 3

In Phase ac Polarogram of a Mixture of Cu^{2+}, Pb^{2+}, In^{3+}, Cd^{2+} and Zn^{2+}

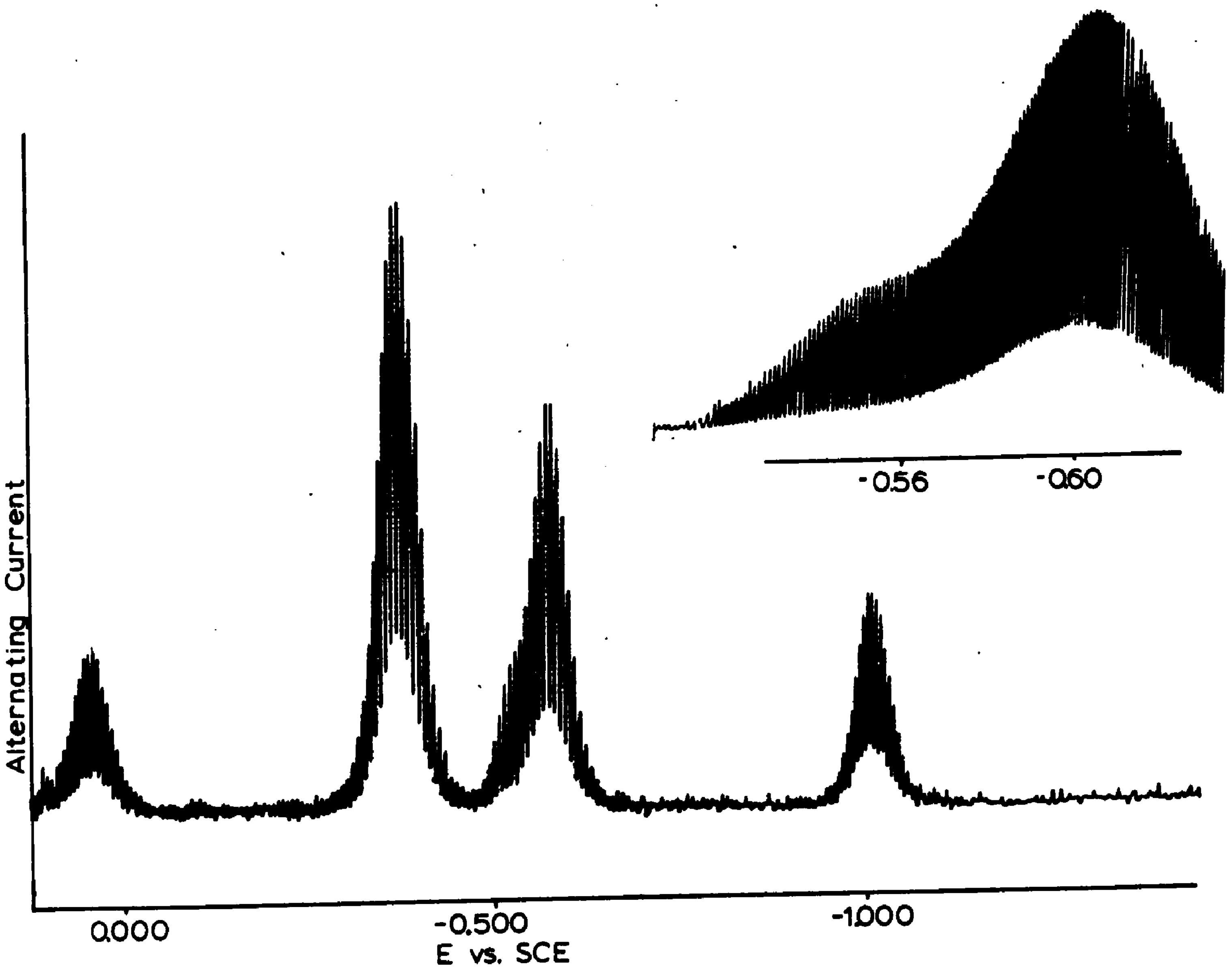
Alternating Current
0.000
-0.500
-1.000
E vs. SCE
-0.56
-0.60

FIGURE 4

Three Consecutive, Coincidental ac Polarograms of 1m$\underline{M}$ Cd^{2+}

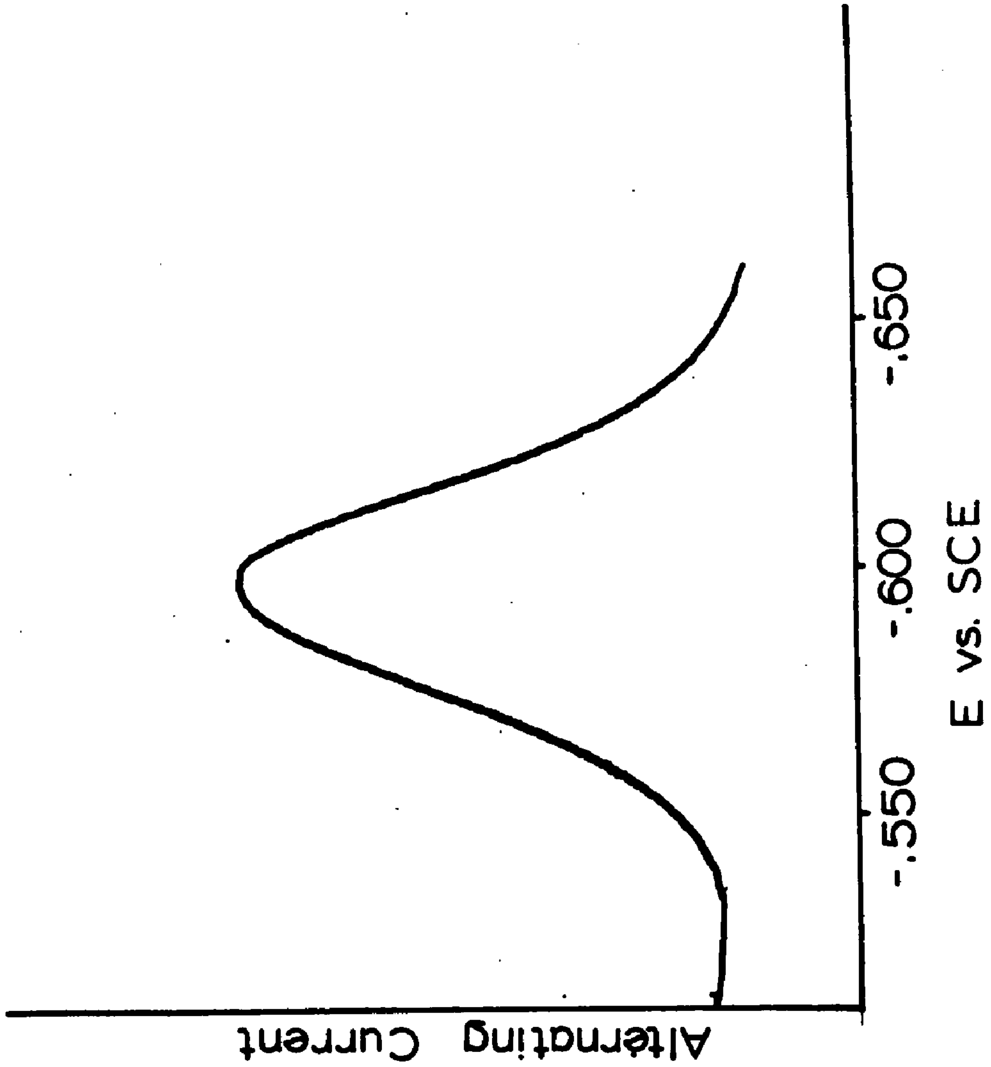
Alternating Current
-.550
-.600
-.650
E vs. SCE

test are shown in Figure 4. These data were obtained after a half hour warm-up period. It is apparent that the instrument is reproducible to within the limits that the recorder (Mosley model 7030A) can be read.

Ac polarographic theory predicts that if the applied ac voltage is small (10 mv), the fundamental harmonic current that flows in an ac esperiment will be directly proportional to the peak-to-peak magnitude of the applied ac voltage. Figure 5 shows a plot of the inphase current as a function of the peak-to-peak magnitude of the ac voltage. As can be seen from the figure, the instrument output agrees well with theory and that applied ac voltages as low as 500μv (1 μv=10^{-6}v) can be easily used on a solution of 5 x 10^{-4}M concentration. Because it is desirable in ac polarography to disturb the system as little as possible from the dc potential, this capability is an important one. The fact that the plot is of cadmium, which is one of the best behaved systems, means that with less ideal systems this 500 μv capability may not be attained.

This reason that ac perturbations as low as 500 v can be used is that the LIA has very high sensitivity (maximum sensitivity is 200 nv, 1 nv=10^{-9}v, full scale which is the equivalent of 400 pa, 1pa=10^{-12}a, full scale) and a very low noise level due to the "frequency lock" and the large amount of filtering. This high sensitivity of the LIA coupled with the usual low level capability of phase sensitive ac polarography means that this instrument should

FIGURE 5

Ac Peak Current versus Peak-to-Peak Applied ac Voltage

1 m$\underline{M}$ Cd^{2+}

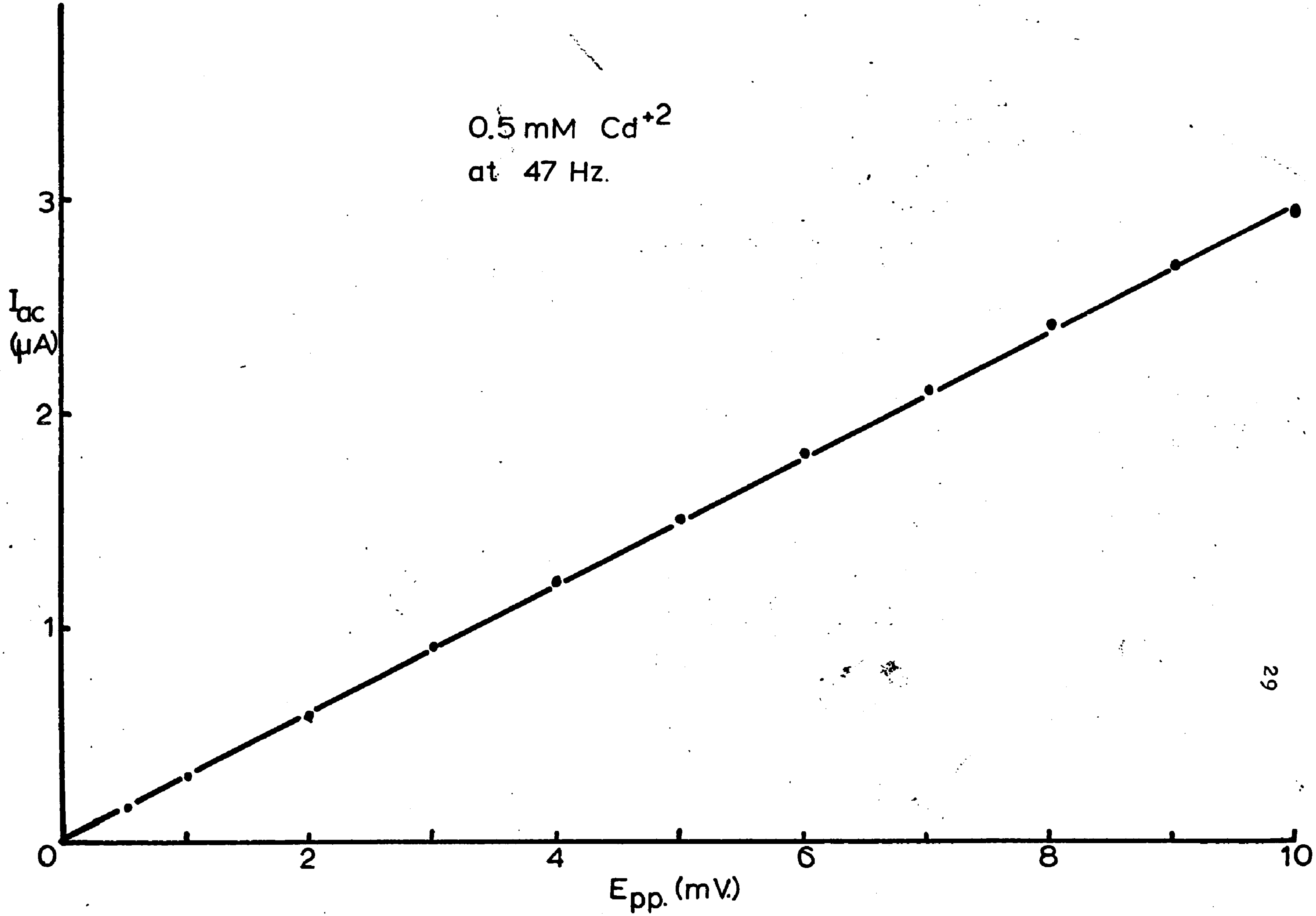
0.5 mM Cd^{+2}
at 47 Hz.
I_{ac} (μA)
3
2
1
0
2
4
6
8
10
$E_{pp.}$ (mV.)

be able to determine extremely low concentrations of ac electroactive substances (19). Although it was not a specific objective in the construction of this instrument to determine extremely low concentrations of electroactive substances, the ability of the instrument to determine low level concentrations was studied as far as was easily obtainable by standard dilution methods and as long as excessively long time constants were not needed. The current should be a linear function of concentration; the experimental data are shown in Figure 6. This plot shows that concentrations as low as 1 x 10^{-7}M can be determined with moderate ease. These data were taken with a hanging mercury drop electrode (HME) and much of the scatter can be attributed to the inability to obtain reproducible electrode areas. Using a mercury pool electrode, as Reinmuth did, should lower the detection limit appropriately, although the ultimate limitation is the ability of the lock-in amplifier to reject the quadrature signals (19). Quadrature signals of about fifty times the full scale sensitivity setting of the LIA can be tolerated. It is possible that even lower concentrations could be determined using a HME if one is willing to spend the time required to use the 100 second time constant or some even longer external time constant. Once again the lower limit attained with other substances will depend upon their reversibility. Cadmium being an ideal case indicates the best (lowest) concentration attainable.

FIGURE 6

Ac Current versus Cd^{2+} Concentration

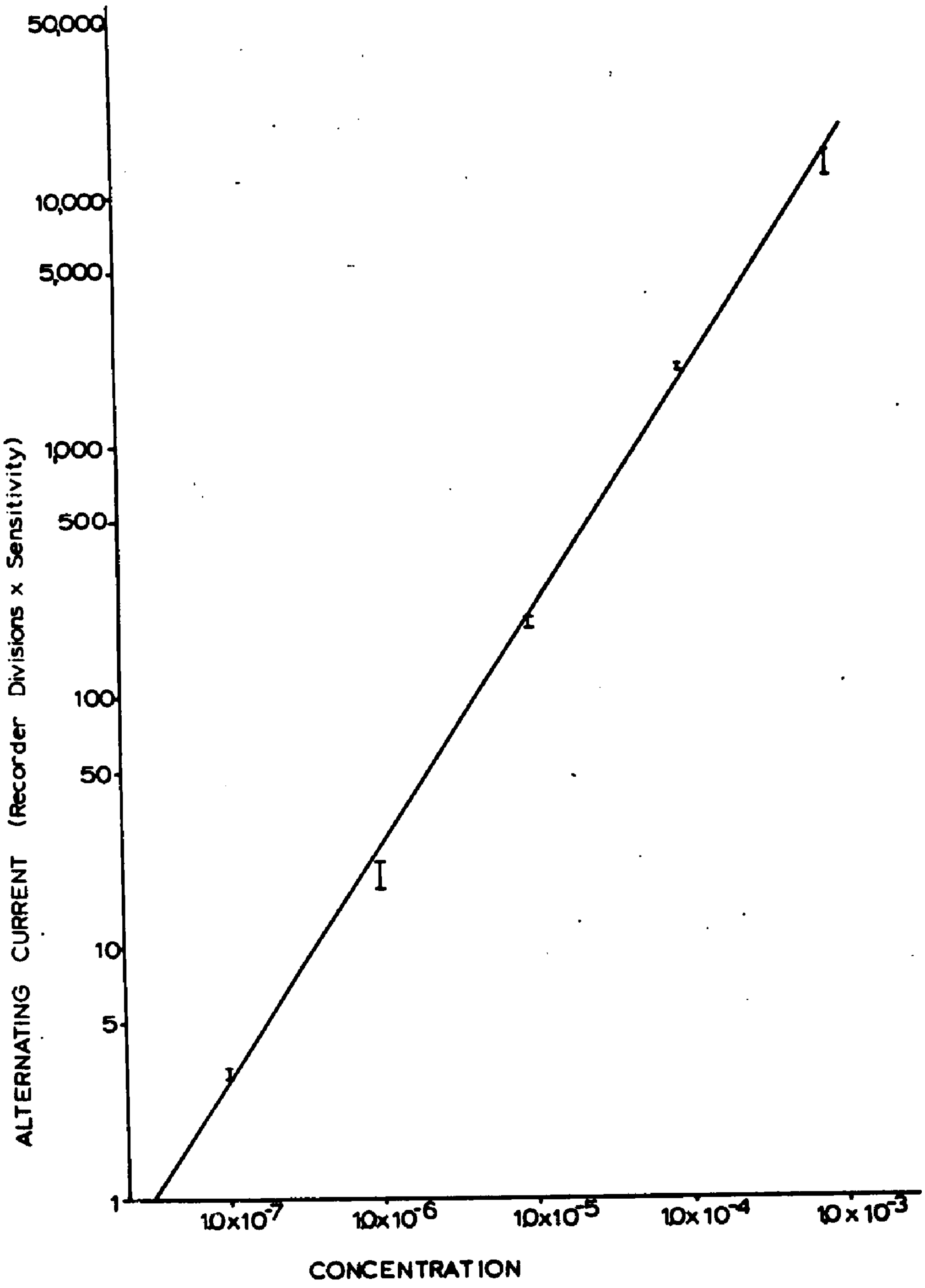
50,000
10,000
5,000
1,000
500
100
50
10
5
1
ALTERNATING CURRENT (Recorder Divisions x Sensitivity)
10x10^{-7}
10x10^{-6}
10x10^{-5}
10x10^{-4}
10 x 10^{-3}
CONCENTRATION

Theoretical treatments of Nernstian systems and experimental data obtained previously predict that the current should increase in a linear fashion with the square root of frequency for the reduction of cadmium ion to the amalgam. The cadmium system was studied as a function of frequency; the results are shown in Figure 7. From the excellent linearity it is apparent that the cadmium system obeys the Nernstian criterion and that the frequency and sensitivity calibrations of the LIA are accurate (at least on a relative basis).

The above tests indicate that the instrument operates adequately as a phase sensitive ac polarograph. If the only purpose of the polarograph was to eliminate capacitive currents so that concentrations could be determined from peak height measurements, the above would be adequate. For mechanistic investigations, however, it is important that the phase angle be measured because interpretation of phase angle data is more straightforward than interpretation of current measurements (1). The above data do not indicate the instrument's capability for determining phase angles.

If an ac signal has a phase angle, ϕ, relative to the applied signal, the signal can be resolved into components in-phase and 90° out-of-phase with the applied signal. The appropriate vector representation is shown below:

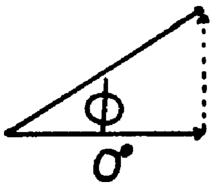

FIGURE 7

Ac Current versus $\omega^{\frac{1}{2}}$ for Cd^{2+} Reduction

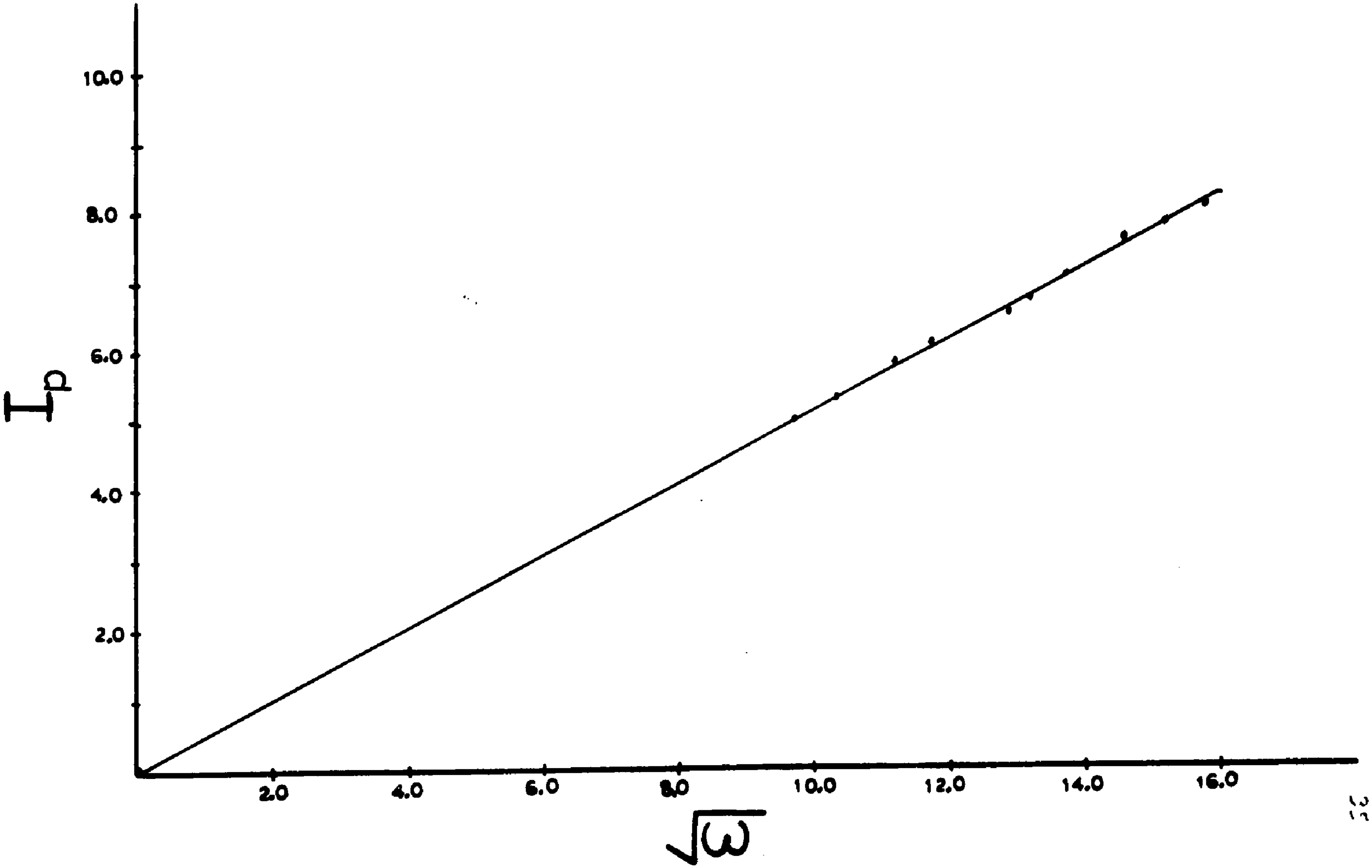
10.0
8.0
6.0
4.0
2.0
I_p
2.0
4.0
6.0
8.0
10.0
12.0
14.0
16.0
$\sqrt{\omega}$

From elementary trigonometry it is obvious that

$$\text{Cot}\,\phi = \frac{\text{in Phase}}{90^{\circ}\ \text{out-of-Phase}}$$

To measure the phase angle, it is necessary to take two polarograms, an in-phase polarogram and a quadrature polarogram. The ratio of the currents at a given potential is the cotangent of the phase angle at that potential. Of course, when the quadrature polarogram is taken, the capacitive contribution to the current is no longer eliminated from the output by the phase sensitive detection. This means that the quadrature signal must be corrected for capacitive current. In the measurement of small phase angles, this becomes the largest source of experimental errors.

Another characteristic of Nernstian reductions not already mentioned is that the phase angle of the current is 45 (1,6). An angle of 45° has a cotangent of 1 which means that the in-phase and quadrature polarograms should have equal current magnitudes (after correcting for the capacitive contribution to the quadrature). Figure 8 shows both the in-phase and quadrature polarograms of a 1m$\underline{\text{M}}$ solution of Cd^{2+}. If the capacitive current is subtracted (displacement of the quadrature signal on the current axis), it is apparent that the two polarograms are the same. Hence, $\cot\phi=1$, $\phi=45^{\circ}$ as is expected for a Nernstian reduction.

The above tests show that the LIA based ac polarograph performs adequately to be useful as a research-quality,

FIGURE 8

Determination of the Phase Angle

A. In-phase Polarogram

B. Quadrature Polarogram

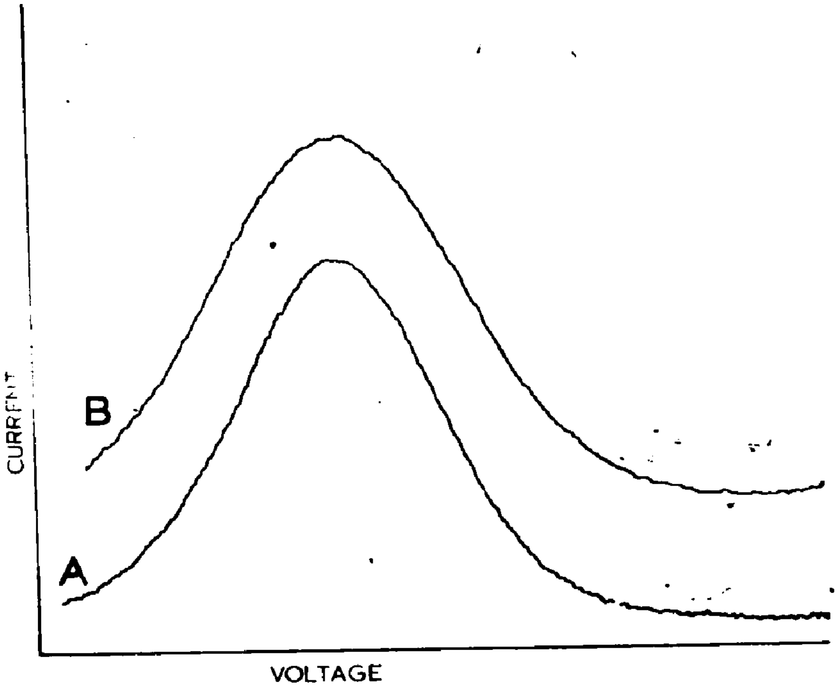
B
A
CURRENT
VOLTAGE

fundamental harmonic ac polarograph. One of the advantages of the LIA polarograph mentioned earilier was that operation as a second harmonic ac polarograph is relatively easy. An external Hewlet-Packard sine wave generator (model 202A) was used to supply the sinusoidal signal and the LIA was tuned for second harmonic operation as previously described. Figure 9 shows the second harmonic ac polarogram which was obtained from a 1 m<u>M</u> Cd^{2+} solution. The sign reversal of the output on passing the peak potential is due to the 180 phase difference between the currents before and after the fundamental peak (1,27,28). The reason that the peaks are of unequal heights is that it is much more difficult to obtain a proper "phase tune" in second harmonic operation. Although capacitive contributions to the current are much smaller in second harmonic operation than in fundamental harmonic operation, it is noticeable that the base line is somewhat more noisy than the base line obtained for fundamental harmonic operation (19,29,30,31). This increased noise is due to the much lower signal levels obtained in second harmonic operation and the subsequent higher sensitivity setting of the LIA needed.

In conclusion, the above shows that this instrument performs all tasks as expected. One problem which is not apparent from the above is that the noise level greatly increases at very low frequency ($<$4Hz). This is due to the so called "1/f" noise (23). This noise can be eliminated from the output by increasing the time constant of the LIA.

FIGURE 9

Second Harmonic ac Polarogram of Cd^{2+}

1 m<u>M</u> Cd^{2+}, 1<u>M</u> KCl, 10 mv p-p applied

Fundamental frequency = 22 Hz

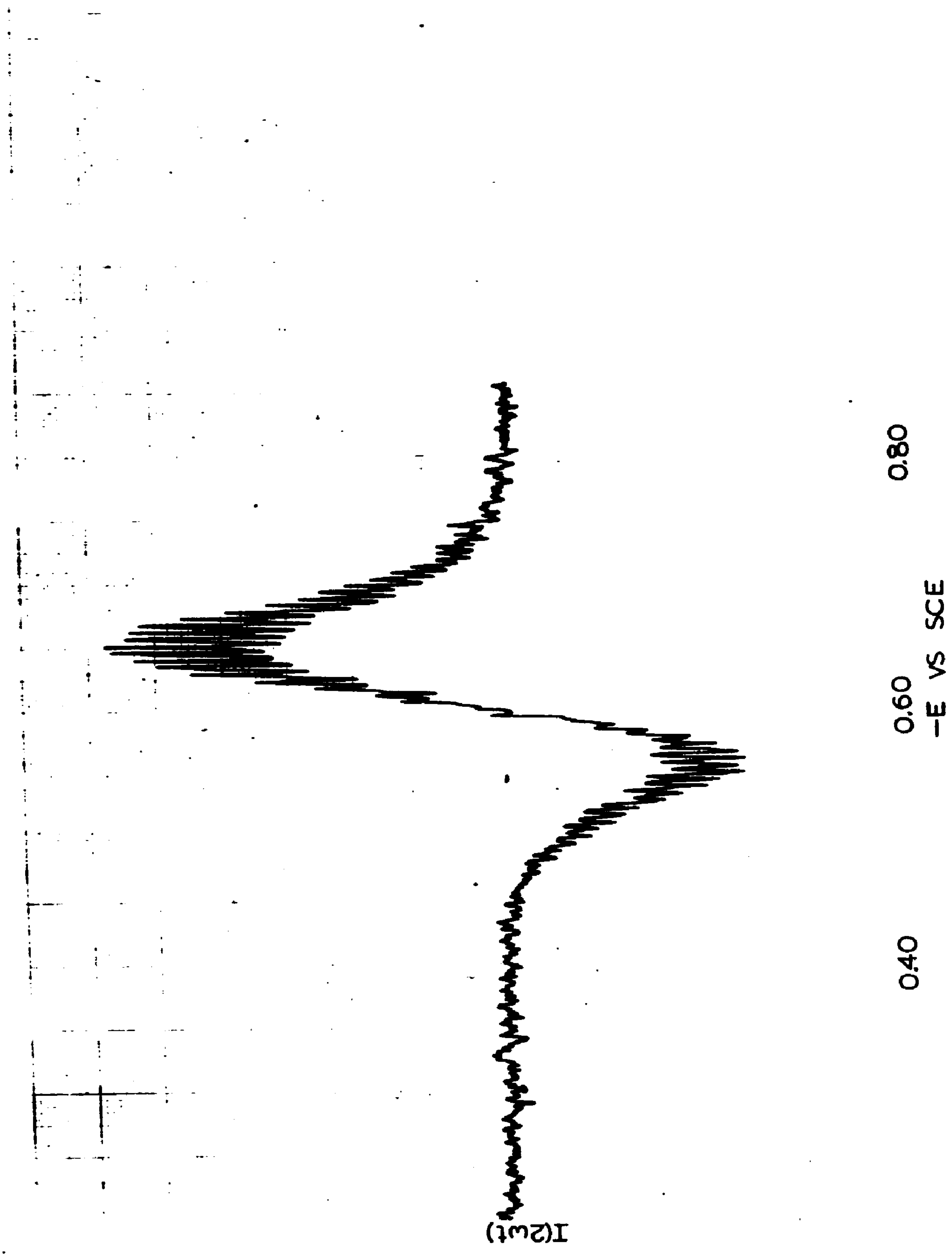
I(2ωt)
0.40
0.60
0.80
−E VS SCE

But this means that the potential scan rate must be decreased so that slewing does not occur which increases the time necessary for each polarogram. This is not a serious limitation, however, because frequencies below 4 Hz are not often used.

The LIA approach is very attractive because it is so simple to construct (all that is needed is an operational amplifier polarograph and a lock-in amplifier) and is capable of giving research-quality data with essentially no calibration.

The Electrochemical Reduction of the Monohalopyridines

Introduction

The mechanism of the electrochemical reduction of the monohalopyridines is interesting because the reduction half-wave potential is a function of pH over a range of pH's determined by the isomer being reduced. This system was previously studied by dc polarography (33). The shift in half-wave potential with pH found previously was consistant with other pH sensitive reductions in that the half-wave potential was independent of pH at extreme values and a linear function of pH at intermediate values of pH. The half-wave potentials were found to be more cathodic in the order: $2I < 4I < 3I < 4Br < 4Cl < 2Br$. Using only dc polarographic data the previous authors proposed two mechanisms, an alkaline and an acidic mechanism (33). The acidic mechanism was simply an overall reaction with no significant details. The alkaline mechanism, however, was far more detailed than was justified by the data available. These two mechanisms are shown below:

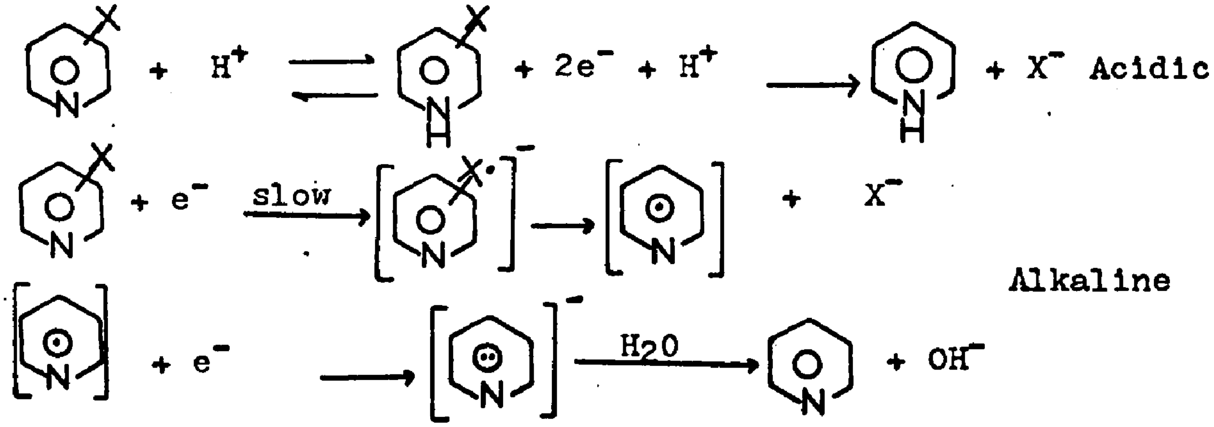

The previous workers apparently used only one buffer to control the pH over the entire range of pH's studied, sodium barbital (pKa of 5,5 diethylbarbituric acid=7.4) and acetic acid (pKa of acetic acid =5.0)(33). They also made no obvious attempt to control the ionic strength of their solutions (33). Using the assumed mechanism, it was possible for them to calculate the acid dissociation constants of the various pyridinium species from the change in diffusion current with pH (33). The calculated pKa values were in such poor agreement with the spectrophotometrically determined literature values that they had to invoke a double layer effect upon the pKa (33). Considering the inadequate buffer capacity and ionic strength control, along with the conclusions drawn without data, the reliability of the previously proposed mechanisms is questionable.

The first step toward verifying (or refuting) the proposed mechanisms was to check the dc polarographic data being careful to maintain good buffer capacity and constant ionic strength. Having reliable dc polarographic data it would then be possible to apply some of the more powerful modern techniques (cyclic voltammetry and ac polarography) to elucidate details lacking from the previous work.

The lack of good buffer capacity and ionic strength control was a serious error on the part of the previous workers (33). The data obtained in this study were significantly different from their data.

Experimental –

All polarographic data were taken on the solid state polarograph described in section 1. Controlled potential electrolyses were performed with a Wenking model 61RH potentiostat. NMR spectra were taken on a Varian model A60A nuclear magnetic resonance spectrometer. Cyclic voltammetry was performed with the triangular wave generator of Enke's design (34).

All chemicals were reagent grade and were used without further purification. Singly distilled water was used. All solutions were 50% aqueous CH_3OH by volume. D_2O and CH_3OD were obtained from Columbia Chemical Company. NaOD was prepared by dissolving Na metal in D_2O. 2-Iodopyridine was prepared by refluxing 2-bromopyridine in concentrated HI after the method of Baker et al. (35); 4-iodopyridine was prepared by diazotization of 4-aminopyridine with $NaNO_2$ and subsequent reaction with KI after the method of Gerely and Iredole (36).

Sodium acetate - acetic acid buffer was used over the pH range 2-6; trishydroxymethylaminomethane (2-amino-2-(hydroxymethyl)-1,3 propanediol) - HCl buffer was used over the pH range 6-8; NH_4^+-NH_3 buffer was used over the pH range 8 - 11. For pH 13 solutions a 0.1 M NaOH solution was used and for pH 0 solutions a 1 M $HClO_4$ solution was used. All solutions (except 1M $HClO_4$) were 0.5 M in $LiClO_4$ to maintain approximately constant ionic strength.

Results

The results of a re-examination of the dependance of the dc polarographic half-wave potential on pH are shown in Figure 10. These data are consistant with those of the previous workers in the order of the reduction half-wave potentials of the various isomers ($2I < 4I < 3I < 4Br < 4Cl < 2Br$) and the linear half-wave potential versus pH regions occur over approximately the same pH ranges. At very low pH the half-wave potentials become independent of pH, but not of isomer, in a manner similar to the data shown by the others. At high pH, however, a major difference between the data can be seen. In the present work all of the iodopyridine isomers reduce at the same reduction half-wave potential at high pH. The previous workers found that at high pH the half-wave potential was independent of pH, but not of isomer. The present data are considered more reliable, in spite of their unusual nature, because of the experimental problems already mentioned. These data, points were found to be reproducible over many runs. The 2-bromopyridine curve appears to level at the same half-wave potential as the iodopyridines; the experimental error in these points, however, is quite large because of the very low current levels and poorly defined diffusion plateaus noted earlier (33).

The single wave obtained from 2-iodopyridine in acid solution was found to separate into tow distinct waves at about pH 8. The second wave had the same half-wave potential

FIGURE 10

Dc Polarographic Half-wave Potential (vs SCE)
versus pH

■ = 2- Bromopyridine

□ = 4- Chloropyridine

▲ = 4- Bromopyridine

△ = 3- Iodopyridine

● = 4- Iodopyridine

○ = 2- Iodopyridine

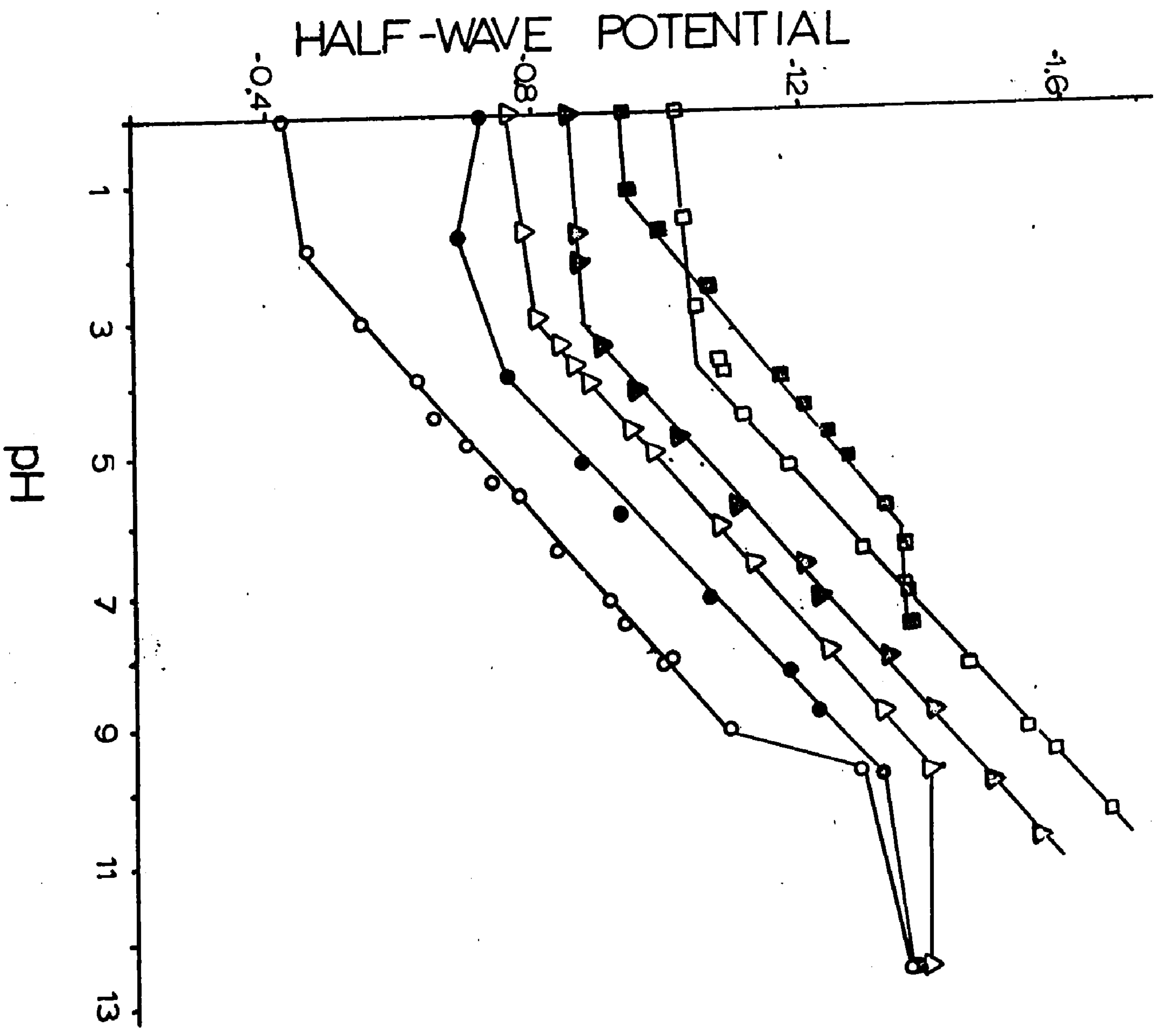
HALF-WAVE POTENTIAL
-0.4
-0.8
-1.2
-1.6
pH
1
3
5
7
9
11
13

as that found for 3-iodopyridine. This is shown in Figure 11. Neither 3-nor 4-iodopyridine showed similar separation. The 4-iodopyridine wave did, however, become more drawn-out at higher pH's indicating that the two half-wave potentials were too close together to allow resolution of the two waves. None of the other isomers showed similar resolution although the diffusion currents of the other waves did decrease at higher pH's were the curves in Figure 10.end. It is assumed that the second wave is not seen with the other isomers because it occurs at potentials more negative than the supporting electrolyte discharge. This is consistent with the inability to obtain polarographic waves of 3-bromopyridine and with both 2 and 3-chloropyridines.

The half-wave potentials were not functions of halopyridine concentration over the range of concentrations used in this work (0.8 - 2.5 m<u>M</u>). It was not possible to obtain polarographic waves of 2-bromopyridine above pH 8 or of 4-bromo or 4-chloropyridine above pH 11 because of the decrease in diffusion current. The decrease in diffusion current was noted by the previous workers who attributed it to a decrease in the amount of pyridinium species in the double layer. Using this interpretation and their polarographic data the acid dissociation constants of the various pyridinium species (in the double layer) were calculated and found to be in very poor agreement with the spectrophotometric values (33). Values of pKa calculated

FIGURE 11

Comparison of the dc Polarographic Responses of 2 and 3-Iodopyridine at pH=8

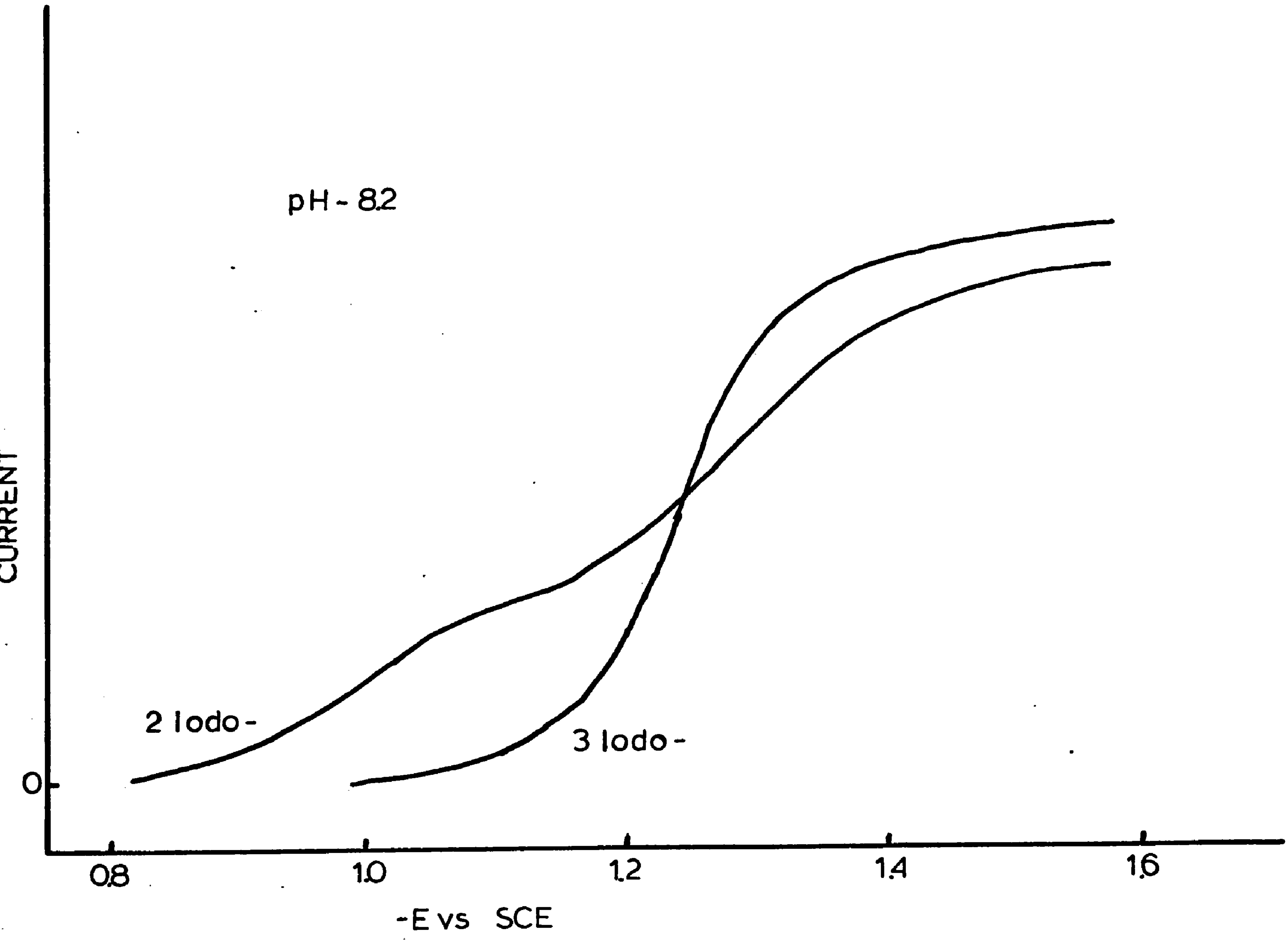
CURRENT
pH - 8.2
2 Iodo-
3 Iodo-
0
0.8
1.0
1.2
1.4
1.6
-E vs SCE

with the present data are in agreement with these of the previous workers (33). The discrepancy between these values and the literature values will be interpreted in a different manner. These data are summarized in table 1.

TABLE I

Summary of dc Polarographic Halopyridine Data

Isomer	$dE_{\frac{1}{2}}/dpH$[a]	$59/\alpha n$ mv[b]	pK'_a[c]	pKa[d]
4-Cl	81.1	91.4	10.6	2.73[e]
2-Br	81.1	91.4	6.8	0.90[f]
4-Br	89.6	91.4	10.5	2.79[e]
2-I	88.0	91.4	8.3	1.82[f]
3-I	83.3	91.4	9	3.25[f]
4-I	86.9	91.4	9	2.93[e]

a.- Slope of the linear portion of the $E_{\frac{1}{2}}$ versus pH curve, mv.

b.- Theoretical slope for the $E_{\frac{1}{2}}$ versus pH curves assuming one hydrogen ion is involved in the reduction and that α n is 0.646 over the entire range. The value of 0.646 was selected because it was approximately the average value of α n determined in this work.

c.- Polarographically determined pKa, determined by setting pKa = pH at that pH where the diffusion current has decreased to one half it's acidic value.

d.- Spectrophotometric pKa values.

e.- From reference (33)

f.- From reference (44)

Values of αn were determined from the slope of the straight line which was obtained when $\log(i_d-i/i)$ was plotted against the applied potential. These values of αn were found to be in good agreement with the values of αn determined from the equation

$$E_{3/4} - E_{1/4} = 0.517/\alpha n \quad (39)$$

and with those reported by the others (33). Because the two values were essentially the same, the simplier E3/4-E1/4 method was used to calculate the bulk of the αn values.

A possible explanation of the merging of the iodopyridine half-wave potentials at high pH would be the formation of a lithium complex with the pyridine which is electroactive at about the same potential regardless of where the substituent is located. This explanation is consistent with the apparent leveling of the 2-bromopyridine curve at the same half-wave potential as the iodopyridines, but is inconsistent with the 4-chloro and 4-bromopyridine data. This hypothesis was disproven when identical data was obtained from solutions to which no lithium ion was added. The solutions which did not contain lithium ion had no metal ion added, the supporting electrolyte was the ammonium - ammonia buffer.

Another explanation of the iodopyridine data which was considered is the reaction of halopyridines with hydroxide ion to form pyridones as shown below:

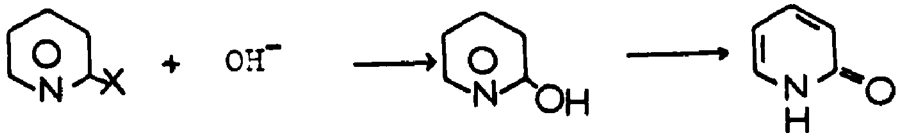

These pyridone reactions are known to occur (37). It was found, however, that, if a pH 13 solution of 2-iodopyridine ($E_{\frac{1}{2}}$=-1.38 V versus SCE) was acidified with perchloric acid to some pH in the linear $E_{\frac{1}{2}}$ versus pH region of 2-iodopyridine, the polarographic wave obtained from the acidified solution had the same half-wave potential and diffusion current constant as would be expected for 2-iodopyridine. If the pyridone reaction was correct, the above observation would require that the reaction be fast, quantitative and reversible. It is known that these reactions are quantitative, but they are neither fast nor reversible (37). For the above reason the pyridone formation reaction was not considered further.

Another possible scheme in which all isomeric iodopyridines would have the same reduction half-wave potential is one in which, under the influence of the potential field around the electrode, the 2-and 4-iodopyridines rearrange to the more stable 3-iodopyridine which is then reduced. There is previous precedent for this typ of rearrangement (38).

This reaction would involve only those iodopyridine molecules which are in the electrical double layer, a small fraction of the bulk concentration. Because only that small fraction in the double layer would rearrange, on acidification, the polarographic wave obtained would be of the unrearranged 2-iodopyridine. In order to test this option, a controlled potential electrolysis of 2-iodopyridine at pH 13 was performed in deuterated solvent. The mercury pool working electrode was maintained at -1.40 V versus SCE until the current had decreased to zero and the product was analyzed by proton magnetic resonance. The product was determined to be 2-deuteropyridine because the integrated intensity of the downfield protons half that of protons was pyridine. Because the rearrangement reaction predicts that the product to be expected in this experiment is 3-deuteropyridine or 2,3-dideuteropyridine, the rearrangement sequence was not considered further. Further discussion of the mechanism will be deferred until it can be discussed in conjunction with the ac polarographic data.

The halopyridine reductions were studied under cyclic voltammetric conditions at a hanging drop electrode (40). No anodic current was observed on the back scan at any sweep rate obtainable with the preent instrument (Ca100 V/Sec). The half-peak potential shifted cathodically as the sweep rate was increased, but not in a manner similar to any of the "diagnostic criteria" available in the literature (40).

The experimental error involved in determining peak potential shifts accurately from oscilliscope traces limits the usefulness of any data obtained in this manner. The increase in peak current with increase in sweep rate was also found to be inconsistent with any of the published predictions (40). These cyclic voltammetric experiments indicate that the halopyridine reductions are totally irreversible (as far as the time scale available from these experiments is able to measure) and they probably reduce by some mechanism which has not been theoretically investigated to date. This total irreversibility is not surprising in view of the overall reaction:

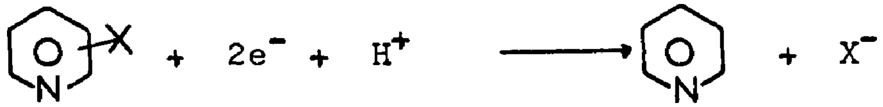

Unfortunately it is not possible, from the cyclic voltammetric data alone, to decide whether the irreversibility is due to the charge transfer reaction or some coupled chemical reaction.

In spite of the apparent total irreversibility of the halopyridine reductions, all isomers which were electroactive under dc polarographic conditions were also electroactive under ac polarographic conditions. The current levels obtained and the effect of frequency upon the current level both much greater than expected for a totally irreversible ac polarographic wave (2,3,4). This indicates that the reduction is either a one step quasi - reversible reduction or a two (or more) step reduction in which at least one of the steps is quasi-reversible. Assuming that the reduction is a one step quasi-reversible reduction, an electron transfer rate constant of about 0.03 cm/sec is calculated from the deviation from linearity of the current versus applied frequency curve at 16 Hz (assuming that the diffusion constant is 10^{-5} cm^2/sec and that the curve will begin to deviate from linearity when $(\omega D)^{\frac{1}{2}} = k_s$) (32). This value of the charge transfer rate constant is only an order of magnitude below that obtained for the "reversible" cadmium ion reduction and is much faster than would be expected for a totally irreversible system (2,3,4,25). If the reduction is a moderately slow charge transfer reaction, as indicated from the calculated value of k_s, some anodic current would be seen on the return scan in the cyclic voltammetric experiments. For these reasons it was decided that the reduction mechanism is not a single step, but at least two steps of which at least one is quasi-reversible. Because the reaction involves only two electrons, it seems unlikely that more than two electron transfer reactions are involved although there could be several chemical reactions.

The addition of one electron to a pyridine molecule will produce a redical ion which should be rather reactive. A controlled potential electrolysis of 3-iodopyridine at pH 3.5 was performed at a stirred mercury cathode held at -1.00 V versus SCE. CO_2 was bubbled through the solution during the electrolysis in the hope that nicotinic acid would be obtained as a product of the electrolysis, thereby supplying chemical proof that a reactive intermediate was involved. The major product of the electrolysis was pyridine. A very small amount of solid material was also isolated from the electrolysis mixture. This solid was analyzed by mass spectrometry. The presence of a series of high mass peaks (m/e 320) separated by the masses of CO_2 and CH_3CO_2 gave indication that a compound similar to the desired one was formed. Because of the very high mass of the peaks, the product is probably some type of polymeric pyridine acid perhaps as shown below:

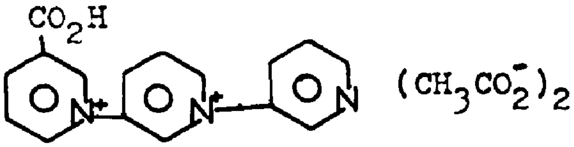

It was not possible to analyze further the solid material because of the extremely small amount of it that was isolated and the questionable purity of that which was obtained. These electrolysis data do, however, add to the ac polarographic indications that the acidic mechanism is a two step reduction with unstable intermediates rather than the one step mechanism proposed previously (33). While these data do not conclusively prove a two step mechanism, they do not refute it either.

Recent theoretical studies of ac polarographic responses of various mechanistic schemes have led to a wealth of relationships which are useful for elucidation of unknown electrochemical reaction mechanisms (1,2,3,4,5,8,9,10,11,12, 13). One of the most powerful of the ac measurements which can be easily accomplished with the present instrument is the phase angle. This was discussed in the first section.

The relationship between phase angle and frequency which is predicted for two step charge transfer reactions is very complicated (9). It would be very difficult to decide between a two step charge transfer reaction and a single step charge transfer step with chemical complications because of the complexity of the relationships which describe both of these cases (1,9,10). For this reason the variation of phase angle with applied frequency was not studied for the halopyridine reductions. It is possible to get essentially the same phase angle versus applied frequency relationship with two different mechanisms by choosing the various rate and equilibrium constants properly.

The phase angle versus applied potential function obtained from the halopyridine reductions is shown in Figure 12. The frastic change in the phase angle function at high pH is a clear indication that the reduction mechanism in alkaline solution is different from the mechanism in acidic solution. These phase angle functions are representative of those obtained for all the electroactive isomers.

The phase angle function obtained at low pH is, fortunately, uncommon. Therefore, it can be interpreted with relative ease. According to the work of Hung and Smith, a function such as that shown in Figure 12 at low pH is to

FIGURE 12

Ac Polarographic Phase Angle versus Applied Potential

15 Hz

○ = Right hand Scale, 3-Iodopyridine at pH = 2.52

● = Left hand Scale, 3- Iodopyridine at pH = 13.

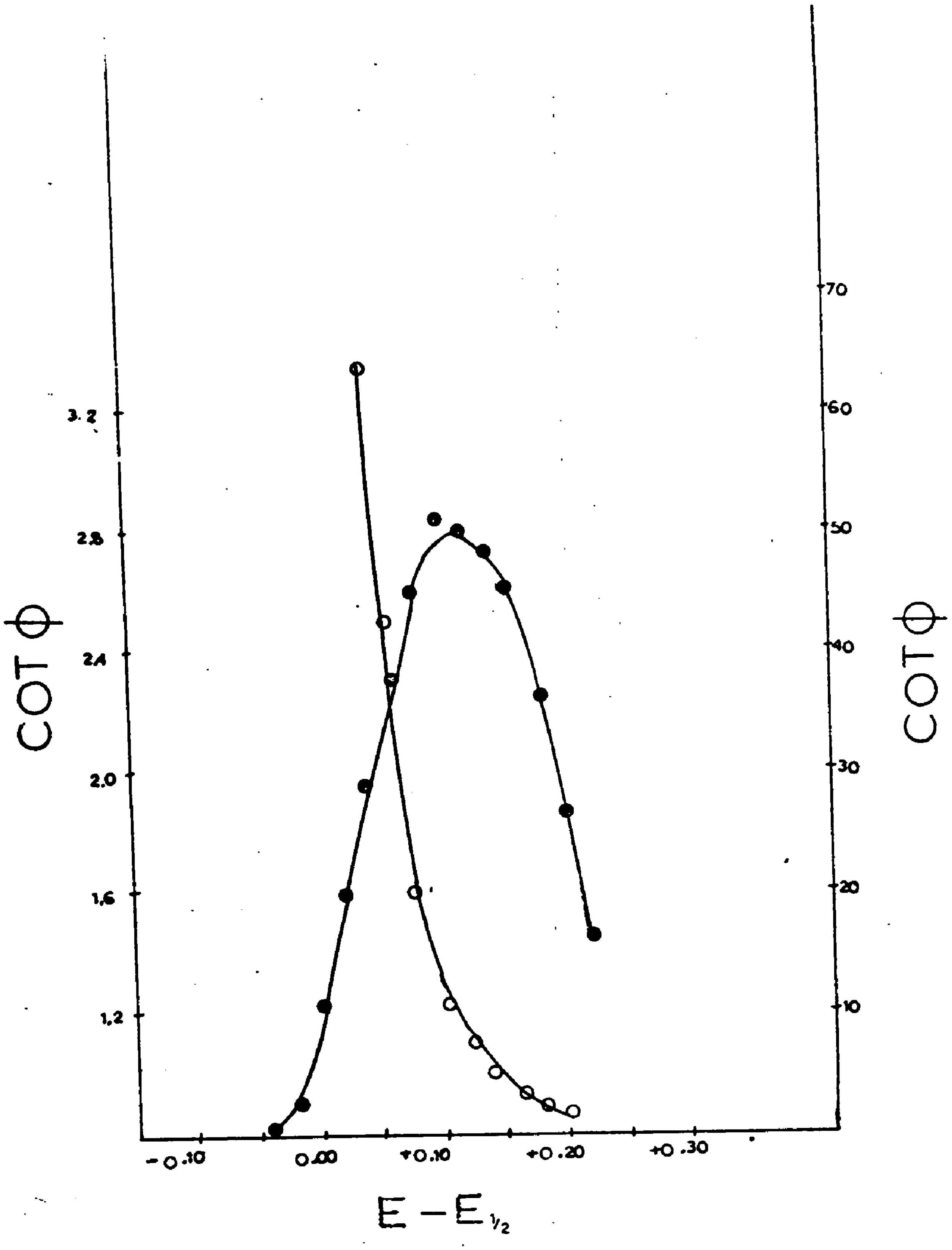
COT Φ
3.2
2.8
2.4
2.0
1.6
1.2
COT Φ
70
60
50
40
30
20
10
-0.10
0.00
+0.10
+0.20
+0.30
E − E½

be expected of an EE mechanism when the first electron transfer rate constant is much slower than the second electron transfer rate constant such as shown below (9):

$$\mathrm{Ox} + n_1e^- \xrightarrow{k_1} \mathrm{Y} + n_2e^- \xrightarrow{k_2} \mathrm{Red} \qquad k_1 \ll k_2$$

For this analysis to be correct, the half-wave potential of the second reduction step must be more anodic than the half-wave potential of the first reduction step (9). It is to be expected that the radical ion formed by adding one electron to a halopyridine would be easier to reduce than the starting halopyridine (this means that the half-wave potential limitation set above is a reasonable requirement).

Phase angles are generally independent of electrode geometry and mass transfer variables (1). A two step mechanism, however, such as that proposed above, would be expected to have a geometry dependent phase angle (9). This geometry dependence of the phase angle will appear in the form of a phase angle which is a function of the drop time of the dropping mercury electrode (9). Because the drop time of the dropping mercury electrode is a function of the mercury column height, a two step reduction would have a phase angle which is a function of the height of the mercury column (9,41). It was found that the phase angle measured in the reduction of 3-iodopyridine decreased when the drop time of the electrode was increased (column height lowered). This is consistent with the recent theoretical predictions (9). The only systems which are expected to give phase angles which are functions of the mercury column height are multistep charge transfer, ion-amalgam charge transfers, and second or higher order coupled chemical reactions (9,13). Of the possible mechanisms only the two step charge transfer reaction seems reasonable in this case.

Considering the slope of the $E_{\frac{1}{2}}$ versus pH functions (figure 10, table 1) and the above data it is now possible to write a mechanism for the reduction of the halopyridines in acidic solution. The slope of the $E_{\frac{1}{2}}$ versus pH curve indicates that the reductions involve one hydrogen ion (42). Assembling all of this information, the following reaction sequence is written for the electrochemical reduction of the monohalopyridines in acidic solution:

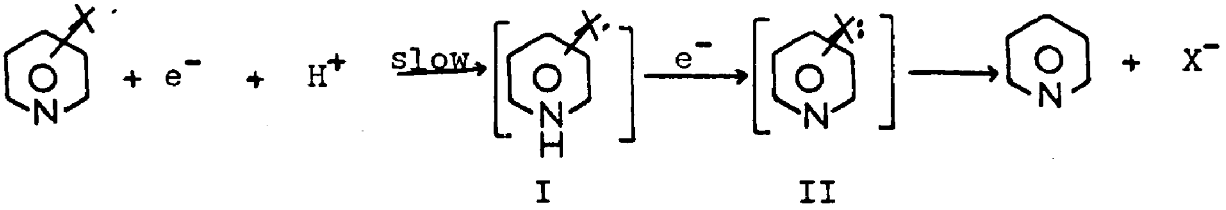

This mechanism is similar to the one written by the previous workers for the halopyridine reduction in alkaline solution (33). Considering the above mechanism, it is apparent why the polarographically determined pKa's are so different from the spectrophotometrically determined pKa's. The polarographic pKa is a measure of the acidity of radical I and not of the ground state pyridinium ion. This is analogous to the difference between the ground state pKa and the excited state pKa, which can be a spectacular difference (43). It is not surprising that radical I is much less acidic than the ground state pyridinium ion because radical I is uncharged while the pyridinium ion is positively charged.

The pH independence of the half-wave potential in very acid solution is also easily explained by the above mechanism. At very low pH, the major pyridine species in the bulk of the solution is the pyridinium ion. Hence, at low pH, the hydrogen ion will not be involved in the electron transfer reaction (the hydrogen ion will already be on the nitrogen). The pH at which the half-wave potential begins to deviate from the low pH limit is shown in Table 2 and can be seen to be related to the spectrophotometric pKa value. It is to be expected that the actual pKa values will be different from the spectrophotometric value because of differences in solution composition (ionic strength).

The high pH mechanism is not as clear as the low pH mechanism. The phase angle data reported in Figure 12 at high pH are not as unusual as the low pH data. A maximum in the cotangent versus applied potential curve is expected for quasi-reversible reductions, chemically coupled single step reductions, and multistep charge transfer reactions (1,9,11). The single step quasi-reversible reduction is disregarded when considering the acidic mechanism. Multistep charge transfer reactions which give maxima in the $\cot\Phi$ versus potential curve usually give values of $\cot\Phi$ larger than those obtained in this investigation and so the multistep charge transfer scheme is disregarded (9). A maximum which occurs after the half-wave potential indicates a coupled chemical reaction occuring after the charge transfer reaction (EC mechanism)(1). If the alkaline

TABLE 2

pH at which the Half-wave Potential becomes a Function of pH

Isomer	pH[a]	pKa[b]
4-Cl	3.8	2.73
2-Br	1.2	0.90
4-Br	3.2	2.79
2-1	2.0	1.82
3-1	3.0	3.25
4-1	2.5	2.93

a. pH at which the half-wave potential begins to deviate from the low pH limit

b. Spectrophotometrically determined pKa's mechanism is as proposed by the previous workers, a phase angle function similar to that obtained at low pH would be expected. From the above arguments it appears that the alkaline mechanism is a two-electron simgle-step charge transfer reaction followed by a rapid chemical reaction.

The critical data which must be explained by the alkaline mechanism is the equivalence of the dc polarographic half-wave potentials of all the iodopyridines. Several possible explanations of this have already been discussed.

Assuming that the EC mechanism is correct, a mechansim is written for the alkaline halopyridine reduction in which the carbon-halogen bond is polarized by the electric field in the neighborhood of the electrode prior to reduction. This polarization can be written in a formal sense by writing the resonance form of the iodopyridine shown below:

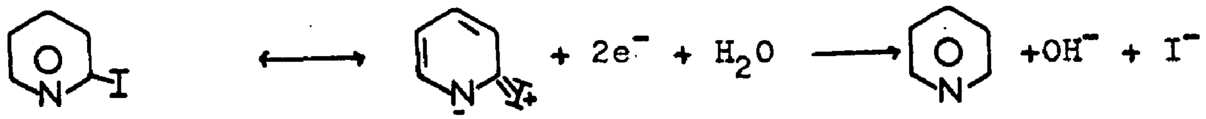

III

A structure similar to III was written by Brown and McDaniel to explain some of thier pKa data (44). One can object to using a resonance form as the electroactive species, but this is only a formalization to show the polarization of the bond. The reason that this polarization is necessary (change of mechanism) is probably because the intermediate radical shown in the acidic mechanism is too unstable unless it is stabilized by a proton.

This mechanism explains the pH independence of the half-wave potential at high pH and the equivalence of the half-wave potentials of all the iodopyridine isomers and is not inconsistent with the ac polarographic data.

The Reaction of Uranium (III) with Nitrate

Introduction

The chemistry and electrochemistry of uranium have been extensively studied by many workers. Uranium chemistry is complicated by the existence of many stable oxidation states (6+,5+,4+,3+) and numerous hydrolysis and polynuclear products (45). Therefore, a complete and consistent picture has not been obtained. Part of the problem lies with the limitations of the techniques which have been applied previously - e.g. dc polarography. Ac polarography has been applied to the uranium system only to the extent of finding that an ac reduction wave could be obtained from uranyl (U(VI)) solutions (32).

The first reported electrochemical reduction of uranium was by Herasymenko, but other than indicating that U(VI) could be electrochemically reduced, this work was of little importance (46). Strubl studied the reduction of uranyl solutions in 2 N $NH_2OH \cdot HCl$ and found tow dc polarographic reduction waves with half-wave potentials of -0.28 and -1.08 V versus SCE respectively (47). The height of the second wave was found to be 2½ times that of the first wave.

Harris and Kolthoff studied the polarographic reduction of uranyl ion in 0.01 - 0.20 M HCl (48). They found that the uranyl reduction took place in two steps. The first reduction wave had a half-wave potential of about -0.18 V versus SCE and the second wave had a half-wave potential of about -0.92 V versus SCE. The first was found to be a one-electron reversible wave because a plot of $\log(i/i_d-i)$ versus potential gave a straight line of 0.062 V slope. This is a necessary, but not sufficient criterion for reversibility; the reversibility of the first reduction step was conclusively shown to be reversible by other workers (49). A plot of $\log(i/i_d-i)$ versus E for the second uranyl wave did not give a straight line for Harris and Kolthoff, but Kritchevsky found that this could be resolved into two straight line segments (48,50). He claimed this as proof that the second wave was really a compound wave of U(V) $\rightarrow$ U(IV) $\rightarrow$ U(III) where the half-wave potentials for the individual steps are close together. This conclusion agreed with the conclusion of Harris and Kolthoff. The U(V) $\longrightarrow$ U(IV) reduction was irreversible (non-Nernstian) while the U(IV) $\rightleftharpoons$ U(III) reduction was reversible (50).

It has been well established that uranyl ion exists as UO_2^{2+} (48,49). Because the first uranyl wave is a reversible one-electron reduction and there is no hydrogen ion effect on the half-wave potential, the pentavalent uranium species was established as UO_2^+ (48,49). The first uranyl wave has thus been rather convincingly shown to be

$$UO_2^{2+} + e^- \overset{rev}{=} \quad UO_2^+$$

Uranium (V) disproportionates in the presence of hydrogen ion via the following sequence (49,51):

$$2UO_2^+ + 4H^+ \rightarrow UO_2^{2+} + U^{4+} + 2H_2O$$

This is a little surprising in view of the stability of Nb(V) and Pu(V) (51). The effect of hydrogen ion on the rate of disproportionation has been studied (49,52,53). The disproportionation of uranium (V) occurs slowly at pH=2 (51). Below pH 2 the rate of disproportionation increases and at higher pH hydrolysis products are formed which also increase the rate of disproportionation (51). Thus it is necessary to maintain the hydrogen ion concentration at about 10^{-2} $\underline{M}$ if appreciable concentrations of uranium (V) are to be generated and maintained.

The effect of disproportionation of the electrolysis product upon the polarographic currents has been studied from a theoretical viewpoint (54). The effect of uranium (V) disproportionation upon the current observed from the first uranyl wave has been studied experimentally (52).

The electrochemical reduction of uranium (IV) was studied by Kritchevsky who found that the $U(IV) \rightleftharpoons U(III)$ couple was reversible (50). He found that, contrary to Kolthoff's observations, the half-wave potential of the second uranyl wave was a function of pH. He studied the $U(IV) \rightleftharpoons U(III)$ couple as a function of acid (HCl or $HClO_4$) and of acid concentration and decided that the couple $U^{4+} + e^- \rightleftharpoons U^{3+}$ was reversible with $E^{o\prime} = -0.886$ V versus SCE in 1M HCl. Above pH2 hydrolysis products of U(IV) caused half-wave potential shifts and decreased the diffusion current. He explained the "apparent" irreversibility of this couple previously noted as due to the slow hydrolysis of U(IV) (48). If U(IV) solutions were allowed to stand the plot of $\log(i/i_d - i)$ versus E was a straight line, but did not have the theoretical slope, 60 mv.

The conclusion from the above work is that the second wave of the uranyl reduction is believed to be a composite of the irreversible $U(V) \rightarrow U(IV)$ and the reversible $U(IV) \rightleftharpoons U(III)$ reductions. The exact route by which the UO_2^+ ion loses its oxygen atoms to become U^{4+} or UOH^{3+}, which is probably the reason for the irreversibility,, is not known with certainty although several workers have studied the problem (50,55).

Uranium (IV) hydrolyzes to UOH^{3+} via the reaction

$$U^{4+} + 2H_2O \rightleftharpoons UOH^{3+} + H_3O^+$$

with a pKa of 1.45 (51). At high pH U(IV) hydrolyzes to a polymeric form, but Kraus and Nelson found no evidence for any hydrolysis product intermediate between UOH^{3+} and the polymer (51).

Harris et. al. found that when nitrate ion is added to a uranyl solution the observed limiting current of the second uranyl wave $(U(V) \rightarrow U(III))$ is greatly increased. They assumed that the increased current was due to the reduction of nitrate ion which was in some way catalyzed by a uranium species. Using the Ilkovic equation with

$D=1.92 \times 10^{-5}$ cm^2/sec (the diffusion constant of nitrate ion) they predicted that five electrons were involved and that the product of reduction was N_2. They also found that chlorate ion does not react (nitrate impurities in $KClO_3$ could be determined by this method).

Collat and Lingane studied the nitrate-uranium reaction by controlled potential electrolysis. A solution of UO_2^{2+} and NO_3^- was electrolyzed at -1.1 V versus SCE until the current dropped to a low value (close to zero)(57). The products of electrolysis were analyzed by standard chemical means and were found to be NH_2OH and a little NH_3 for the nitrate and the uranium was incorrectly reported to be present as U(IV). Because the potential of the electrode used in the electrolysis was on the diffusion plateau of the U(V) ⟶ U(III) wave, the product of the uranium reduction must be U(III). A rather large amount of hydrogen ion was also consumed in the process. They proposed that there was a catalytic reaction involving U(III) and NO_3 as shown below:

$$\begin{tikzcd} U(IV) + e^- \arrow[r, shift left] & U(III) \arrow[l, shift left] \arrow[l, bend left=60, "NO_3^-"] \end{tikzcd}$$

The kinetics of the above reaction were studied by Koryta using a dc polarographic technique (58). The method involved measuring the increase in the diffusion current as a function of nitrate concentration. The rate of the catalytic reaction was determined from the equation:

$$(i_k/i_d) = 0.81\ (k_c t)^{\frac{1}{2}}$$

where i_k is the diffusion current at a particular nitrate concentration, i_d is the diffusion current when no nitrate is present, k_c is the rate of the catalytic reaction and t is the drop time of the electrode. Koryta found that t the reaction was first order in nitrate ion and involved the oxidation of U(III) to U(IV). The k_c^o (rate divided by the nitrate concentration) was 1.6×10^6 mol^{-1} liter sec^{-1}. He did not study the rate of the catalytic reaction as a function of uranyl concentration.

The reason for the hydrogen ion consumption noted by Collat and Lingane is the competing catalytic oxidation of U(III) by hydrogen ion

$$U^{3+} + H^+ \rightarrow U^{4+} + H^o$$

as well as consumption of hydrogen ion by the nitrate

$$6U^{3+} + NO_3^- + 7H^+ \rightarrow 6U^{4+} + NH_2OH + 2H_2O$$

This reaction has not been well-studied, but is known to occur (59). One result of the present work will show that, under the conditions used here, the reaction of U(III) with H^+ is slow enough that it can be assumed not to affect the analysis of the uranium data.

The above, while far from a complete survey of the uranium literature, gives the background for the present study and indicates some of the complexities of the system. The overall uranyl system is then:

$$UO_2^{2+} + e^- \xrightleftharpoons{rev} UO_2^+ \qquad 1.$$

$$2UO_2^+ + 4H^+ \longrightarrow UO_2^{2+} + U^{4+} + 2H_2O \qquad 2.$$

$$UO_2^+ + e^- \longrightarrow UO_2 \qquad 3.$$

$$UO_2^+ + e^- \longrightarrow U^{4+} + 2H_2O \qquad 4.$$

$$U^{4+} + e^- \xrightleftharpoons{rev} U^{3+} \qquad 5.$$

$$6U^{3+} + NO_3^- + 7H^+ \longrightarrow 6U^{4+} + NH_2OH = 2H_2O \qquad 6.$$

$$U^{3+} + H^+ \longrightarrow U^{4+} + H^0 \qquad 7.$$

Purpose of uranium study

There are two reasons for re-examining the catalytic uranium (III) - nitrate reaction using modern electrochemical techniques. First, although the system has been well-studied, and the reaction of U(III) with nitrate has been known for a long time, to date no mechanism for the reaction has been written. The mechanism must explain why nitrate will oxidize U(III) while perchlorate and chlorate will not.

The second reason for pursuing this research is the fact that many papers have appeared recently dealing with theoretical predictions of ac polarographic responses for various reduction pathways (1,2,3,4,5,8,9,10,11,12, 13). To date, however, there have been very few experimental studies. The only previous experimental use of the available theory was reported by Smith who studied the catalytic chlorate - titanium (III) system (12):

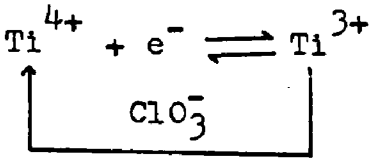

The data gathered would thus serve two purposes: to explain the mechanism and to supply experimental tests of the existing, but experimentally untested, wealth of theoretical predictions.

Experimental

All solutions were aqueous 0.01 N in HCl and 0.1 N in KCl. Uranyl acetate (Fisher, Certified Reagent) was used without further purification as the source of uranyl ions. Uranium tetrachloride prepared by reaction of UO_3 (Alfa Inorganic Chemical Company) with hexachloropropene (J.T. Baker Chemical Company) after the method of Hermann and Suttle was used as the source of U(IV) ions (60). Potassium nitrate (Baker, Analyzed Reagent) was used without purification as the source of nitrate ions.

All polarographic data were taken on the solid state polarograph described in section 1. The cell was kept in a Faraday cage with temperature control provided by the controlled atmosphere of the room (a constant temperature water bath was found to introduce excessive noise into the output of the lock-in amplifier and so was not used). Controlled potential electrolyses were performed with a Wenking model 61RH potentiostat at a sturred mercury cathode; the anode compartment was separated by an ultrafine sintered glass disk. The data were displayed on a Mosley model 7030A XY recorder.

The phase angle was determined by taking the ratio of the in-phase current and the quadrature current after correcting the quadrature current for the capacitive contribution as shown in section 1.

The frequency calibration of the LIA was used as is to determine the applied frequency. The voltage calibration of the LIA was also used as is. The applied potential was 10 mv peak-to-peak and was measured with the lock-in before each run. The in-phase setting of the LIA was determined by tuning the LIA phase adjustment for minimum output at an initial (dc) potential where no faradaic current flowed. This tuning procedure achieved two things: first it compensates for phase shifts in the instrument and it also accomplishes a rough "iR compensation." Because a dropping mercury electrode is used, the iR compensation is only correct at one point in the drop growth. Uncompensated iR losses were not serious because the correction of the quadrature signal for capacitive current was the greatest source of experimental error. The LIA was operated at a long time constant (10 seconds) and the scan rate was very slow (1-2 mv/sec) so that the dropping electrode noise could be eliminated without serious loss in resolution.

Results

Proof of a Chemical Oxidation of U(III) by NO_3^-.

It has been assumed in the previous work that the reduction of the nitrate ion was a purely chemical reaction of nitrate and U(III). The previous data could be explained, however, by an electrochemical reduction of the nitrate with the uranium species acting as an "electron bridge" to lower the overpotential of the nitrate ion. The controlled potential of Collat and Lingane was performed with nitrate in the solution and, hence, did not establish whether the reaction was chemical or electrochemical.

In order to establish that the reaction is a chemical reaction, a controlled potential electrolysis of uranium (IV) with no nitrate in solution was performed at -1.1 V versus SCE. When the current had dropped to a low value (it is not possible to get to zero current because of the oxidation of U(III) by hydrogen ion) the potentiostat was disconnected and a platinium electrode was inserted into the solution. The potential of the electrode was measured (versus the SCE) with a Corning model 12 pH meter. Due to the reaction of the U(III) with hydrogen ion, the potential was not steady and thus a potentiometric titration was not possible. However, when a potassium nitrate solution was added to the electrolysis solution, the green U(IV) color immediately appeared and the platinium electrode potential changed by several hundred millivolts. Because of the reaction of U(III) with hydrogen ion and the subsequent inability to electrolyze completely the U^{4+} to U^{3+} it was not possible to do a true potentiometric titration. However, the rapid change in electrode potential on addition of nitrate (from about -500 mv to -200 mv versus SCE) clearly indicates a chemical reaction between U(III) and NO_3^-.

When the electrochemically generated U(III) solution, to which excess nitrate ion had been added, was allowed to stand under nitrogen, the green U(IV) color of the solution turned dark brown over a period of about one-half hour. The dark colored solution was stable under nitrogen for several days, but faded in 1-2 hours in air. The color also faded when solvent was removed with suction from a water aspirator; however, if the solvent was boiled off, a black precipitate was formed.

The brown solution color changed to the yellow uranyl (U(VI)) color immediately upon addition of H_2O_2 to the solution. Addition of concentrated hydrochloric acid to the dark colored solution did not change the color so long as the solution was kept under nitrogen. It was not possible to remove the colored species from the aqueous phase with any of the common organic solvents used for this purpose (Et_2O, C_6H_6, $C_6H_5CH_3$, MIBK, $CHCl_3$). The colored species did not "precipitate" on addition of either tetraphenylborate, tetrabutylammonium, or hydroxide ions. The visible absorption spectrum of the colored aqueous phase showed approximately constant absorbance over the entire visible region. It was not possible to obtain a meaningful infrared spectrum of the colored species because it was not possible to remove it from the aqueous solution.

If an acidified solution of KNO_3 was added to the electrolytically generated U(III) solution and allowed to stand under nitrogen, the development of the brown color was greatly diminished, compared to the color developed when a neutral solution of KNO_3 was used.

The above data suggest the possible formation of some type of uranium - NO (or NO_2) compound analegous to the "brown ring test" ferrous - NO compound. An experiment to synthesize the proposed compound by direct chemical reaction was performed. A solution of uranium tetrachloride was electrolyzed, as before, but, after the potentiostat was disconnected, NO gas (along with nitrogen) was bubbled through the U(III) solution. The dark color did not form in this experiment nor in an analogous experiment in which NO_2 was bubbled through the electrolysis solution. No dark colored species was found to form when NO gas was passed through a uranium (IV) solution either. While these attempted chemical preparations did not succeed in proving the existence of the suspected compound, they did not disprove the possible dormation under the conditions of the reaction U^{3+} + excess NO_3^-.

Because of the greatly decreased color (essentially not formed) when an acidified KNO_3 solution was reacted with electrolytically generated U^{3+} and because the attempted chemical syntheses were failures, the dark color of the solution is considered as do to the formation of colloidal UO_2 which is formed when the pH is raised by the consumption of hydrogen ions in the reaction:

$$6U^{3+} + NO_3^- + 7H^+ \longrightarrow 6U^{4+} + NH_2OH + 2H_2O$$

The colloidal UO_2 is assumed to dissolve slowly in acid, but is rapidly oxidized to soluble uranyl by H_2O_2. It has not been possible to rule out completely a uranium NO or NO_2 complex, but in view of the lack of information on these compounds, except in liquid NO_2, the colloidal UO_2 formation seems reasonable (61).

The electrolysis experiments reported above confirm the chemical oxidation of U(III) to U(IV) by nitrate ion.

This chemical oxidation does not, however, rule out a possible electrochemical reaction also.

Ac Polarographic Behavior of U(VI) and U(IV), No nitrate.

An examination of the ac polarographic response of uranium solutions was undertaken for the reasons already stated. Only the second uranyl (U(VI)) wave (U(V) ⟶ U(IV) ⟶ U(III)) and the uranous (U(IV) ⟶ U(III)) waves were studied.

The second uranyl wave has been shown to be a composite wave of the irreversible U(V) → U(IV) and the reversible U(IV) ⇌ U(III) reductions (50). The ac polarographic wave obtained for this overall U(V) ⟶ U(III) reduction will be assumed to be due only to the reversible U(IV) ⇌ U(III) reduction (i.e. the U(V) → U(IV) reduction does not contribute to the ac current) for reasons given below.

The assumption that the observed ac wave is due only to the reversible U(IV) ⇌ U(III) couple is reasonable because the U(V) → U(IV) couple is irreversible (50).

Smith has shown that a plot of log $((I_p/I)^{\frac{1}{2}}-(I_p-I/I)^{\frac{1}{2}})$ versus potential (where I_p is the peak current and I is the current at a given potential) should be a straight line of slope (120/n) mv for a reversible reduction at 25°C (1). When an analysis of the rising current portion of the second uranyl wave was performed, this plot had a slope of 89 mv. A similar plot of the data from the reduction wave obtained from a solution containing U(IV) gave a straight line of 91 mv slope. These two results agree within experimental error (± 4mv) for these plots which are shown in Figures 13 and 14.

It has also been shown that the width of a reversible ac polarographic peak at half-height is (90/n) mv (1). The half-peak width found for the second uranyl ac wave is 95 mv, in reasonable agreement with an n value of 1.

The above data support the assignment of the second ac polarographic uranyl wave as due to the $U(IV) \rightleftharpoons U(III)$ (one electron) couple. The first electron transfer of the compound wave $(U(V(\rightarrow U(IV))$ is then seen as a complication of the $U(IV) \rightleftharpoons U(III)$ reduction. This is discussed further below.

That the plots of $\log((I_p/I)^{\frac{1}{2}}-(I_p-I/I)^{\frac{1}{2}})$ for the second uranyl wave and the U(IV) wave give the same non-integer value of n from the equation slope=120/n mv supports the assignment, but is a little disturbing. These non-integer values of n can be explained in two eays. First, if the reduction is not a one electron (single step) process, the slope of the line will vary with the difference in half-wave potentials of the individual steps as shown by Smith (62). Because the uranium (IV) reduction can not be more than one electron and because the slopes are the same in the two cases, the above explanation has been discounted. Second, the deviation from an integer value of n may reflect the non-perfectly reversible behavior of the system and/or the chemical reactions which precede and follow the electron transfer.

FIGURE 13

$\log((I_p/I)^{\frac{1}{2}}-(I_p-I/I)^{\frac{1}{2}})$ versus E for the second uranyl Wave, 0.25 m<u>M</u> UO_2^{2+}, 22 Hz

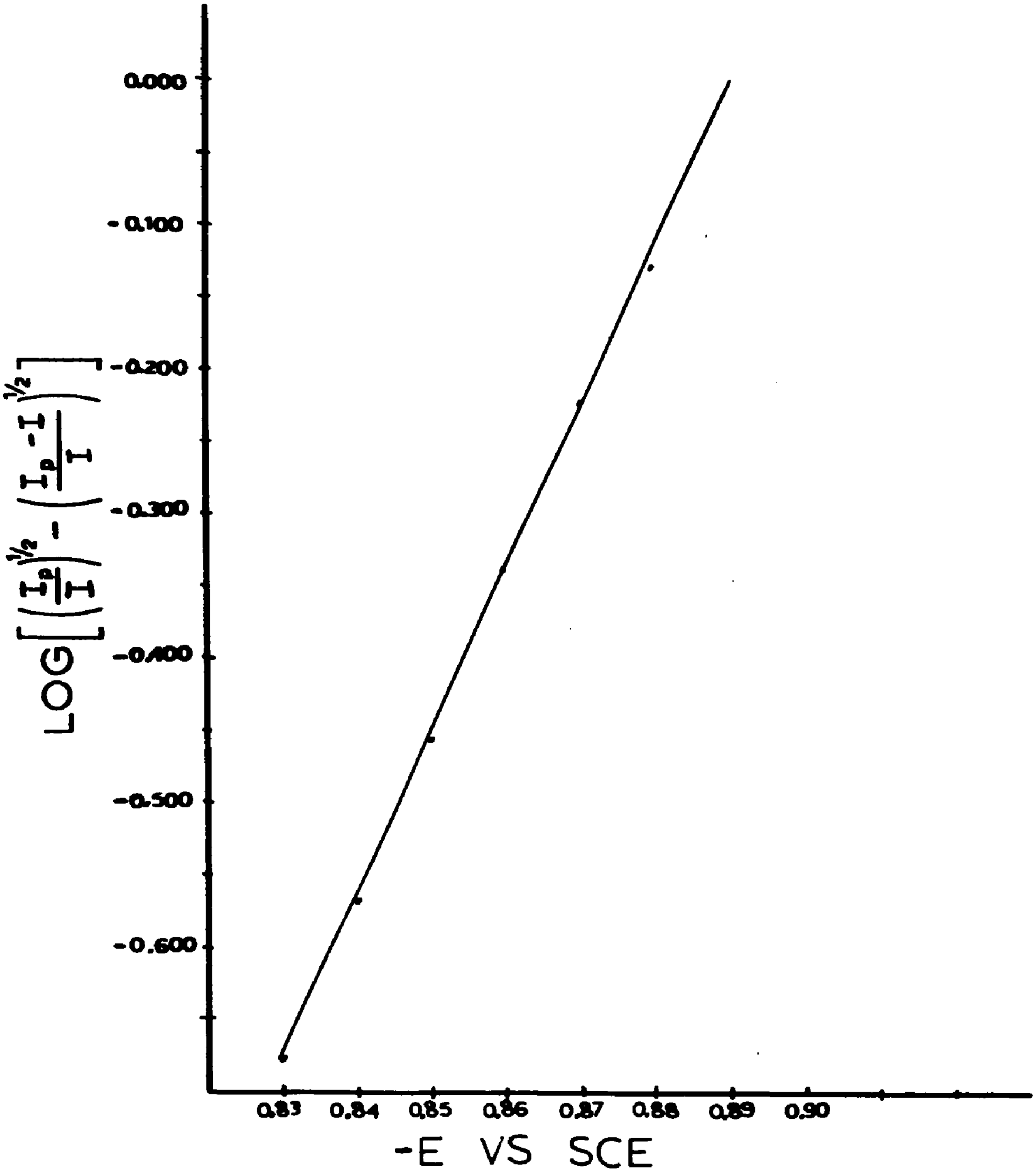
0.000
-0.100
-0.200
-0.300
-0.400
-0.500
-0.600
$\mathrm{LOG}\left[\left(\frac{I_p}{I}\right)^{1/2}-\left(\frac{I_p-I}{I}\right)^{1/2}\right]$
0.83
0.84
0.85
0.86
0.87
0.88
0.89
0.90
-E VS SCE

FIGURE 14

Log$((I_p/I)^{\frac{1}{2}}-(I_p-I/I)^{\frac{1}{2}})$ versus E for the Uranous Wave

0.2 m*M* U^{4+}, 22 Hz, $\xi=(I_p/I)^{\frac{1}{2}}-(I_p-I/I)^{\frac{1}{2}}$

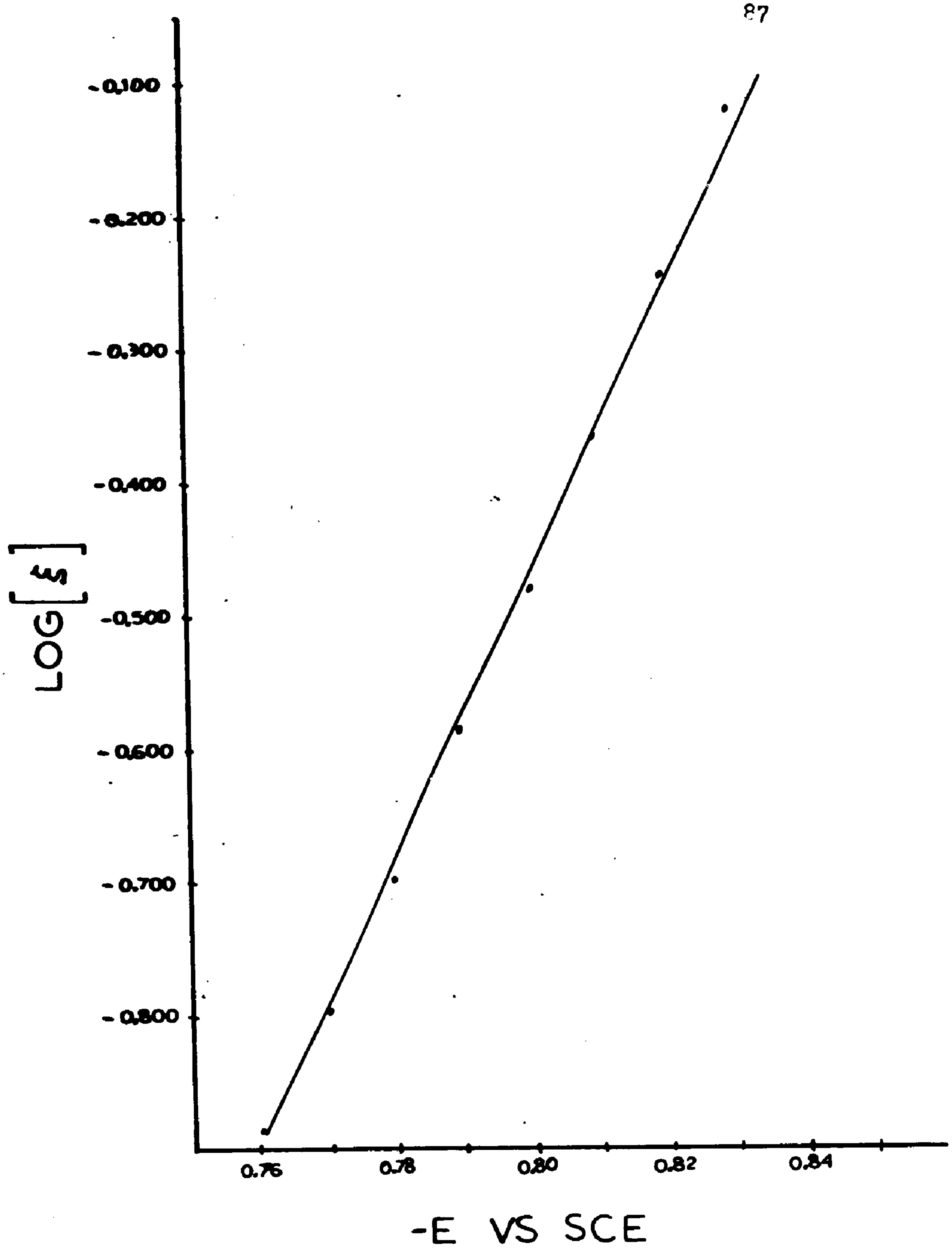
- 0.100
- 0.200
- 0.300
- 0.400
- 0.500
- 0.600
- 0.700
- 0.800
LOG [ξ]
0.76
0.78
0.80
0.82
0.84
-E VS SCE

Ac polarographic theory predicts that the cotangent of the phase angle obtained from a quasi-reversible reduction should be directly proportional to the square root of the applied frequency (1). The slope of the straight line obtained when cot is plotted against the square root of frequency will have a slope of

$$2^{\frac{1}{2}}/k_s(\exp(-\alpha j)+\exp(\beta j))/D^{\frac{1}{2}} \qquad (1)$$

where k_s is the electron transfer rate constant, α is the transfer coefficient, $\beta = 1-\alpha$, D is the diffusion coefficient and j is $(nF/RT)(E-E_{\frac{1}{2}})$. If the phase angle is measured at the half-wave potential, the equation of the slope of the line can be written as

$$\text{slope} = D^{\frac{1}{2}}/2^{\frac{1}{2}}k_s \qquad (2)$$

The variation of the cotangent of the phase angle of the second uranyl wave with the square root of frequency is shown in Figure 15. The slope of the straight line obtained for the uncomplicated (by nitrate reaction) uranyl reduction is 0.02 $\sec^{-\frac{1}{2}}$. Using equation (2) above and assuming a value of the diffusion constant of $1X\ 10^{-5}\text{cm}^2/\text{sec}$ a value of 0.1 cm/sec is calculated for k_s. This value compares favorably with the value of 0.34 cm/sec found for the electron transfer rate constant of the "reversible" cadmium ion reduction (25). Because of this high value of k_s and the linear increase in peak current with the square root of frequency up to 200 Hz (see figure 24), the second ac polarographic uranyl wave is established as due only to the reversible one electron reduction of U(IV).

It is to be expected that the variation of cotϕ of the uranium(IV) reduction with the square root of frequency (no nitrate in solution) will be the same as that observed

FIGURE 15

Cotangent of Phase Angle versus Frequency,
Second Uranyl Wave

• = No Nitrate, 0.25 m$\underline{M}$ U(VI)
△ = 0.085 m$\underline{M}$ NO_3^-, 0.145 m$\underline{M}$ U(VI)
◬ = 0.196 m$\underline{M}$ NO_3^-, 0.145 m$\underline{M}$ U(VI)
* = 0.394 m$\underline{M}$ NO_3^-, 0.145 m$\underline{M}$ U(VI)
+ = 0.34 m$\underline{M}$ NO_3^-, 0.25 m$\underline{M}$ U(VI)
▫ = 1.09 m$\underline{M}$ NO_3^-, 0.25 m$\underline{M}$ U(VI)
○ = 0.025 m$\underline{M}$ NO_3^-, 0.25 m$\underline{M}$ U(VI)
● = 0.064 m$\underline{M}$ NO_3^-, 0.25 m$\underline{M}$ U(VI)
⊙ = 0.113 m$\underline{M}$ NO_3^-, 0.25 m$\underline{M}$ U(VI)
⊕ = 0.258 m$\underline{M}$ NO_3^-, 0.25 m$\underline{M}$ U(VI)

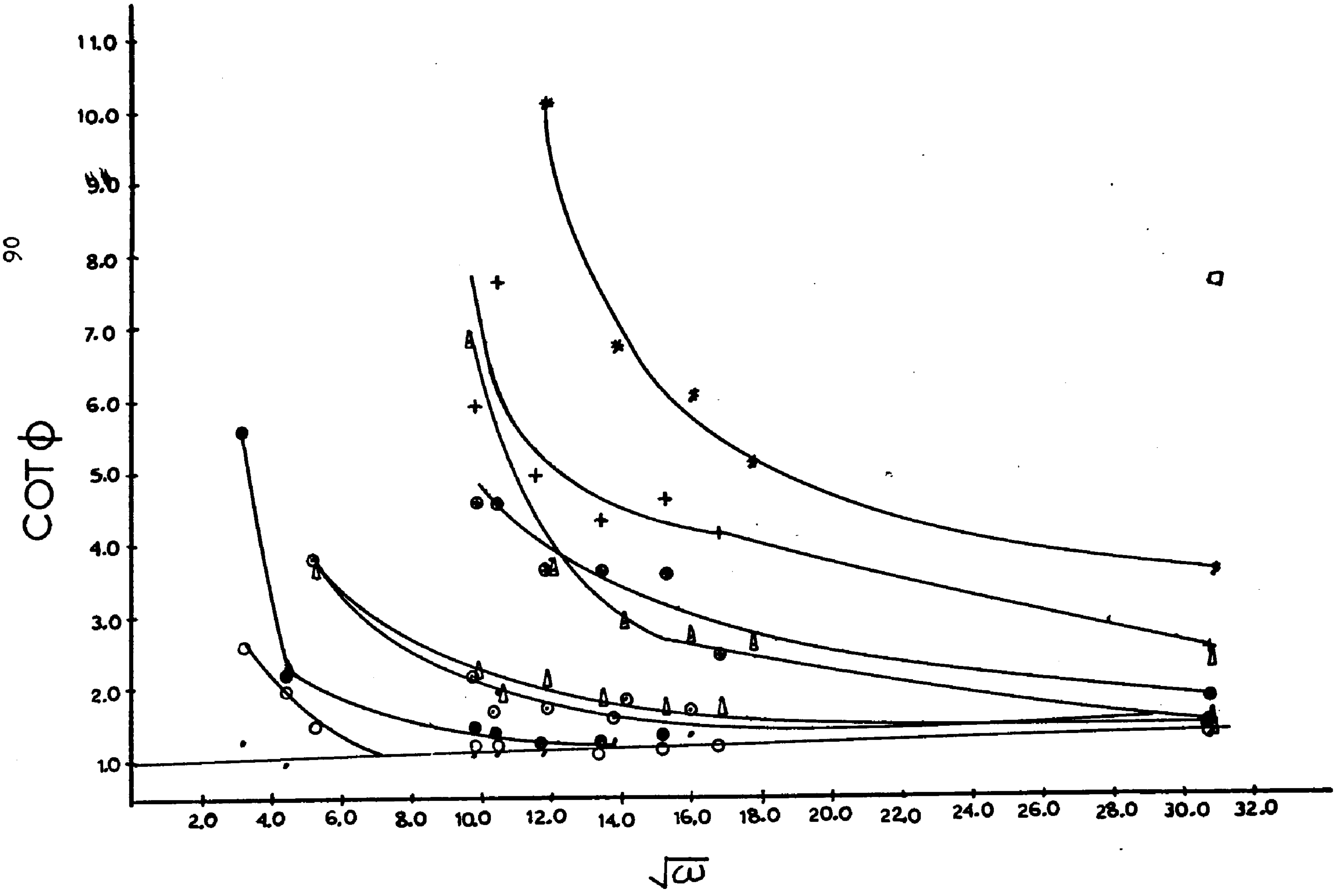

COT Φ
11.0
10.0
9.0
8.0
7.0
6.0
5.0
4.0
3.0
2.0
1.0
2.0
4.0
6.0
8.0
10.0
12.0
14.0
16.0
18.0
20.0
22.0
24.0
26.0
28.0
30.0
32.0
√ω

for the second uranyl wave. These data are reported in Figure 16. Unfortunately, the experimental scatter of the U(IV) data is so bad that no straight line can be drawn. The reason for this high degree of scatter in the U(IV) data is the complicated aqueous chemistry of U(IV) around pH 2. It was previously noted that the reversibility of U(IV) solutions depend upon the age of the solutions (50). This observation was attributed to a slow hydrolysis of uranium (IV) to some unknown species (probably UOH^{3+} as later shown by Kraus (51)).

Theoretical ac polarographic studies predict that a reversible reduction will give ac currents with phase angles of 45° ($\cot\phi = 1$) at all potentials (1). A plot of cot versus applied potential for the uranium (IV) reduction (fresh U(IV) solution) is shown in Figure 17. As seen from this figure, the $U(IV) \rightleftharpoons U(III)$ couple behaves as a reversible couple ($\cot\phi = 1$ at all potentials) up to a little beyond the peak ($E_p = -0.825$), past the peak the phase angle becomes greater than 45° ($\cot\phi < 1$). A phase angle greater than 45° is characteristic of adsorption of the electroactive species (1). There is no other way, to my knowledge, that a phase angle greater than 45° can be obtained. Because the adsorption does not appear until potentials after the peak, a U(III) species is probably responsible.

The relationship between the applied potential and the cotangent of the phase angle for the second uranyl wave is shown in Figure 18. The variation of the phase angle is seen to be considerably different from the behavior of the

FIGURE 16

Cotangent of Phase Angle versus Applied Frequency,

Uranous Wave

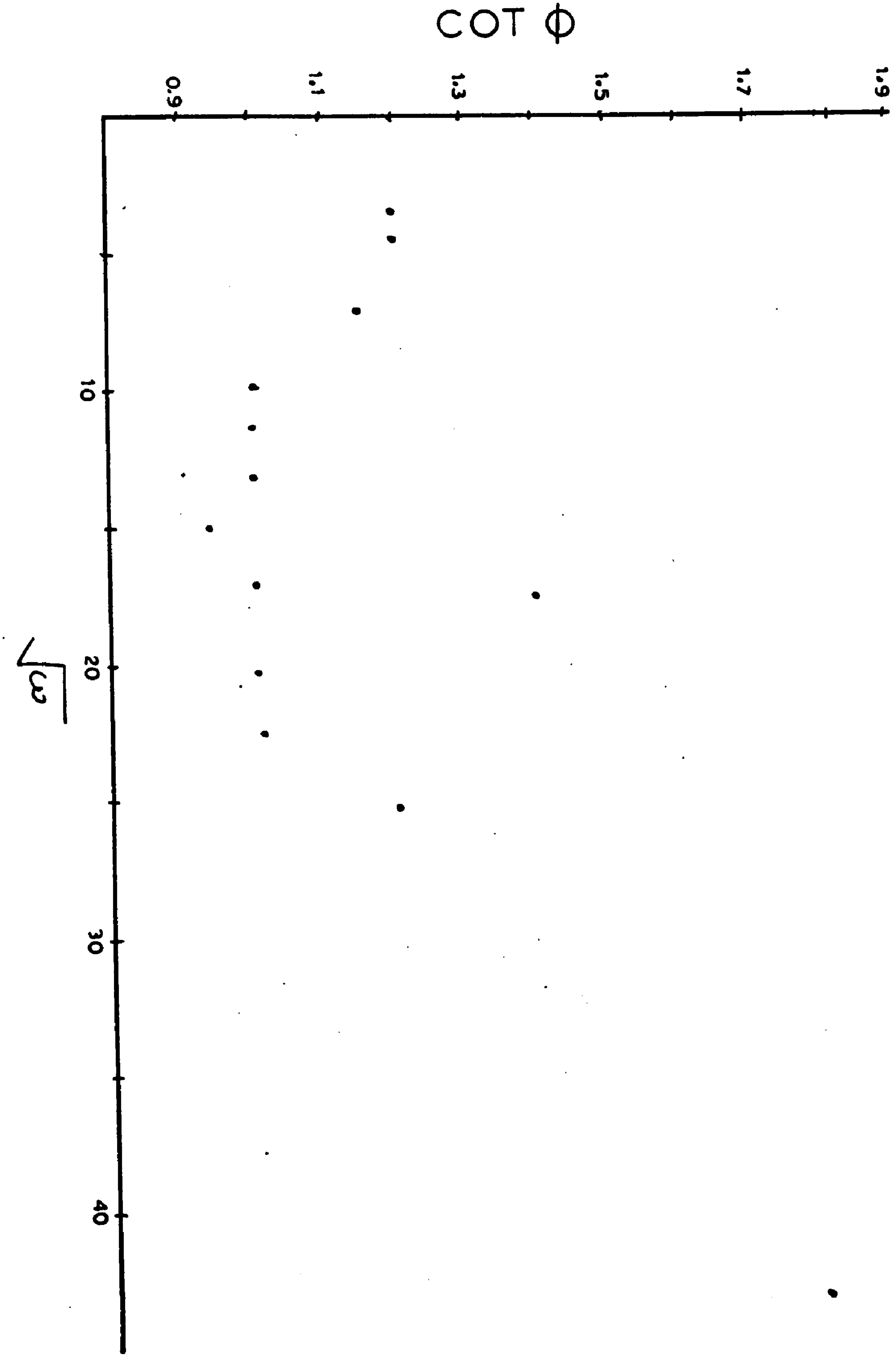
COT Φ
0.9
1.1
1.3
1.5
1.7
1.9
10
20
30
40
$\sqrt{\omega}$

FIGURE 17

Cotangent of Phase Angle versus Applied Potential,
Uranous Reduction

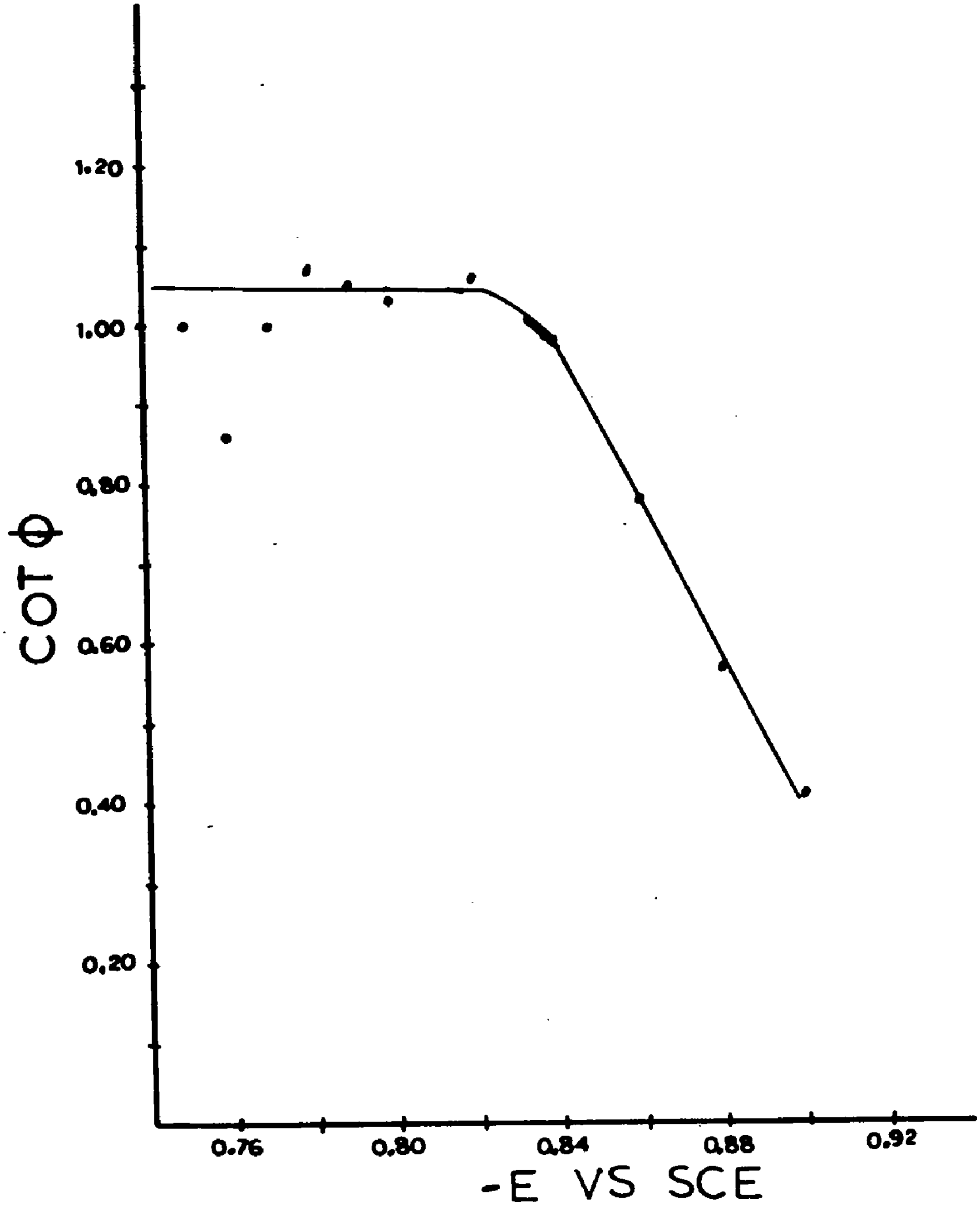
1.20
1.00
0.80
0.60
0.40
0.20
COT Φ
0.76
0.80
0.84
0.88
0.92
-E VS SCE

FIGURE 18

Cotangent of Phase Angle versus Applied Potential, Second Uranyl Reduction, 0.25 m<u>M</u> U(VI)

● = 22 Hz

○ = 28 Hz

⊙ = 300 Hz

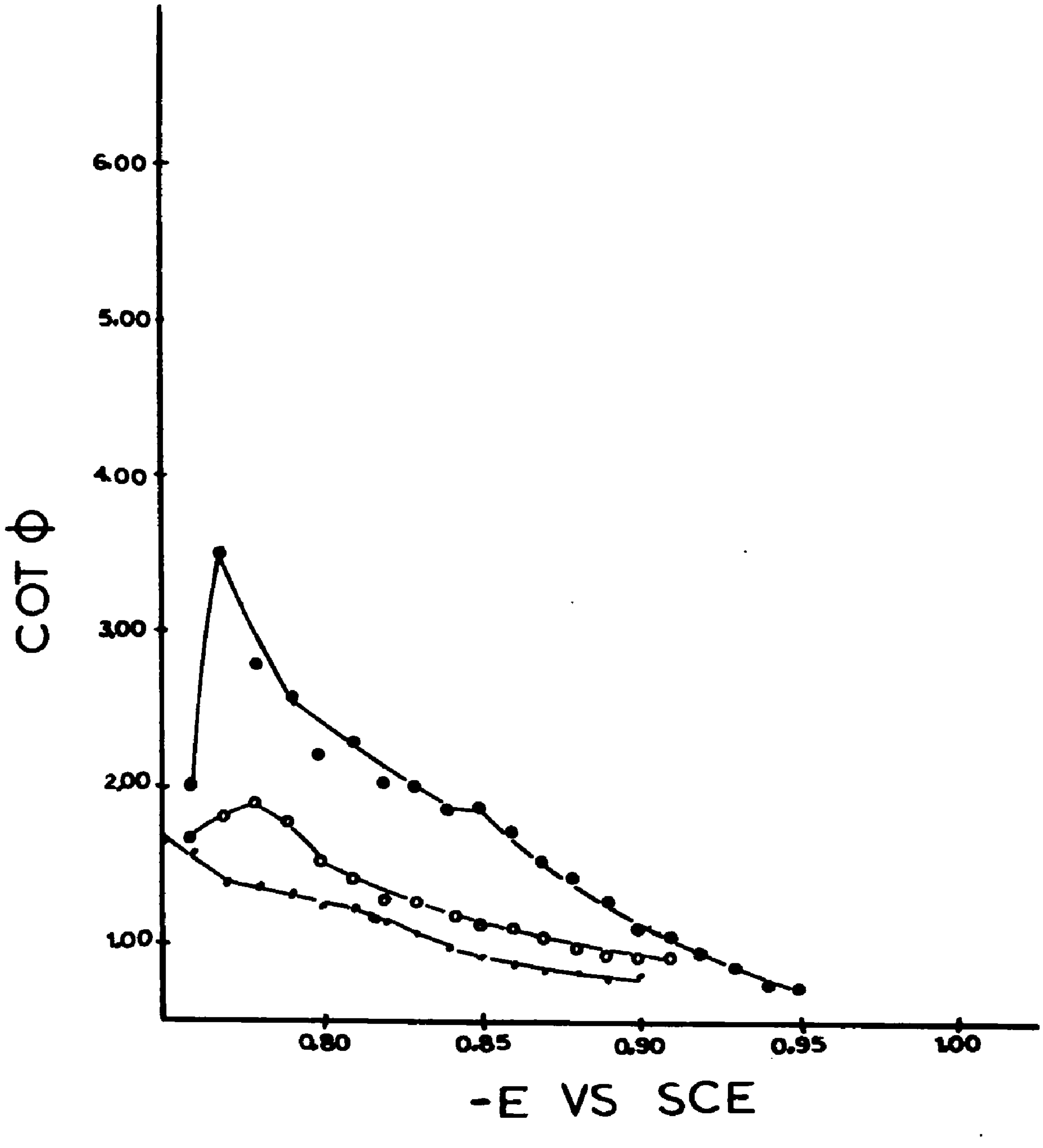
6.00
5.00
4.00
3.00
2.00
1.00
COT Φ
0.80
0.85
0.90
0.95
1.00
-E VS SCE

$U(IV) \rightleftharpoons U(III)$ couple. The adsorption noted in the U(IV) reduction does also appear in the uranyl reduction at high potentials but, before the peak, the wave does not have the characteristic reversible phase angle. If we assume that the ac wave seen for the second uranyl reduction is due to the U(IV)   U(III) reaction, the phase angle behavior is similar to the behavior expected of a reversible reduction preceded by a chemical reaction (1). If this is true, the mechanism for the reduction of U(V) to U(III) is then

$$UO_2^+ + e^- \longrightarrow UO_2 \qquad (8)$$

$$UO_2 + 4H^+ \longrightarrow U^{4+} + 2H_2O \qquad (9)$$

$$U^{4+} + e^- \longrightarrow U^{3+} \qquad (10)$$

and not

$$UO_2^+ + 2H^+ \longrightarrow UO^{3+} + H_2O \qquad (11)$$

$$UO^{3+} + 2H^+ + e^- \longrightarrow U^{4+} + H_2O \qquad (12)$$

$$U^{4+} + e^- \longrightarrow U^{3+} \qquad (13)$$

A recent more rigorous treatment of the ac polarographic response of a Nernstian system with a preceding coupled chemical reaction, such as shown below, indicates that phase angle functions such as those shown in Figure 18 are expected in this case (following chemical reactions give mirror images of these functions) if the chemical reaction rate constants and/or the equilibrium constant are small (8).

$$Y \underset{k_2}{\overset{k_1}{\rightleftharpoons}} Ox + ne^- \longrightarrow Red \qquad Keq = k_1/k_2$$

Because the controlled potential electrolysis experiments indicated the formation of UO_2 which apparently reacts slowly with hydrogen ion, it seems that the mechanism postulated above for the reaction of U(V) to U(III) (reactions

8 - 10) is reasonable. Theoretically it should be possible to determine the rate of reaction of UO_2 with hydrogen ion from the present ac polarographic data if the equilibrium constant for the reaction were known. Because the equilibrium constant is not known and the task of evaluation of the rate with a known equilibrium constant is a complicated job, no attempt was made to evaluate the rate of reaction of UO_2 with hydrogen ion. These data do establish, however, with little uncertainty that the electron transfer step occurs before the U(V) is deoxygenated.

The effect of the reaction of U(III) with nitrate ion on the ac polarographic behavior of U(VI) and U(IV).

The effect of catalytic regeneration of starting material upon the ac polarographic response has been considered theoretically (1, 12). The most striking feature of the theoretical predictions is the unique cotϕ versus square root of applied frequency dependence. A reproduction of the theoretical curves derived assuming a simple catalytic mechanism

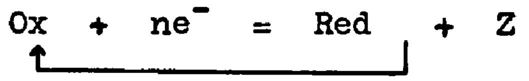

$$Ox + ne^- = Red + Z$$

is shown in Figure 19.

It has been assumed that the catalytic oxidation of U(III) involves a simple catalytic reaction:

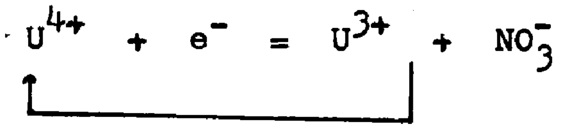

$$U^{4+} + e^- = U^{3+} + NO_3^-$$

and in particular that the preceding reduction of U(V) to

FIGURE 19

Theoretical Cotangent of Phase Angle versus Frequency,[a] Simple Catalytic Mechanism

[a] From Reference (12)

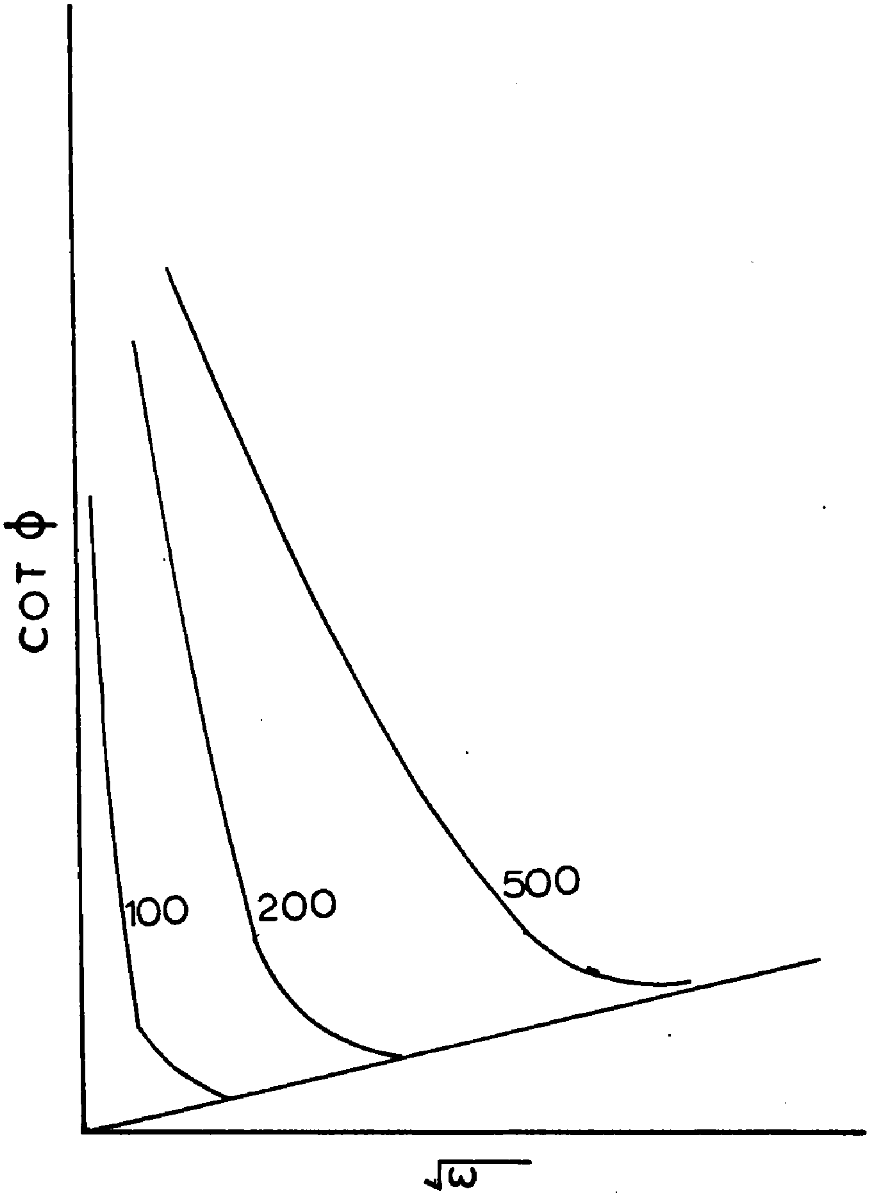
COT φ
100
200
500
√ω

U(IV) does not affect the catalytic response of the system. The effect of nitrate upon the phase angle versus square root of frequency relationship of the second uranyl wave is shown in Figure 15. The qualitative agreement between theory and experiment is evident. A similar ac polarographic study of the Ti (III) - ClO_3^- reaction also gave excellent agreement between theory and experiment (63). This agreement shows that either the approximation of a simple catalytic mechanism is valid or that the variation of cotϕ with frequency is not very sensitive to slight deviations from the theoretically assumed mechanism.

Theoretical treatments of the catalytic mechanism predict that the phase angle as a function of applied potential should have the same symmetry as that function in the absence of a catalytic reaction (1,12). The phase angle versus applied potential curve of the second uranyl wave in the presence of nitrate ion is shown in Figure 20. Comparison of Figure 20 and Figure 18 shows that the catalytic reaction affects not only the magnitude of the phase angle, but also the symmetry of the cotϕ versus applied potential curve, contrary to theoretical predictions. The disagreement between theory and practice is a manifestation of the difference between the true mechanism and the simple catalytic mechanism. No hint of this disagreement was obtained from the cotϕ versus frequency plot, indicating that the cotϕ versus potential criterion is probably more sensitive to slight changes in mechanism than is the cotϕ versus frequency. Smith has studied some more complicated catalytic type mechanisms such

FIGURE 20

Cotangent of Phase Angle versus Applied Potential,

Second Uranyl Wave with Nitrate,

0.25 mM U(VI), 0.34 mM NO_3^-

○ = 28 Hz

⊙ = 44 Hz

● = 150 Hz

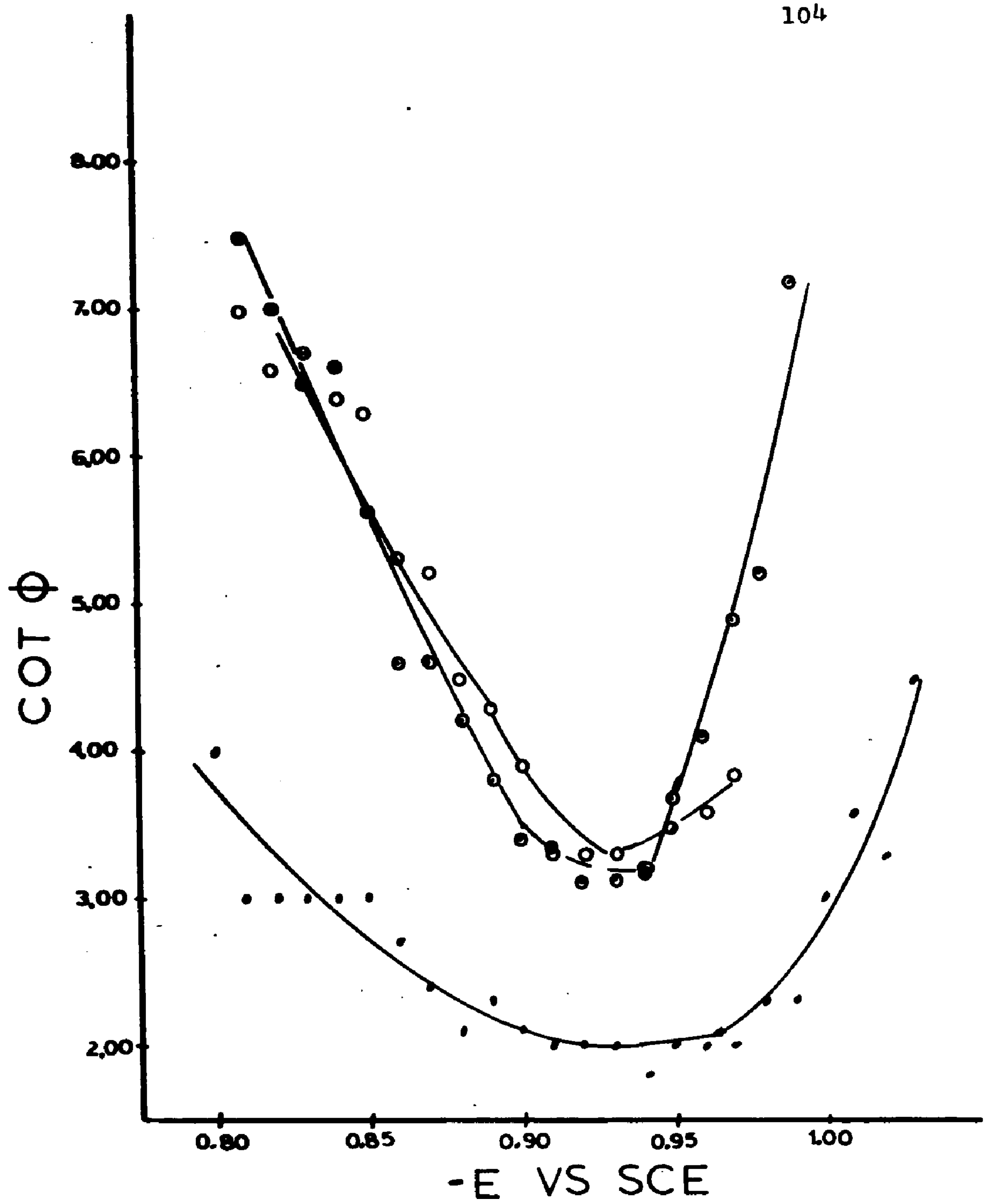
8.00
7.00
6.00
5.00
4.00
3.00
2.00
COT Φ
0.80
0.85
0.90
0.95
1.00
-E VS SCE

as those shown below (10,63):

$$\begin{tikzcd} Y \arrow[r, shift left, "k_1"] & Ox \arrow[l, shift left, "k_2"] & + \; ne^- \; = & Red \arrow[ll, bend left] & + \; Z \end{tikzcd}$$

$$\begin{tikzcd} Y \arrow[r, shift left, "k_1"] & Ox \arrow[l, shift left, "k_2"] & + \; ne^- \; = & Red \arrow[lll, bend left] & + \; Z \end{tikzcd}$$

and has pointed out that systems which show evidence for more complicated mechanisms from the potential dependence of $\cot\phi$ may not show anything unusual in the $\cot\phi$ - frequency behavior. This appears to be the case in this instance (i.e. a more complicated mechanism is apparent from the $\cot\phi$ versus potential data, but a simple catalytic mechanism is suggested from the $\cot\phi$ versus frequency results). Further examination of the $\cot\phi$ versus potential curve for the second uranyl wave in the presence of nitrate shows that the phase angles greater than 45° are no longer present which is consistent with the adsorption of some U(III) species because it is to be expected that the adsorption would decrease as the catalytic reaction rate increases. The most unusual feature of this function is the minimization of the cotangent of the phase angle around the peak of the ac wave. To my knowledge, no system thus far treated theoretically predicts that the cotangent of the phase angle should reach a minimum as shown in Figure 20. The fact that no theoretical treatment has thus far predicted the above behavior is not surprising because the uranium system presents a problem which is much more complicated than the previously considered mechanistic schemes (1,2,3,4,5,8,9,10, 11, 12, 13).

The phase angle versus applied potential function for the uranium (IV) reduction (fresh solution) with nitrate added is shown in Figure 21. It is apparent from the figure that the adsorption of U(III) is no longer present (just as it was no longer present when nitrate was added to the uranyl solution above). More important than the disappearence of the U(III) adsorption is the observation that the symmetry of the wave with nitrate (or lack of symmetry) is more nearly the same as the symmetry of the curve without nitrate in solution (compare Figures 21 and 17). It would appear that when U(IV) is reduced in the presence of nitrate the reaction is more nearly approximated by the simple catalytic mechanism than is the reduction of U(VI) in the presence of nitrate. This conclusion is not surprising in view of the fact that using uranium (IV) eliminates several preceding chemical and electrochemical reactions.

The rate of reaction of U(III) with nitrate ion and the mechanism of the reaction

From the measurement of the phase angle (cot ϕ) it is possible to determine the rate of the chemical reaction if the mechanism is known (1,2,3,4,5,8,9,10,11,12,13). The equations derived by Smith which relate the measured phase angle to the rate of chemical reaction are shown below for the simple catalytic case (12, 63):

$$\cot \phi = \frac{\left(\frac{2\omega}{\lambda}\right)^{\frac{1}{2}} + \left((1+g^2)^{\frac{1}{2}} + g/1 + g^2\right)^{\frac{1}{2}}}{\left((1+g^2)^{\frac{1}{2}} - g/1 + g^2\right)^{\frac{1}{2}}} \quad . \qquad (1)$$

FIGURE 21

Cotangent of Phase Angle versus Applied Potential, Uranous Reduction with Nitrate

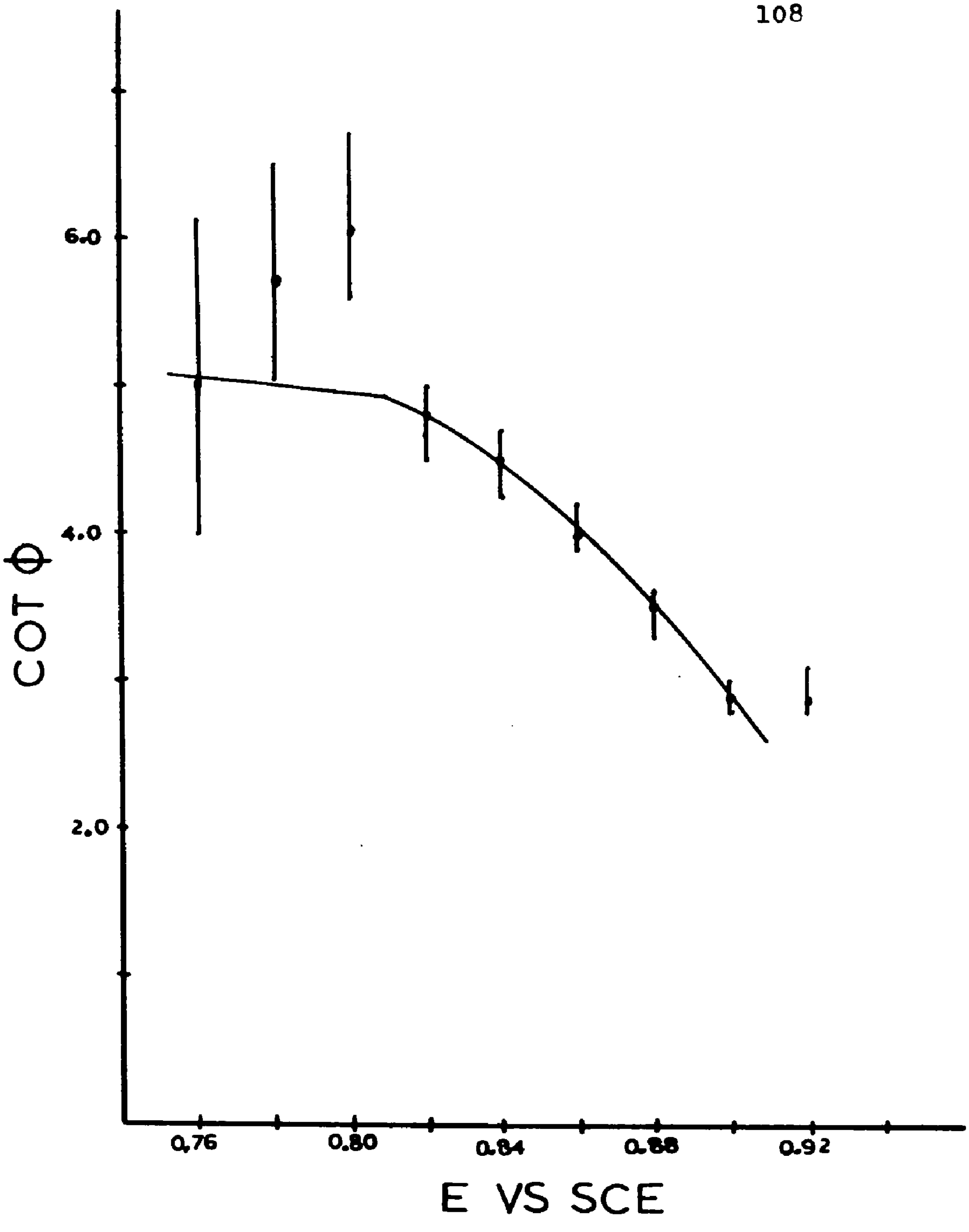
6.0
4.0
2.0
COT Φ
0.76
0.80
0.84
0.88
0.92
E VS SCE

$$\cot\phi_{max} = \frac{\dfrac{(2\,\omega\,D)^{\frac{1}{2}}}{k_s f((\alpha/\beta)^{-\alpha} + (\alpha/\beta)^{\beta})} + ((1+g^2)^{\frac{1}{2}} + g/1+g^2)^{\frac{1}{2}}}{((1 + g^2)^{\frac{1}{2}} - g/\ 1+g^2)^{\frac{1}{2}}} \qquad (2)$$

Equation (2) was used for the calculation of the rate constants in this work using $\cot\phi_{max}$ as the phase angle at the peak of the ac wave. The equation was simplified by assuming that $\alpha = 0.5$ (32) and that the first term does not contribute significantly to the phase angle (this is valid because k_s is relatively large and $(2\omega D)^{\frac{1}{2}}$ is rather small). The simplified equation used in this work is then:

$$\cot\phi_{max} = \frac{((1+g^2)^{\frac{1}{2}}+g/1 + g^2)^{\frac{1}{2}}}{((1+g^2)^{\frac{1}{2}} - g/1 + g^2)^{\frac{1}{2}}} \qquad (3)$$

The working curve shown in Figure 22 was constructed from equation (3). This working curve shows the phase angle as a function of the parameter g $(k_c/\omega$, where k_c is the rate of the catalytic reaction and is the circular frequency of measurement). From a measured phase angle at a known frequency, the rate of the reaction could be determined by finding that value of $\cot\phi$ on the ordinate and the corresponding value of g on the abscissa and hence the value of k_c. This method is usable only for those rates and frequencies where the phase angle is large enough to be measured accurately. This simplified equation gave reasonable agreement with the rates determined by Koryta using a dc polarographic technique (58). Because the extrapolation method

FIGURE 22

Working Curve for Determination of Catalytic Reaction Rates from Phase Angle Data

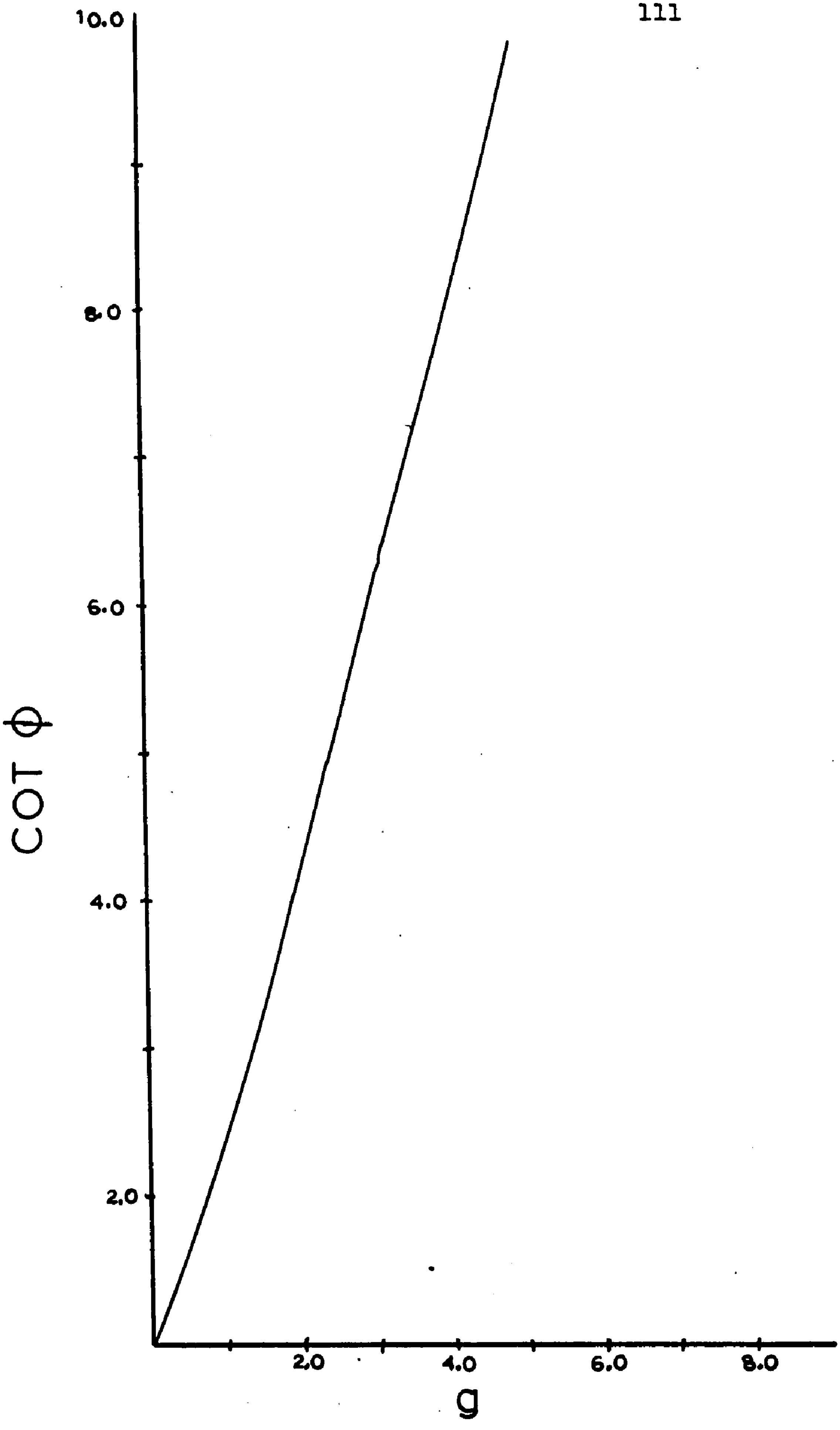
10.0
8.0
6.0
4.0
2.0
COT Φ
2.0
4.0
6.0
8.0
g

is used to determine the quadrature signals in evaluating the phase angles, the range of rates measurable by this method is limited. The errors and noise level involved with this instrument limited the usable phase angles to about $\cot^{-1} 10$. A different method of evaluating the rate of reaction was used in those cases where the phase angle was close to 0°. This other method will be discussed below. Because values of the reaction rates obtained from the phase angle measurements are in good agreement with those reported in previous work, the simplyfing assumptions used to develop the working curve used are reasonable (i.e. a simple catalytic mechanism, $\cot\phi$ at peak = $\cot\phi_{max}$, first term in equation (2) does not contribute a measurable amount to the phase angle) (58).

The rate of reaction as a function of nitrate concentration determined by this method from the data of the second uranyl wave is shown in Figure 23. The first order dependence of the rate on nitrate concentration agrees well with the previous work of Koryta (58); however, due to the scatter of the experimental points, the unity reaction order with respect to nitrate is not unambiguous. Assuming that the reaction is unity order in nitrate the value $k_c^o = k_c/(NO_3^-)$ is found to be 1.3×10^6 sec^{-1} M $liter^{-1}$ (at 0.145 mM uranium (VI) concentration) which is in good agreement with the value of 1.6×10^6 sec^{-1} M $liter^{-1}$ found by Koryta (58). Because measurements of small phase angles are doomed to high experimental errors by virtue of the large capacitive correction necessary and in view of the many approximations

FIGURE 23

Rate of Reaction of Nitrate ion with U(III) Determined from Phase Angle Data

○ = 0.145 m<u>M</u> U(VI)

● = 0.25 m<u>M</u> U(VI)

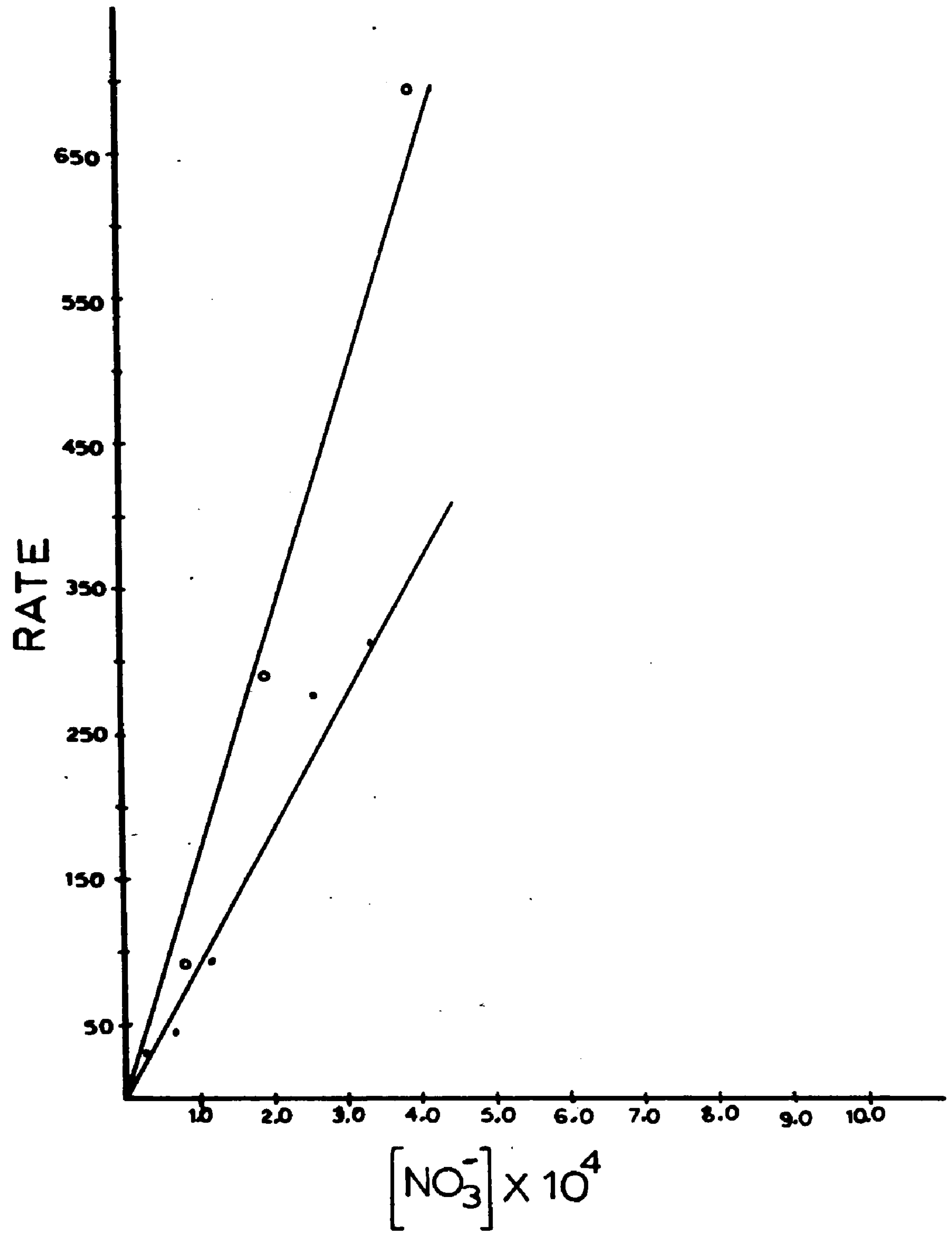
RATE
650
550
450
350
250
150
50
1.0
2.0
3.0
4.0
5.0
6.0
7.0
8.0
9.0
10.0
$[NO_3^-] \times 10^4$

made, too much importance should not be placed on the specific values of the rate constants, but the interpretation should be based upon the change in rate of reaction with change in concentration of reactant. The above is simply stating that an underlying assumption in this work is that errors will be more or less the same so that trends will be accurate even though specific rates may be in error. It appears from this rate study at two different uranium concentrations that the rate of reaction increases as the concentration of uranium decreases. This will be discussed in more detail below.

Because the reaction is so fast at reasonable nitrate concentrations, the phase angle soon becomes too small to measure with any tolerably small experimental error at usable frequencies (i.e. below those frequencies where charge transfer kinetics begin to become important). For the above reason a new method, based upon a recent paper by Smith was devised (64). This method does not involve the measurment of phase angles, but rather current levels (very analogous to the dc method previously). Therefore it does not have the experimental error limitation of the phase angle evaluations. If one considers the effect of a catalytic reaction upon the alternating current which flows in an ac polarographic experiment, it can be shown that, in the limit where the rate of the catalytic reaction is much faster than the applied frequency (g very large, $\cot\phi$ very large), the current is given by (64):

$$I(\omega t) = \frac{n^2F^2AC_o^* \, (k_cD_o)^{\frac{1}{2}} \, \Delta E}{4RT \cosh^2(j/2)} \sin(\omega t) \qquad (4)$$

where $I(\omega t)$ is the ac current, n is the number of electrons involved, F is the Faraday, A the area of the electrode, C_o^* the bulk concentration of Ox, k_c the rate of the catalytic reaction, D_o the diffusion constant of Ox, ΔE the peak-to-peak magnitude of the applied ac voltage, R the gas constant, T the absolute temperature, j is a function of the difference between the potential of measurment and the half-wave potential, ω is the circular frequency ($2\pi f$) and t is time. Because the measurment which is performed is the RMS value of the ac current, the sine term becomes a constant (0.707). Comparing equation (4) with the expression derived for a simple reversible ac polarographic wave (1,64):

$$I_{rev} = \frac{n^2F^2AC_o^* \, (\omega D_o)^{\frac{1}{2}} \, \Delta E}{4RT \cosh^2(j/2)} \sin(\omega t) \qquad (5)$$

it becomes apparent that the only change in current magnitude is that in the limiting case the current is independent of frequency and is proportional to the rate of reaction while the magnitude of the uncomplicated charge transfer current is the diffusion controlled value (i.e. $I_{rev} \propto (\omega)^{\frac{1}{2}}$). Dividing equation (5) by equation (4) yields:

$$I_{rev}/I(\omega t) = (\omega/k_c)^{\frac{1}{2}}$$

and hence

$$k_c = \omega/(I_{rev}/I(\omega t))^2$$

This means that the rate of the catalytic reaction can be evaluated by measuring the current (peak current is used) without nitrate present and then the current, at the same frequency, with nitrate present and taking the ration of the two. It is necessary, of course, that the phase angle be measured also to be sure that it is close to 0° to confirm the validity of the limiting law approximation.

It is necessary for the terms in $\cosh^2$ to cancel if the above equations are to be valid for the determination of rate constants. Cancelling the $\cosh^2$ terms assumes that the peak in the presence of the nitrate occurs as far from the reversible half-wave potential as the peak without nitrate does. The peak potential shifts with added nitrate, but so does the half-wave potential so that this assumption states that these two potentials shift by the same amount. If this assumption is not valid, an error of 100 mv will introduce an error of about a factor of 2 in the measured rate constant. An error of 100 mv is larger than any possible error in this work. Even if the assumption is not valid, the error introduced will again be a constant one so that the trends will still be valid.

The variation of peak current with frequency as a function of nitrate concentration is shown in Figure 24. At high nitrate concentration and low frequency the peak current is found to obey the limiting law given above, equation (4): the current is independent of frequency and greater than the diffusion controlled case (because the limiting law is valid when $k_c \gg \omega$, the theory predicts that the

FIGURE 24

Variation of Peak Current with Frequency at Various Nitrate Concentrations, Second Uranyl Wave

● = No Nitrate, 0.25m*M* U(VI)

○ = 0.064 m*M* NO_3^-, 0.25 m*M* U(VI)

(= 0.34 m*M* NO_3^-, 0.25 m*M* U(VI)

+ = 0.113 m*M* NO_3^-, 0.25 m*M* U(VI)

⊙ = 0.258 m*M* NO_3^-, 0.25 m*M* U(VI)

⊗ = 1.09 m*M* NO_3^-, 0.25 m*M* U(VI)

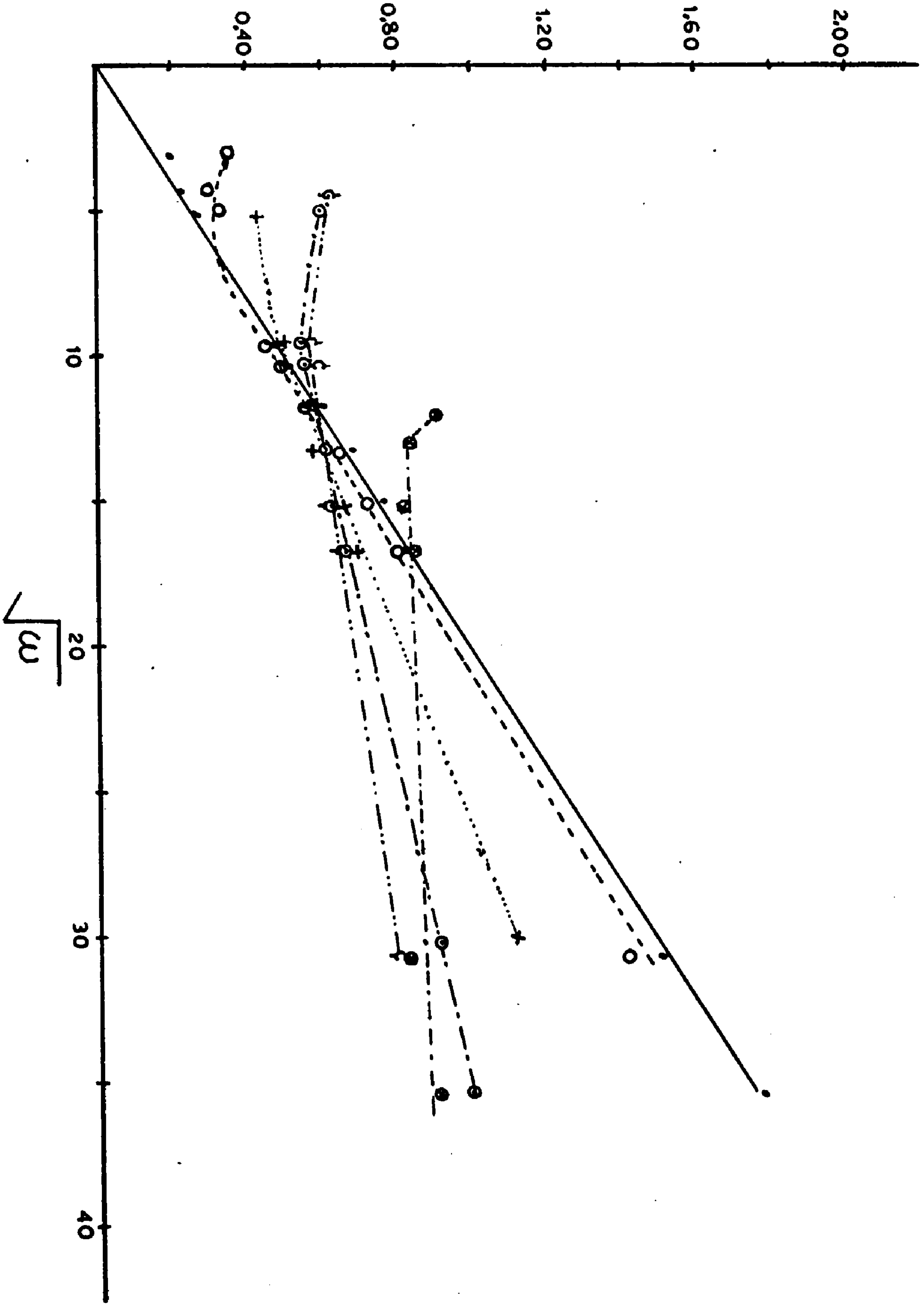
I_p
0.40
0.80
1.20
1.60
2.00
$\sqrt{\omega}$
10
20
30
40

current will be greater than the diffusion limited case). At higher frequencies, however, where the limiting approximation is no longer valid, some rather unexpected behavior is noted. The current is found to decrease with increasing frequency over a narrow region and then to increase (more or less linearly) with the square root of frequency, but at a decreased slope from the diffusion controlled case. At very high nitrate concentrations the peak current is almost independent of frequency, but remains less than the diffusion controlled current.

The theory of the simple catalytic mechanism predicts that the ac current will be described by the equation shown below (the limiting equation is obtained from this by letting $k_c \gg \omega$)(64):

$$I(\omega t) = \frac{n^2F^2AC_o^* (\omega D_o)^{\frac{1}{2}} \Delta E}{4RT \cosh^2(j/2)} (2/T^2 + U^2)\sin(\omega t + \phi) \quad (6)$$

where $T = ((1 + g^2)^{\frac{1}{2}} + g/ 1 + g^2)^{\frac{1}{2}}$

and $U = ((1 + g^2)^{\frac{1}{2}} - g/ 1 + g^2)^{\frac{1}{2}}$ $\qquad g = k_c/\omega$

Introducing the equation for the diffusion controlled wave (equation (5)) and remembering that the current measured is the RMS value (the sine terms become constants) yields equation (7) below

$$I(\omega t) = I_{rev} (2/T^2 + U^2)^{\frac{1}{2}} \quad (7)$$

which by algabraic manipulation can be rearranged to give

$$I(\omega t) = I_{rev}(1 + g^2)^{\frac{1}{4}} \quad (8)$$

Because $(1 + g^2)$ can not be less than unity without introducing imaginary numbers, the catalytic current can not be less than the diffusion controlled current. Hence, the theory of the simple catalytic mechanism fails to predict the observed current behavior in this case; in fact it predicts the oposite effect.

The explanation of the unusual current variations noted above lies in recalling that at high frequencies (small g) the effect of the catalytic reaction will be small because the current reversal takes place before the catalytic reaction can proceed to any great extent. If the data at high nitrate concentration and at high frequency are treated as if the catalytic reaction is not taking place, it can be seen that this behavior predicts either a non-reversible electron transfer step or a coupled chemical reaction.

If there is a preceding chemical reaction involving the formation of a nitrate complex (es) which is not electroactive, the current level would decrease at high frequencies where the potential varies faster than the dissociation of the complex to the electroactive form. At low frequencies the effect would be negligible because the dissociation reaction would be able to keep up with the rate of potential changes. Uranium (IV) complexes with nitrate ion are known, but are not very stable (65,66,67). The peak current as a function of nitrate concentration at high frequency is shown in Figure 25. Assuming that the lowering of the current is due to the formation of an electroinactive nitrate complex and that the current is

FIGURE 25

Variation of Peak Current at 150 Hz with Variation in Nitrate Concentration, 0.25 m_M_ U(VI)

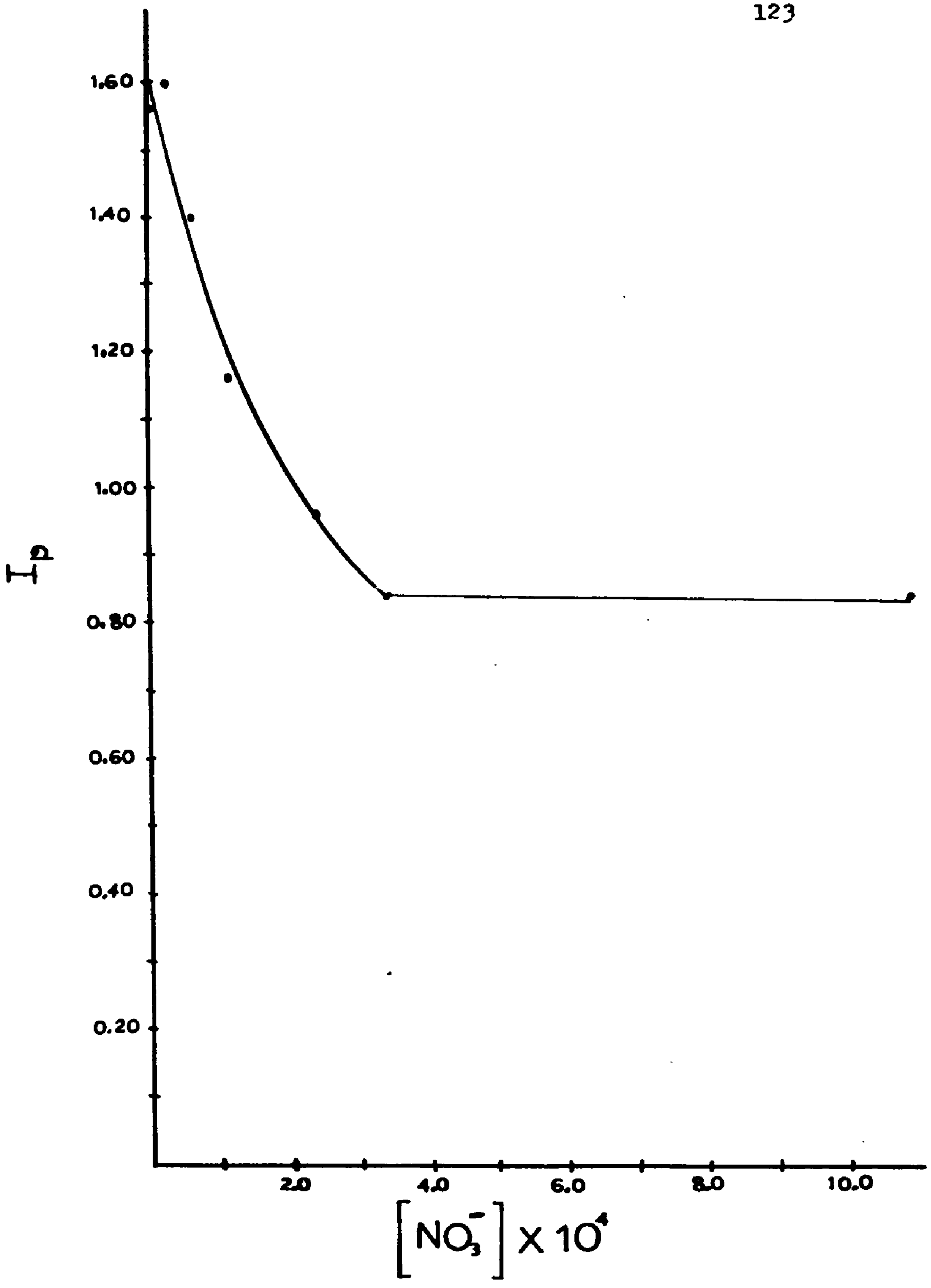
1.60
1.40
1.20
1.00
0.80
0.60
0.40
0.20
I_p
2.0
4.0
6.0
8.0
10.0
$[NO_3^-] \times 10^4$

a measure only of the uncomplexed U(IV), the calculated formation constant of the complex $(U(NO_3)^{3+})$ is log K = 5.5; this is in poor agreement with the value of log K = 0.36 found by other workers (65,67).

The effect of a chemical reaction which follows the charge transfer step producing an electroinactive complex would be expected to give similar results (if we scan from the opposite direction, the following chemical reaction would become a preceding reaction in exactly the same manner). In view of the poor agreement between the calculated formation constant and the literature value of the U(IV) - NO_3^- complex, further discussion of the current function is deferred until the mechanism is introduced.

Koryta had studied the rate of this reaction as a function of nitrate concentration, but had neglected to consider the effect of uranium concentration. He also assumed that the reaction was first order in nitrate and did not check to see if the experimental data had sufficient scatter to fit with some other reaction orders. The Koryta data were reevaluated considering the possibility of non-unity orders; the data were found to agree within the same limits of scatter (approximately) with several non-unity orders. The results of this reevaluation are shown in Figure 26. Because the rate of U(V) disproportionation increases with changes in pH from 2 (either direction), the effect of hydrogen ion on the reaction rate

FIGURE 26

Reevaluation of Koryta's Data assuming non-unity Orders

● = 1. First Order Reaction, $X = \frac{1}{2}$

○ = 2. 4/3 Order Reaction, $X = 2/3$

● = 3. 3/2 Order Reaction, $X = 3/4$

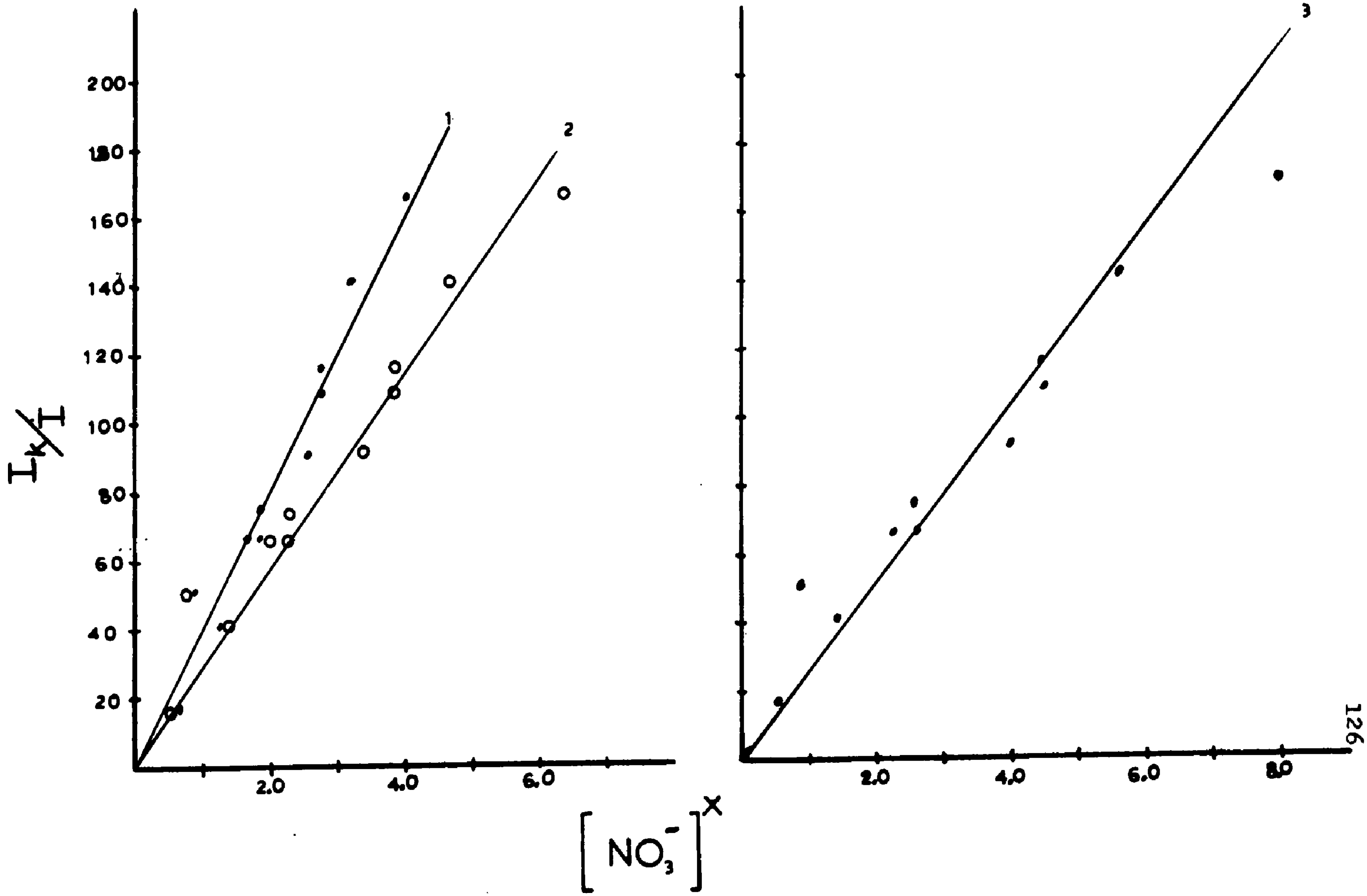
I_k/I
200
180
160
140
120
100
80
60
40
20
2.0
4.0
6.0
8.0
1
2
3
$[NO_3^-]^x$

was not studied; all measurments were made at pH=2.

The rate of reaction as a function of nitrate and uranium concentration was studied by the current ratio technique explained above. These data are summarized in Figure 27. The reaction is first order (more or less) in nitrate in agreement with previous work and the phase angle data (58). The apparent negative order with respect to the uranium concentration which was mentioned with reference to the phase angle data is clearly confirmed by the current ratio data. Figure 28 shows a plot of k_c^o as a function of uranium concentration obtained from the data in Figure 27.

Because the previous worker did not study the effect of uranyl concentration, the data can not be compared. A brief study was performed to ascertain if this negative order was the result of the method of measuring the rate or a fact of the reaction. The rate was determined by the dc method used by the previous author at two uranyl concentrations. The results were in good agreement with those obtained by the ac current ratio technique. This strongly suggests that the negative order is a true phenomenum of the reaction and not an artifact of the method of measurment. Once again the importance of the rate data is the change in rate with concentration and not the specific numbers at any particular concentration. The experimental error involved in making measurements by the ac current ratio technique is less than that involved using the phase angle technique; however, assuming that the $\cosh^2$ terms cancel in the current functions

FIGURE 27

Rate of Reaction of U(III) with NO_3^- Determined by Current Ratio Technique as Function of Nitrate Concentration

⊙ = 0.004 m*M* U(VI)
⊗ = 0.04 m*M* U(VI)
○ = 0.102 m*M* U(VI)
● = 0.205 m*M* U(VI)

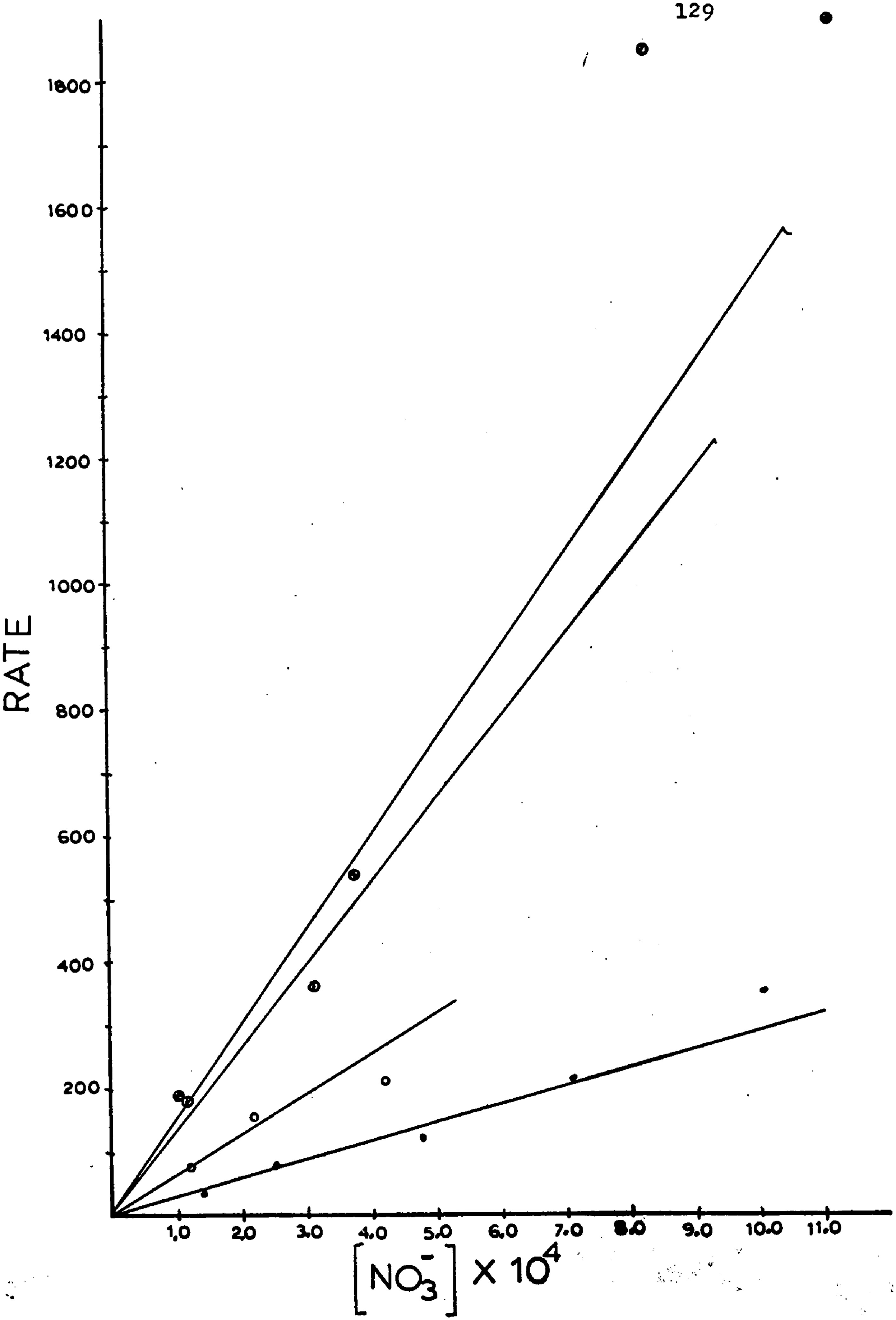
RATE
1800
1600
1400
1200
1000
800
600
400
200
1.0
2.0
3.0
4.0
5.0
6.0
7.0
8.0
9.0
10.0
11.0
$[NO_3^-] \times 10^4$

FIGURE 28

Variation of k_c^o with U(VI) Concentration Determined by Current Ratio Technique

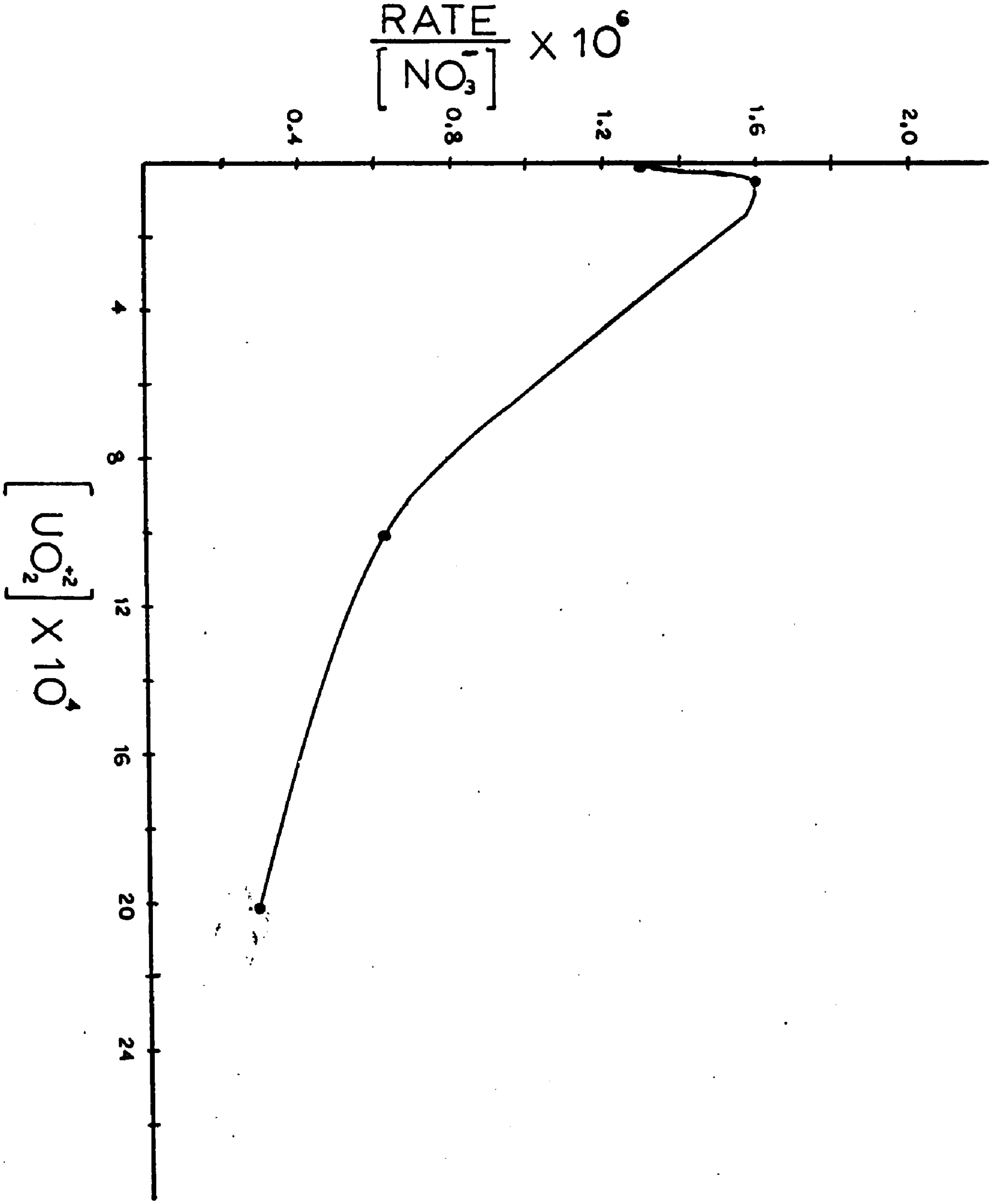
$\frac{\text{RATE}}{[NO_3^-]} \times 10^6$
0.4
0.8
1.2
1.6
2.0
4
8
12
16
20
24
$[UO_2^{+2}] \times 10^4$

introduces another error not present in the phase angle method.

The rate law which can be written from the data shown in Figures 27 and 28 is of the form:

$$\text{rate} = k_1(NO_3^-)^x - k_2(UO_2^{2+})^y \qquad (9)$$

where x and y are not necessarily unity (the possibility of non-integer values of x and y is introduced because of the experimental error precluding a more precise statement). The rate referred to above, equation (9), is the rate of dissappearence of U(III) when phase angle measurements are used and the rate of appearence of U(IV) when current measurements are used. From the rate law it is clear that the reaction mechanism is not simply a collisional reaction of U(III) and NO_3^-; there is a competing reaction involving some uranium species which removes reactants from the sequence. It is also apparent from the above rate law that the rate controlling step does not involve uranium! This presents a dilemma because the nitrate ion does not reduce at these potentials if uranium is absent.

The mechanism of the uranium catalyzed electrochemical reduction of nitrate ion written from all of tese data is shown below:

$$U^{4+} + e^- \rightleftharpoons U^{3+} \qquad (A)$$

$$(\text{slow}) \quad NO_3^- + 2H^+ + e^- \xrightarrow{U(IV)} NO_2 + H_2O \qquad (B)$$

$$(\text{fast}) \quad 5H^+ + 5U^{3+} + NO_2 \longrightarrow 5U^{4+} + NH_2OH + H_2O \qquad (C)$$

$$U^{3+} + NO_3^- \longrightarrow U^{4+} + N(C) \qquad (D)$$

The above reaction sequence is interpreted in the following manner, after U(IV) is generated at the electrode by the reduction of U(V): addition of an electron to the U(IV) at the electrode can do two things; the electron can reduce U(IV) producing U(III) (reaction (A)) or it can be passed to a nitrate ion "associated" with the U(IV) to produce NO_2 (reaction (B)). The NO_2 then chemically reacts (reaction (C)) with the U(III) produced viz reaction (A) thereby giving rise to the catalytic current. Reaction (D) represents the termination reaction and because it depletes the NO_3^- concentration near the electrode it causes the negative order with respect to uranium. The U(III) which diffuses away from the electrode reacts chemically with nitrate ion in the diffuse double layer, lowering the effective concentration of nitrate available for reaction (B). Reaction (B) must be faster than reaction (D). The product of reaction (D) would diffuse away from the electrode and so would not enter into any more reactions. Because the amount of U(III) which diffuses away from the electrode is proportional to the bulk concentration of uranyl, the effect of the termination reaction (reaction (D)) on the rate is proportional to the bulk uranyl concentration.

The reason for the zero order dependence on uranium in the rate controlling step is that only a small fraction of the total nitrate concentration is "associated" with U(IV). This means that there is a large excess of U(IV) over that needed by the nitrate. At very low uranium concentrations a decrease in the reaction rate is noted (see Figure 28) showing that at these concentrations the amount of U(IV) around the electrode is no longer in large excess over that needed by the nitrate.

In essence the uranium (IV) acts as an "electron bridge" from the electrode to the nitrate ion. A mechanism similar to this was originally proposed for the "catalysis" of nitrate by some other ions (La (III), Ce (III)), but was later discounted by others who were, however, unable to decide what is the correct mechanism (56,68).

Another mechanism which is consistent with the rate data is shown below:

$$\begin{array}{llll}
U^{4+} + e^- & \rightleftharpoons & U^{3+} & \text{(E)} \\
2H^+ + U^{3+} + NO_3^- & \longrightarrow & U^{4+} + NO_2 + H_2O & \text{(F)} \\
2NO_2 & \longrightarrow & N_2O_4 & \text{(G)} \\
2H_2O + 3N_2O_4 & \longrightarrow & 2NO + 4H^+ + 4NO_3^- & \text{(H)} \\
3H^+ + NO + 3U^{3+} & \longrightarrow & 3U^{4+} + NH_2OH & \text{(I)} \\
UO_2^+ + NO_2 + 2H^+ & \longrightarrow & U^{4+} + NO_3^- + H_2) & \text{(J)}
\end{array}$$

Sequence E - J was discounted because reaction F, due to its very large equilibrium constant, predicts that the concentration of U^{3+} and of NO_3^- around the electrode would be very close to zero and reaction (J) will not go for thermodynamic reasons.

Other metal ions have been reported to "catalyze" the electrochemical reduction of nitrate (68,69,70). Because these data are not reproducible and there is a question as to whether the waves occur at the same potential as "uncatalyzed" nitrate reduction, there is a great deal of doubt as to the interpretation of the previous observations.

The unusual variation of the ac peak current with applied frequency can now be discussed in terms of the proposed mechanism. From sequence (A) - (D) it is seen that the electron given to a uranium (IV) species "associated" with a nitrate ion does not go to reducing the uranium, but to reducing the nitrate. At low frequencies this electron transfer occurs fast enough that the U(IV) can also be reduced before the ac potential reverses and, hence, the current measured is that predicted by the theoretical equations of a catalytic mechanism. At high frequencies there is not enough time for all the "associated" U(IV) species to be reduced to U(III) and the current contribution from the catalytic sequence is small. Hence, the current is determined by the current due to the "unassociated" U(IV) and the current due to electron transfer to nitrate (probably non-Nernstian). The irreversibility of the electron transfer introduced in this manner would reduce the current below the diffusion controlled value. Non-Nernstian charge transfer reactions give non-linear plots of current versus square root of frequency. The apparent contradiction with the above data (Figure 24) is resolved if one recalls that the current should be zero at zero frequency. If the origin is included the current curves deviate significantly from reversible (linear) behavior.

The rate of the catalytic oxidation of U(III) by hydrogen ion was determined from the phase angle of the ac polarographic wave at -0.90 V versus SCE of a 1.96 m*M* solution of uranium (VI). The rate was approximately 2 sec^{-1}. This rate is sufficiently slow relative to the rate of oxidation by nitrate ion that hydrogen ion is assumed not to contribute to the measured rates of the earlier experiments.

Conclusions

The catalytic reduction of nitrate ion is still not fully understood. Previous work has been characterized both by lack of agreement and by poor reproducibility among the various workers. Catalysis by uranium is somewhat different from catalysis by other metal ions in that the data have been more reproducible, but lack of agreement in conclusions has been equally bad. At least part of the blame for the confusion surrounding these reductions can be placed on the complexity of the uranium chemistry. The techniques used by previous workers were more or less classical electrochemical techniques such as dc polarography, potentiometry, etc. which are somewhat limited in terms of mechanistic data which can be obtained.

As with virtually all mechanistic investigations, this work has not conclusively proven the proposed mechanism; it has indicated that the mechanism is more complicated than previously assumed and one possible mechanism has been disproven. The crucial question which any other mechanism must explain is: if the reaction is negative order with respect to uranium, why is uranium necessary for the nitrate reduction to proceed at all? The mechanism proposed in the present work explains this on the basis of a rate controlling step not involving uranium except as a "catalyst" and a depletion of the nitrate in the reaction layer by a chemical reaction of uranium and nitrate.

REFERENCES

1. D. E. Smith in "Electroanalytical Chemistry," A. J. Bard, ed., Volume 1, Marcel Dekker, New York, N.Y.,1966.
2. D. E. Smith and T.G. McCord, Anal. Chem., 40, 474 (1968).
3. B. Timmer, M. Sluters-Rehbach and J. H. Sluyters, J. Electroanal. Chem., 14, 169 (1967).
4. B. Timmer, M. Sluyters-Rehbach and J. H. Sluyters, Ibid., p 181.
5. H. Matsuda, Z. Elektrochem., 62, 977 (1958).
6. P. Delahay, "New Instrumental Methods in Electrochemistry," Interscience, New York, N.Y., 1954.
7. S. Glasstone, K.J. Laidler and H. Eyring, "The Theory of Rate Processes," McGraw Hill, New York, N.Y., 1941.
8. T. G. McCord and D.E. Smith, Anal. Chem., 41, 116,131 (1969).
9. H. L. Hung and D. E. Smith, J. Electroanal. Chem., 11, 425 (1966).
10. H. L. Hung, J. R. Delmastro and D. E. Smith, Ibid., 7, 1 (1964).
11. H. L. Hung and D. E. Smith, Anal. Chem., 36, 922 (1964).
12. D. E. Smith, Ibid., 35, 602 (1963).
13. J. R. Delmastro and D. E. Smith, Ibid., 39, 1050 (1967).
14. J. J. Lingane, "Electroanalytical Chemistry," Interscience, New York, N.Y., 1958.
15. J. Heyrovsky, J. Kuta, "Principles of Polarography," Czechoslovak Academy of Sciences, Prague, 1966.
16. E. R. Brown, T. G. McCord, D. E. Smith and D. D. DeFord, Anal. Chem., 38, 1119 (1966).
17. S. W. Hayes and C. N. Reilley, Ibid., 37, 1322 (1965).
18. T. Takakashi and E. Niki, Talanta, 1, 245 (1958).
19. D. E. Smith and W. H. Reinmuth, Anal. Chem., 32, 1892 (1960).
20. D. D. DeFord, Division of Analytical Chemistry, 133rd National Meeting, ACS, San Francisco, Calif., April 1958.

21. W. M. Schwarz and I. Shain, Anal. Chem., 35, 1770 (1963).

22. G. L. Booman and W. B. Holbrook, Ibid., p. 1793.

23. Instruction Manual, Precision Lock-in-Amplifier model HR-8, Princeton Applied Research Corp., Princeton, N.J., 1965.

24. "How the lock-in-amplifier works," Brower Laboratories Inc., Westboro, Mass.

25. J. K. Frischmann and A. Timmick, Anal. Chem., 39, 1507 (1967).

26. H. Bauer and P. J. Elving, Ibid., 30, 341 (1958).

27. M. Senda and P. Delahay, J. Amer. Chem. Soc., 83, 3763 (1961).

28. I. Tachi and M. Senda, Bull. Chem. Soc. Japan, 28, 632 (1955).

29. D. E. Smith, Anal. Chem., 35, 1811 (1963)

30. W. Erbelding and W. D. Cooke, Division of Analytical Chemistry, 140th National Meeting, ACS, Chicago, Ill., Sept. 1961.

31. G. W. C. Milner, "Principles and Applications of Polarography," Interscience, New York, N.Y., 1963.

32. B. Beyer and H. H. Bauer, "AC Polarography and Tensammetry," Interscience, New York, N.Y., 1963.

33. J. Holubek and J. Volke, Coll. Czech. Chem. Commun., 27, 680 (1962).

34. W. D. Weir and C. G. Enke, Rev. Sci. Instru., 35, 833 (1964).

35. W. Baker and R. F. Curtis and M. G. Edwards, J. Chem. Soc., 83 (1951).

36. E. Gergely and T. Iredole, J. Chem. Soc., 3226 (1953).

37. Pyridine and Derivitives in "Hetrocyclic Compounds," chapter VI, E. Klingsberg, ed., Interscience, New York, N.Y., 1961.

38. Hertog and Wibaut, Rec. Trav. Chim., 51, 940 (1932).

39. L. Meites in "Treatise on Analytical Chemistry," I. M. Kolthoff and P. J. Elving, eds., Interscience, Vol. 1, No. 4, 2334 (1963).

40. R. S. Nicholson and I. Shain, Anal. Chem., 36, 706 (1964).

41. I. M. Kolthoff and J. J. Lingane, "Polarography," Interscience, New York, N.Y., 1952.

42. L. Meites, "Polarographic Techniques," Interscience, New York, N.Y., 1955.

43. E. L. Wehry and L. B. Rogers in "Fluorescence and Phosphorescence Analysis," D. N. Hercules, ed., Interscience, New York, N.Y., 1966.

44. H. C. Brown and D. H. McDaniel, J. Amer. Chem. Soc., 77, 3752 (1955).

45. F. A. Cotton and G. Wilkinson, "Advanced Inorganic Chemistry," Interscience, New York, N.Y., 1962.

46. P. Herasymenko, Trans. Faraday Soc., 24, 272 (1928).

47. R. Strubl, Col. Czech. Chem. Commun., 10, 466 (1938).

48. W. E. Harris and I. M. Kolthoff, J. Amer. Chem. Soc., 67, 1484 (1945).

49. D. M. H. Kern and E. F. Orleman, Ibid., 71, 2102 (1949).

50. E. S. Kritchevsky and J. C. Hindman, Ibid., 71, 2096 (1949).

51. K. A. Kraus, F. Nelson and G. L. Johnson, Ibid., p. 2510.

52. J. Koryta and J. Koutecky, Col. Czech. Chem. Commun., 20, 423 (1955).

53. B. McDuffie and C. N. Reilley, Anal. Chem., 38, 1881 (1966).

54. D. M. H. Kern and E. F. Orleman, J. Amer. Chem. Soc., 75, 3058 (1953).

55. W. E. Harris and I. M. Kolthoff, Ibid., 69, 446 (1947).

56. I. M. Kolthoff, W. E. Harris and G. Matsuyama, Ibid., 66, 1782 (1944).

57. J. W. Collat and J. J. Lingane, Ibid., 76, 4214 (1954).

58. J. Koryta, Col. Czech. Chem. Commun., 20, 667 (1955).

59. J. F. Suttle in "Inorganic Syntheses," Vol. V., T. Moeller, ed., McGraw-Hill, New York, N.Y., 1957 p. 145.

60. J. A. Hermann and J. F. Suttle, Ibid., p. 143.

61. C. C. Adison and B. J. Hathaway, J. Chem. Soc., 1468 (1960).

62. H. L. Hung and D. E. Smith, J. Electroanal. Chem., 11, 237 (1966).

63. D. E. Smith, Anal. Chem., 35, 610 (1963).

64. D. E. Smith and T. G. McCord, Ibid., 40, 474 (1968).

65. L. G. Siller, Inorganic Ligands in "Stability Constants of Metal ion Complexes," The Chemical Society, London, 1964 p. 170.

66. S. Ahrland, Acta. Chem. Scand., 5, 1271 (1951).

67. N. P. Ermolaev and N. M. Krot, Radiokhimiya, 4, 678 (1962).

68. M. Tokuoka, Col. Czech. Chem. Commun., 4, 444 (1932).

69. M. Tokuoka and J. Ruzicka, Ibid., 6, 339 (1934).

70. L. Meites, J. Amer. Chem. Soc., 73, 4115 (1951).

VITA

Ronald Frank Evilia

Born December 28, 1943, Meriden, Connecticut

Parents - Alexander and Ida Evilia

Married the former Deborah Ann Baer, one child, Christopher David

Preliminary education - Meriden public school system

Undergraduate training - BA Lehigh University, 1965

Societies - Society Sigma Xi, American Chemical Society

Publications - "Ac polarography with simplified phase sensitive detection," Anal. Chem., 39, 1885 (1967) (with A. J. Diefenderfer).

"Electrochemical Studies of the Monohalopyridines," J. Electroanal. Chem., in press (with A. J. Diefenderfer).